Sound control in windy weather

Master Thesis

Jonas Buchholdt

Aalborg University
Electronic Engineering and IT

This report is compiled in LaTeX. Additionally Mathworks MATLAB®, Inkscape, and Xfig are used to draw figures and charts.

AALBORG UNIVERSITY
STUDENT REPORT

Electronic Engineering and IT
Aalborg University
http://www.aau.dk

Title:
Sound control in windy weather

Theme:
Signal Processing and Acoustics

Project Period:
MSc, 10th Semester 2019

Project Group:
Jonas Buchholdt

Participants:
Jonas Buchholdt

Supervisor:
Sofus Birkedal Nielsen

Number of Pages: 222

Date of Completion:
?th June 2019

Abstract:

Will come later

Preface

This report is composed by Jonas Buchholdt during the 10th semester of Electronic Engineering and IT at Aalborg University. The general purpose of the report is *Signal Processing and Acoustics* .

For citations, the report employs the Harvard method. If citations are not present by figures or tables, these have been made by the authors of the report. Units are indicated according to the SI standard.

Aalborg University, May 30, 2019

Jonas Buchholdt
<Jbuchh13@student.aau.dk>

Contents

Glossary

ADC Analog to Digital Converter. 59

DSP Digital Signal Processor. 78

FDTD Finite-Difference Time-Domain. 14

FFT Fast Fourier Transform. 58, 92

FIFO First In First Out. 59

FOH Front Of House. 5

IFFT Inverse Fast Fourier Transform. 58, 92

IP Internet Protocol. 163

PA Public Address System. 3, 4

PCB Printed Circuit Board. 61

SPL Sound Pressure Level. 3, 4, 5, 9, 10, 11, 12, 15, 16, 19, 22, 23, 24, 27, 28, 29, 34, 37, 38, 39, 41, 42, 43, 46, 47, 51, 56, 58, 64, 68, 69, 70, 71, 72, 73, 81, 82, 90, 91, 97, 98, 99, 100, 101, 102, 104, 105, 106, 107, 108, 109, 111, 112, 117, 118, 119, 125, 126, 141, 176, 178, 193, 194, 195, 196, 204, 206

UDP User Datagram Protocol. 163

USB Universal Serial Bus. 57, 60

Chapter 1

Introduction

1.1 Live venue sound challenges

This section explores the challenges of producing sound in an outdoor environment. The challenge of producing a good sound experience for the audience highly depend on the calibration method and the atmosphere condition. It is well known that acoustically wave propagation is strongly affected by the inhomogeneous atmosphere doing the outdoor sound propagation. This inhomogeneous atmosphere shifts the calibration of the sound system which affects the intelligibility. In section 1.1.1 an overview of high Sound Pressure Level (SPL) Public Address System (PA) system is discussed.

1.1.1 Acoustics at live venue

An outdoor PA system is an essential sound reinforcement concept today. It is used to address information, music or just entertainment where the number of audiences is large, sometimes more than 10.000 audiences. The number of the audience makes it difficult to address the information to a large number of the audience without the reinforcement of the information. The reinforcement is nearly always done from a stage with a sizeable PA system and sometimes delay unit in the middle of the audience area. The stage lifts the artist while the PA system is designed to cover the audience area with sound. The optimal PA system covers the area with a linear frequency spectrum in the audible frequency range with a homogeneous SPL. Today, the used speaker is a line source array flown in both side of the stage and is therefore only close to the audience in front of the stage. The line source array is an array of small identically wide speakers attached to each other, to form a vertical line of speakers. An example of a line source array is shown in Figure 1.1

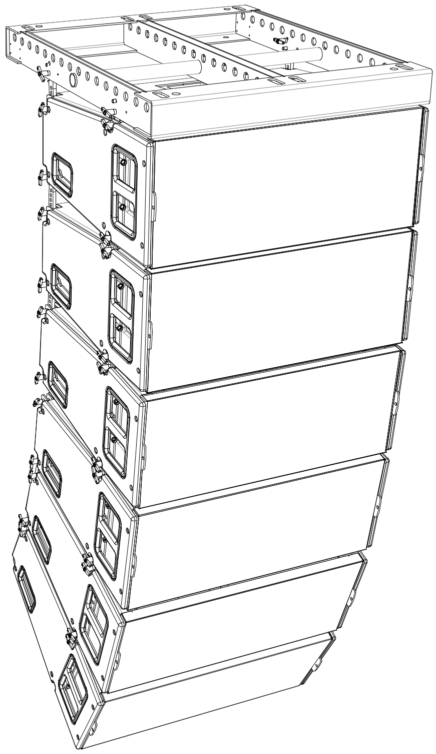

Figure 1.1: The figure shows an illustration of a KUDO line source array from L-Acoustics [L-Acoustics, a]

Every speaker or a small group of the line source array can be controlled individually, both in sound coverage area angle and SPL. The benefit of using the line source array design is that the coupling between the speaker makes a line acting source. With an optimised control system of the line source array, the audience area is covered with sound such that all audience can hear the information without damage the ear of the frontal audience. An optimised line source array has, for example, an optimised main lobe such that the lower part of the main lobe lays flat along the audience area. The following Figure 1.2 shows a graphical illustration of the outdoor PA venue concept.

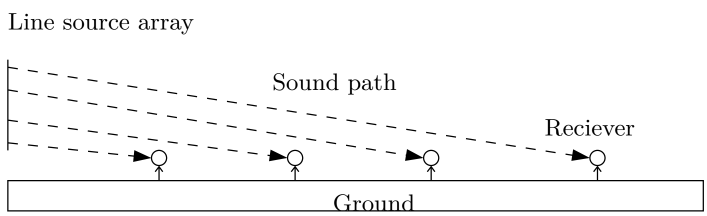

Figure 1.2: The figure illustrate the concept of outdoor PA venue

As shown in Figure 1.2, the distances from one element in the line source array to the receiving audience dependent on the audience position. The distance indicates that the signal to every line source element has to be set individually to cover the audience area wit ha homogeneous SPL. The individual control of the source is necessary because of the wave amplitude decay with distances. This phenomena is addressed in section 2.1. The adjustment is not as simple as just supply the upper speaker with more power. A sound wave is a mechanical movement of the particle in the air, which condensate and compression the air molecule, then low pressure and high pressure respectively. The movement of the molecule depends on the medium, and in this thesis, the medium is limited to air. The SPL is the pressure divination of the instantiates atmospheric pressure. The atmospheric pressure, therefore, set a lower bound on the condensation while very high pressure changes the speed of sound and distort the wave as it propagates. To ensuring that the information is communicated to the audience without distortion, the limitation is addressed in section 2.2.3. The medium in the air is not constant and varies over time regarding pressure, wind, humanity and temperature. The analysis starts with the experience for live concert of the author in section 1.1.2, next section 2.2 address the impact of homogeneous atmospheric effect on sound propagation. Then section 2.2 address the impact of inhomogeneous atmospheric effect on sound propagation.

1.1.2 Author experience of live concert

The Author of the thesis has experience with live concert both as an audience and as a sound engineer. The aspect of being the sound engineer and an audience to a live concert is very different. As a sound engineer, the area for controlling the sound is a secured area with a tent as protection. The tent roof often shadows for the high frequency, and the walls make standing waves of the low frequency because the distance between parallel tent walls fits with the wavelength for the low frequency. The sound engineer control area is defined as the Front Of House (FOH). The FOH is often equipped with an additional speaker, and the sound engineer does not fully know how it sounds outside the FOH, but base there mixes on experience ??. The aspect of being an audience depends on where the audience is regarding the stage. In close hand to the stage the SPL is high and often to high especially in the low frequency. The low frequency is often made as a vertical array at the ground or two end-fire arrays and shall be able to exhibit all audience by an audible low frequency spectrum typically from 25 Hz but one company extends down to 13 Hz. Therefore the SPL just in front of the subwoofer has a very high SPL. This position is not comfortable to be at in longer period, and the high SPL mask the higher frequency. The optimal audience position is in the centre of the stage and not as long from the stage as the delay towers. The average SPL is often less than 102 dB SPL since the sound engineer try to keep a maximum average SPL at 102 dB SPL just in front of the FOH. Moreover, it is the stereo sweet spot. This position is the only position where the stereo image is optimal. The stereo perspective problem is a hot topic nowadays, both L-Acoustics [L-Acoustics, 2019] and D&B Audiotechnik [d&b audiotechnik, 2019] have made there own solution to the problem. The idea is to fly many small line source array above the stage and assign every musician to there own line source array. The concept minimises the interference between two line source array playing the same mono signal. Near the delay towers or approximately 50 m from the main stage, the low frequency spectrum is still sharp and audible but something happens to the high frequency. Often the high frequency disappears for a few seconds and gets back. This phenomenon altering through the full concert. Behind the delay towers, the line source array in the delay tower reproduces the sound such that the audience in the back also gets the high frequency spectrum. The question is why does the high frequency disappear for a short period when the low frequency does not? This analysis focus on finding the atmospheric condition which cause the phenomena.

Part I

Problem Analysis and Requirements

Chapter 2

Analysis of sound propogation in outdoor venue

2.1 Ideal geometric spreading loss

When a line source generates a sound wave, the wave field exhibits two fundamental difference spatially directive regions, near-field and far-field. In near-field, the wave propagates as a cylindrical wave wherein the far-field the wave propagates as a spherical wave. When the wave propagates as a cylindrical wave, the wave propagates only in the horizontal plane, and therefore the attenuation is 3 dB Sound Pressure Level (SPL) per doubling of distance. For a spherical wave propagation, the wave propagates in all direction. Therefore the attenuation is 6 dB SPL per doubling of distance. The near-field and far-field attenuation are based on non-absorption homogeneous atmospheric conditions. The border between the near-field and far-field depends on the hight of the array and the frequency. The distance can be calculated with Fresnel formula Equation 2.1, where the wavelength λ is approximated to $\frac{1}{3f}$ [Bauman et al., 2001]

$$d_B = \frac{3}{2} f \cdot H^2 \sqrt{1 - \frac{1}{(3f \cdot H)}} \tag{2.1}$$

Where:

d_B	is is the distance from the array to the end of near field	[m]
f	is the frequency	[kHz]
H	is the hight of the array	[m]

In equation Equation 2.1 it can be calculated that less than 80 Hz radiate directly intro spherical wave on the exit of the speaker no matter the hight of the line source array. The following Figure 2.1 shows a horizontal cut of the near-field, far-field from a line source array.

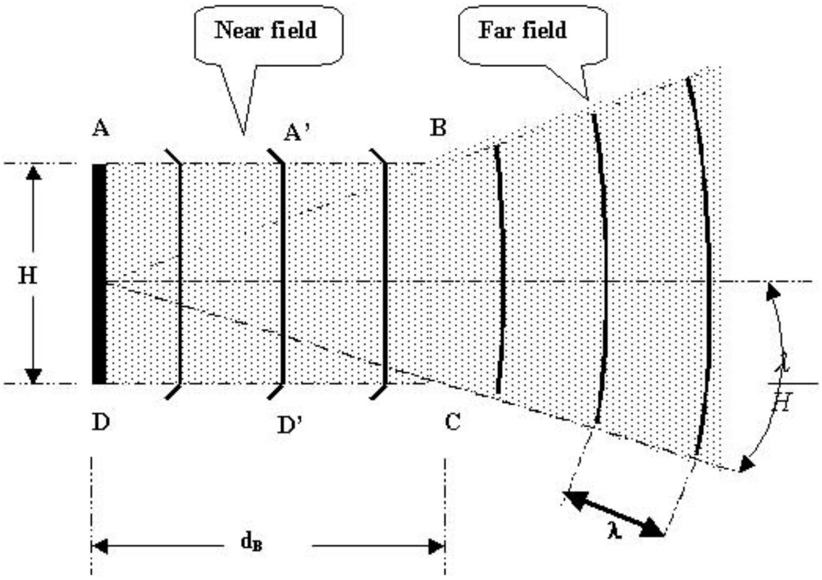

Figure 2.1: The figure shows horizontal cut of a SPL radiation pattern of a line source array [Bauman et al., 2001].

As seen in Figure 2.1, the wave propagating as a plane cylindrical wave in the near-field, where the coverage area for every double of distance is twice as big. Since the coverage area is twice as big, the SPL is the half for the doubled distance. When the wave excites distance d_B, the wave propagates intro far-field where the coverage area is four times higher while travelling the double of distance and therefore the SPL is four times less. In far-field, the wave propagates as a spherical sound source. The following Figure 2.2 gives two examples with different hight.

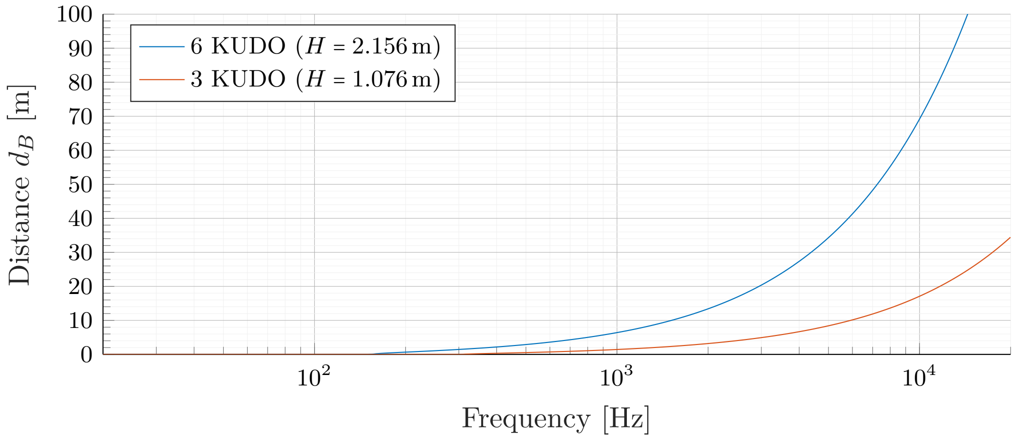

Figure 2.2: The figure shows two hight example calculated from Equation 2.1.

As seen in Figure 2.2, while the hight is the double, the far-field is moved four times as far back.

2.2 Homogeneous atmospheric conditions

This section aims to analyse the sound wave propagation in homogeneous atmospheric conditions. It is well known that the sound wave propagation is highly depending on the atmospheric conditions. The propagation depends on the atmospheric pressure, wind, temperature and humanity, where the two latter moreover is frequency dependent. The attenuation difference in frequency for temperature and humanity can be above 80 dB SPL [Corteel et al., 2017]. The following sections introduce a brief discussion of homogeneous atmospheric conditions effect on sound propagation.

2.2.1 Humidity and temperature impact

The temperature and humidity have three impacts on wave propagation from a line source array, directionality of the speaker, the speed of sound and a lowpass effect. The following description starts with the latter.

Lowpass effect The effect of humidity and temperature on wave propagation act as a lowpass filter while the wave propagates. The low frequency remains without any additional attenuation where the high frequency highly depends on the atmospheric condition. In other words, attenuation in the high frequency range does not only depends on the spreading loss but also temperature and humanity. Therefore, for long distance, the atmospheric conditions have a high influence on the frequency spectrum delivered to the audience. Humanity and temperature attenuation are already well studied and standardised. Standard [ISO 9613-1:1993] gives an overview of calculating the SPL attenuation concerning the frequency, distance, temperature and humanity. The article [Corteel et al., 2017] gives some examples of attenuation at a distance of 100 m. The article shows that if humanity increases proportionally to the temperature, the lowpass effect is small. If the change in temperature and humanity is the opposite of each other, for example, high temperature but dry, the attenuation in high frequency is significant. The following Figure 2.3 shows the worst-case scenario from [Corteel et al., 2017].

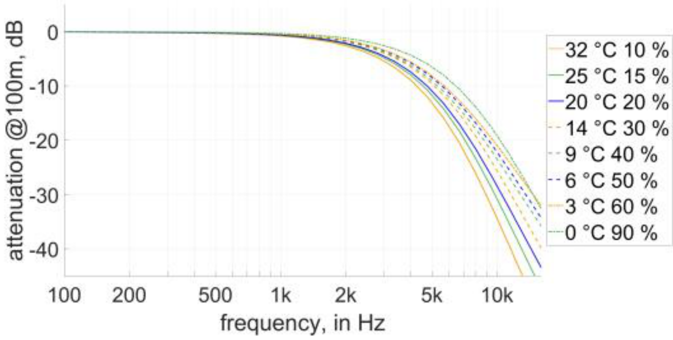

Figure 2.3: The graph shows the attenuation in dBwith respect to frequency, humanity and temperature [Corteel et al., 2017].

As shown in Figure 2.3 the attenuation in the high frequency is significant and excite 30 dB SPL within the audible frequency range. The attenuation is such markedly that applying more power does not cover the attenuation without an extreme high-pressure driver which is only in theory. Extreme high-pressure drivers introduce high distortion as is explained in section 2.2.3

Speed of sound The second consequence is the speed of sound. At temperature range from 0 °C to 40 °C the speed of sound with respect to humanity change is sparse and mostly only depend on temperature. At 0 % humidity, the speed of sound increases with 0.6 m/s for every increasing degree °C. At humanity higher that 0 % the speed of sound increase with respect to humanity, depends on temperature. The wave propagation speed start at 331.5 m/s at 0 °C and 0 % humanity. The following Figure 2.4 shows the speed of sound with respect to humanity and temperature.

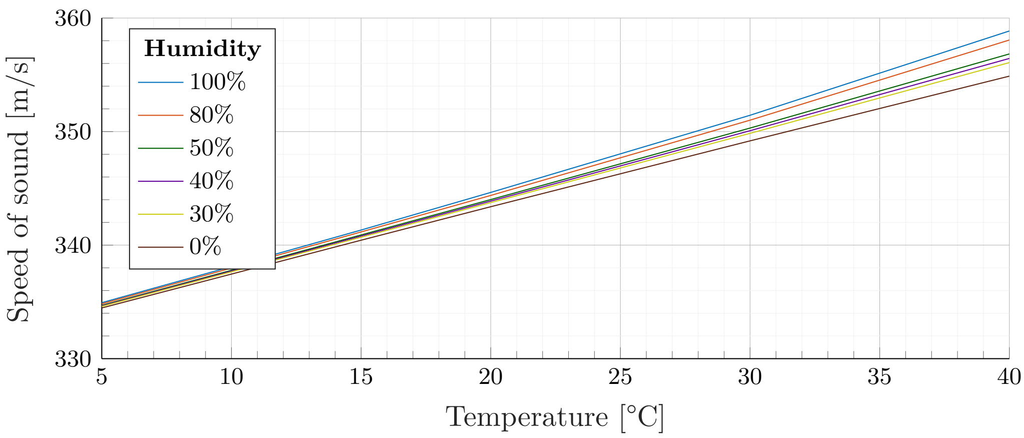

Figure 2.4: The figure shows the increase of sound speed with respect to humanity and temperature [Bohn, 1987] [Wong and Embleton, 1985]

As seen in Figure 2.4, the effect of humidity is negligible compared to the effect of temperature changes, but as the temperature increases the humidity gets significant. At a temperature of 40 °C the speed of sound is changed 4 m/s from 0 % humidity to 100 %

Directivity The directivity of a line source array in the mid and high frequency is always controlled mechanically by a horn because the wavelength is short compared to the size of the speaker. At low frequency, the wavelength is too long to be controlled mechanically by a horn. Therefore the directional pattern is controlled via cancellation from a backwards pointing speaker. The directivity of both the low frequency and the high frequency driver sufferers from temperature increased. At the high frequency, the main lobe gets narrower when the mechanical horn gets warmer, and the effect is notable when the sun directly heats up the horn. When the surface of the horn heats up by the sun, the temperature can get much warmer in the horn that the air temperature. Therefore the surface of the horn affect the directivity of the high frequency by radiate warm air from the surface. The resend that main lope gets narrower is that the wavelength gets shorter at higher temperature [Levine et al., 2018]. The directivity of the low frequency is affected as in the high frequency with the temperature increase. The difference is not as significant as in the high frequency since there is no surface heat. The directivity is then not affected due to the sunlight, but only the temperature increasing and decreasing. As in the high frequency temperature differences change the wavelength, and then the length between the speaker in a cardioid low frequency does not match the optimised distance between the speaker more.

2.2.2 Wind impact

The wind influence is depending on the angle of the wind direction with respect to the direction of sound propagation. A homogeneous wind is a laminar wind flown with the same homogeneous speed. The following analysis assumes homogeneous laminar wind flow from one direction. The analysis is of both oblique wind and parallel wind with respect to the frontal direction of the line source array. The analysis starts with the latter.

Parallel to sound propagation When the wind flows in the same direction as the sound wave propagation, the wind flow in m/s is an addition to the speed of sound. When the wind flows in the opposite direction, it is a negative addition. In other cases, the influence is complicated since the wind deflect the sound waves.

oblique- and crosswind The effect of homogeneous oblique- and crosswind on sound propagation from a speaker is rarely studied, and the effect on high frequency seems to be unclear. One author has addressed the problem in a simulation of a low frequency source [Ostashev et al., 2005] where the author of [Ballou, 2008] have practical experience with high power sound system and indicate that crosswind effect might be frequency dependent. The author indicates that the frequency dependency might be due to the directionality of the high frequency drivers. The author of [Ostashev et al., 2005] has simulated a homogeneous crosswind effect on an omni-directional source at 100 Hz. The author of [Prospathopoulos and Voutsinas, 2007] implemented a ray tracing method with a vector based interpolation as shown in Figure 2.5.

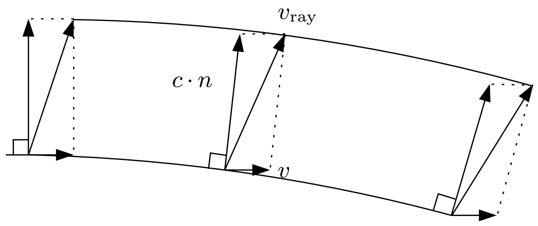

Figure 2.5: The figure shows a geometrical ray tracing calculation scheme of calculate the resulting wave direction at crosswind [Prospathopoulos and Voutsinas, 2007], [Ostashev et al., 2005]

Where:

c	is the speed of sound	[m/s]
n	is the normal unit vector	[m]
v	is the speed of wind	[m s]
v_{ray}	is the resulting sound ray	[m]

As seen in Figure 2.5, the ray vector v_{ray} is an addition of the sound speed vector $c \cdot n$ and the speed of wind v. The wave speed and wavelength, therefore, depend on the speed of the wind and the angle between the wind and the sound propagation. The following Equation 2.2 calculate the speed of sound in the v_{ray} direction with respect to the wind speed and angle.

$$c_r = c + ||v||_2 \cdot sin(\theta) = ||c \cdot n + v||_2 = ||v_{\mathrm{ray}}||_2 \tag{2.2}$$

Where:

θ	is the angle of the wave with respect to the wind	[°]
c_r	is the resulting speed of sound	[m/s]

As the wave propagating, the resulting v_{ray} increases in the direction of the wind. The article [Ostashev et al., 2005] simulates the effect of crosswind in a Finite-Difference Time-Domain (FDTD) simulation with a wind speed of 102.9 m/s. For the acceptable condition to a concert, the wind speed is less than 20 m/s. Otherwise, the audience is escorted from the stage to the exit, and the speaker system is taken down to ensure safety. The following Figure 2.6 shows a simulation result from

[Ostashev et al., 2005], where the source is an omnidirectional 100 Hz spherical source while the wind has a constant uniform wind speed from left. The simulation is done in two dimensions.

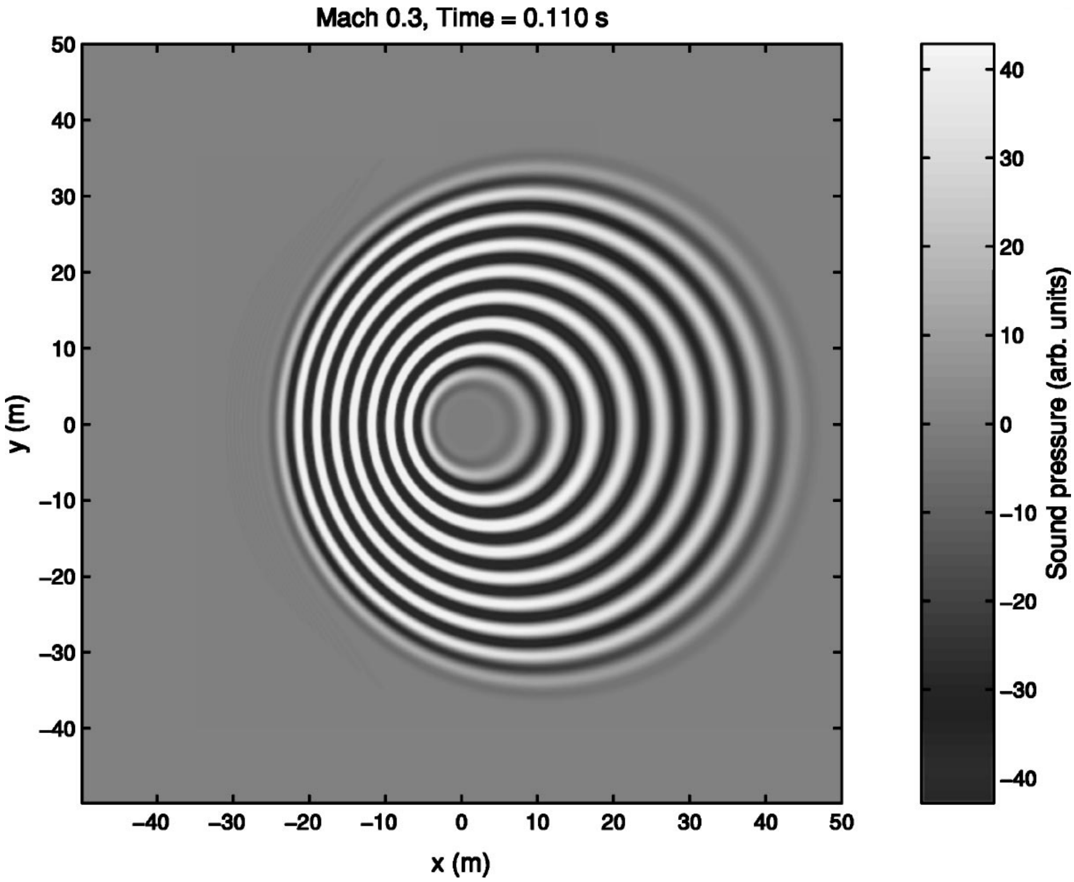

Figure 2.6: The figure shows a simulation of a 100 Hz omnidirectional source with a uniform constant wind speed from left with speed of 102.9 m/s [Ostashev et al., 2005].

As seen in Figure 2.6, the homogeneous crosswind does not affect the direction of the wave from a low frequency spherical source. It only affects the time of arrival to the audience.

2.2.3 Pressure impact

The influence of atmospheric pressure change is low compared to the effect of wind, humanity and temperature. The average atmospherical absorption from 4.0 kHz to 16.0 kHz with fixed temperature and variable humanity, increases with 2 dB SPL while going from 101.33 kPa to 54.02 kPa. The atmospheric pressure then only have a negligibility influence on sound propagation and is generally not frequency dependent.

Beside the small impact of pressure difference in the atmosphere, the high pressure generated by the speaker does have a tremendous influence on the sound propagation.

There are three states in the propagation way that can produce distortion concerning the pressure. The design of the high frequency horn [Czerwinski et al., 1999], the port design of the low frequency driver [Vanderkooy, 1998] and the influence of the sound path. The following description starts with the latte.

Sound path In the sound path, two factors distort the wave doing propagating in air. As described in section 1.1.1 a sound wave is condensation and compresses of the air particle. The air medium, therefore, has a lower limit that cannot be less than vacuum. The higher bound of SPL is then depending on the atmospheric pressure. As an example, at 54.02 kPa the highest SPL before distortion caused be vacuum is 188.6 dB SPL and at 101.33 kPa the highest SPL before distortion caused be vacuum is 194.1 dB SPL.

There is, therefore, a higher limit determined by the atmospheric pressure to vacuum, but distortion occurs much before the limit of vacuum. High pressure in the compression also distorts the sound because of the lack of linear dependency between the particle velocity and stiffness in the sound wave. The stiffness or density increases while the air particle is closer to each other. Therefore SPL increases more than the density of the sound wave which causing the compression of the sound wave to be stiffer and therefore propagate faster than in the condensation of the wave. This speed differences, therefore, produce harmonic distortion, and is even present in SPL less than 120 dB SPL [Czerwinski et al., 1999]. The speed differences transform the sinusoid intro a sawtooth as it propagates which transfer energy to the harmonic of the propagation frequency. The distortion is not only SPL dependent, but also depend on the frequency. The higher the frequency is, the faster the sinusoid transformers intro a sawtooth, therefore, the distortion increases with frequency for constant SPL. The harmonic frequency is higher than the fundamental frequency and therefore, as explained in section 2.2.1, the harmonic has higher attunation with respect to the distance and viscosity. In most cases, the attention is not as high as the increase of the harmonic distortion, and therefore the distortion of the wave propagation is not fully compensated by the viscous losses in the air. [Czerwinski et al., 1999]. The distortion made by air propagation is much less than the distortion in the mouth of the speaker which leads to the next distortion problem produced by high-pressure [Czerwinski et al., 1999].

Driver throat and mouth design High pressure in both horn phase plug, sealed enclosures, vented enclosures and reflex enclosures for low frequency driver cabinet produces distortion as they act as nonlinear components. The latter produce distortion because high pressure makes air turbulence in the vent. In the optimal design, the distortion of air turbulent is low but is always present in high-pressure [Roozen et al., 1998]. The air turbulence is not only caused in the vent of the low frequency driver, but it also occurs in the phase plug of the compression driver if the SPL is high [Czerwinski et al., 1999]. The distortion depends on the moving mass, the stiffness and the viscous losses in the air on the diagram displacement and the SPL. As the air in the high frequency driver compress, it becomes heavier, stiffer and thicker which make nonlinear wave propagation. It typically occurs when the compression chamber exceeds approximately 170 dB SPL. At a higher level, the particle velocity resistance to the air flow increases and the laminar air flow turns intro turbulent air flow. The distortion is also depending on the length of the horn and the expansion rate of the horn flare. To keep the distortion as low as possible for the high frequency driver the displacement of the diaphragm should be kept significantly lower than the hight of the compression chamber [Voishvillo, 2004]. Therefore, to keep the displacement of the high frequency driver as low as possible, the frequency range should be limited.

2.2.4 Ground absorption and reflection

In a concert area, ground absorption and reflection is complicated because there are two very different situations. Before the concert, the area is a local plan area often with mown grass and with ground reflection. An example of a frequency response over mown grass where the measuring hight of the microphone is in the hight of the ear is given in [Piercy et al., 1977]. The measurement shows that the ground reflection affects the frequency response with high interference. A measurement in Appendix A is performed where the ground reflection clearly have a big influence on the received frequency response. In this measurement inhomogeneous airflow is present, but the interference is similar in homogenous airflow [Piercy et al., 1977]. Doing the concert the interesting part is not such ground reflection effect but the audience reflection or absorption. The area along the concert is packed by the audience and therefore, the reflection is not easy to calculate. The absorption and reflection in an outside concert area with a group of audience is rarely studied, but absorption for the audience inside a concert hall is highly studied [Beranek, 2006]. The absorption of the audience is founded to be high in all measured concert hall from 1.0 kHz octave band to 4.0 kHz octave band [Beranek, 2006]. The average absorption a_{sabine} coefficient is calculated to be above 0.80. The method and result can be founded in [Beranek, 2006]. The reflection in the high frequency in the audience area doing concert is therefore assumed to be low. At low frequency, the article [Beranek, 2006] indicate that the absorption decay with frequency beneath 250 Hz, but The octave band for low frequency driver, which is 31.5 Hz, is not measured by [Beranek, 2006]. The low frequency absorption at 31.5 Hz octave band is therefore assumed to low. The low frequency driver is mostly located in front of the stage on a line or in end-fire settings, often with a maximum distance of half the wavelength from acoustical centre to acoustical centre. The distance between the low frequency driver is determined by the half wavelength of the highest frequency, such that they radiate a plan wave [Bauman et al., 2001]. A higher distance between the acoustical centre causes interference in the low frequency in the audience area.

2.3 Inhomogeneous atmospheric conditions

This section aims to analyse the sound wave propagation in inhomogeneous atmospheric conditions. In an inhomogeneous atmosphere, the pressure and speed is a function of position. By this fact, the modelling of a sound wave is very complex and depend on various variables such as temperature and wind speed. The following sections give a short introduction to the effect of inhomogeneous atmospheric conditions.

2.3.1 Atmospheric refraction

When the wind speed, the temperature and humanity is assumed to be homogeneous in the sound field, the sound is travelling in a straight plan wave. Often this is not true, the wind speed increases logarithmically with the hight from the ground to the geostrophic wind [Yang, 2016] in the free troposphere [Rossing, 2014], and the temperature and humanity are inhomogeneous. The geostrophic wind in the free troposphere is located in a hight from approximately 1 km above the ground [Rossing, 2014], [Association, 2003]. The inhomogeneous atmospheric condition makes the speed of sound to depend on the hight from the ground. This inhomogeneous atmospheric condition results in a curved sound path and is defined as atmospheric refraction. For small distances, the atmospheric refraction has a spars effect on the sound travelling path, because the speed of sound is much faster than the speed of the wind and the temperature change. Generally distance up to 50 m is often assumed to have no significant refraction effect [de Oliveira, 2012]. For distances larger than 50 m the refraction is assumed to have a significant influence, especially when the sound source and the receiver are close to the ground. Refraction is frequency and distance dependent and is measured in dB excess attenuation. The means of excess attenuation is that only the effect of wind or temperature is considered, all other atmospherical effect is excluded. A measurement is given in [Piercy et al., 1977] for a point source where the wind speed is 5 m/s. At a distance of 110 m, it is observed that frequency above 400 Hz is refracting where frequency below is rarely effected of refraction. Moreover, at a distance of 615 m the refraction is present in the full measured frequency range from 50 Hz to 3.2 kHz. In the perspective of a live concert the interesting distance is the 110 m from the line source array to the audience rather than the 615 m. Both the downwards and upwards refraction is interesting. In the upwards refraction the audience might be in the shadow zone where for the downwards refraction the high frequency reflection from the ground is assumed to be low when the concert area is full of audience. Therefore the high frequency is refracted down intro the frontal audience, and only sparse reflection of the high frequency propagate to the back part of the audience. The following Figure 2.7 display the phenomena of upwards refraction.

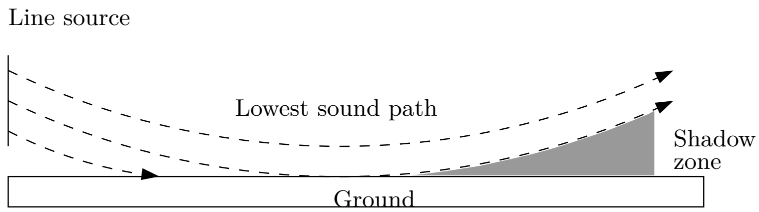

Figure 2.7: The figure illustrates that the shadow zone occurs from an upwards refraction. A line source speaker array contains of many couplet point sources. Every lowest sound path dashed line indicate the lower directional angle of one point source in the line source array.

The following description is based on the distance of 110 m and upwards refraction. As explained in [Piercy et al., 1977] the refraction at a distance of 110 m is highly frequency dependent. At a frequency below 400 Hz the effect is sparse but above the effect is high and may result in 20 dB SPL attenuation at the audience. The reason that the refraction is frequency dependent is that the scale of the wind gradient and temperature gradient close to the ground is small compared to the wavelength of the low frequency [Piercy et al., 1977]. This theory does not follow the shell's law of refraction. Shell's law describes the refraction as a layer change in the medium of propagation. Shell's law of refraction is defined as Equation 2.3

$$\frac{cos(a_1)}{c_1} = \frac{cos(a_2)}{c_2} \tag{2.3}$$

Where:

a_1	is the input angle in the horizontal plan	[°]
c_1	is the sound of speed in the medium of arrival	[m/s]
a_2	is the output angle in the horizontal plan	[°]
c_2	is the sound of speed in the medium of destination	[m/s]

As shown in shell's law Equation 2.3 the frequency dependency is not a factor and are therefore maybe only valid for a laminar wind flow profile. The article [Piercy et al., 1977] only explorer frequency up to 3.2 kHz but since the refraction depends on the wavelength, the distance of refraction wave might be smaller for higher frequency. The attenuation with respect to refraction seems to have a saddle attenuation at 20 dB SPL. A measurement in [Piercy et al., 1977] shows the attenuation for the center frequency of 1.2 kHz with 1/3 octave band filtered airplain noise over mown grass. The measurement is interesting with respect to a concert area and is therefore shown in Figure 2.8

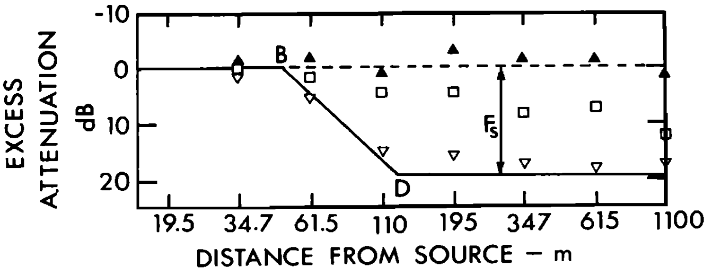

Figure 2.8: Excess attenuation measured for aircraft noise in the 1.2 kHz 1/3 octave band for the ground-to-ground configuration. The vector component of the wind velocity in the direction of propagation for ▲ is 5 m/s, □ is 0 m/s, and ▽ is −5 m/s. The temperature profile is neutral. F_s is the shielding factor, B is the shadow boundary [Piercy et al., 1977]

The following two paragraphs explain the difference between wind refraction and temperature refraction.

Temperature Temperature decreases with respect to the hight at day time and increases at the night time. The increase or decrease is usually approximated as a logarithmic function. In the day time, the sun heats the ground even on a cloudy day, and the concert area is full of audience. Therefore, the eath and audience radiate warm air, which makes the temperature at a low hight warmer than the temperature at higher hight. These phenomena are named lapse where the opposite is defined as inversion. As explained in section 2.2.1, the speed of sound depends on the temperature. Therefore, at day time, the speed of sound in this situation decay with respect to hight. The speed change can be modelled as a change of layer for a plane wave. The output angle of the layer change follows the shell's law when the frequency dependency is excluded. Therefore when the temperature profile is logarithmic, the layer change is a function of hight and change the wave direction. The wave direction of the descript weather condition results in an upwards refraction. Since the temperature is a scalar quantity uniformly over a large area and a function of hight, an identical temperature profile is applicable all around an omnidirectional sound source. Therefore the upwards refraction is uniform all along the speaker in the horizontal plane. The following Figure 2.9 illustrate the phenomena where the temperature decay with respect to the hight and the line source array is omnidirectional in the horizontal plane. The omnidirectionality of the line source array is only present in the low frequency typically below 200 Hz.

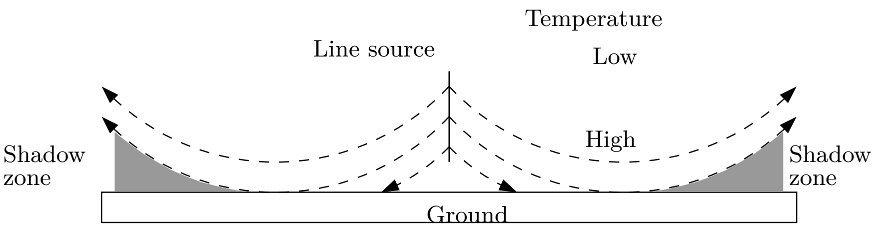

Figure 2.9: Wave refraction of a horizontal omnidirectional line source array in inhomogeneous temperature with lapse profile

When the temperature profile is reversed, the refraction is downwards.

Wind With respect to the wind speed, a concert area is often a protected area with for example barrier, stage and building. This blockage and the ground friction slows down the wind speed near the ground and cause turbulence. Moreover, from nature itself, the wind speed is often logarithmically increased with respect to the hight. When the wave is propagation in the same direction as the wind, the atmospheric refraction refracts the sound wave downwards. When the wave propagates against the wind, the atmospheric refraction refracts the sound wave upwards. The following Figure 2.10 illustrate the phenomena with a logarithmic increasing wind from left, and the line source array is omnidirectional in the horizontal plane.

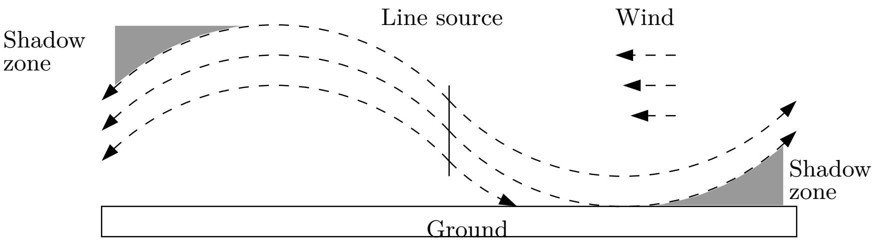

Figure 2.10: Wave refraction of a horizontal omnidirectional line source array in inhomogeneous logarithmically increasing wind profile where the wind gradient points towards left

As shown in Figure 2.7 the refraction is upwards when the wind flows in the opposite direction as the wave propagation. Behind the line array source, the refraction is downwards and is therefore different than for temperature refraction. The refraction of wind is the most dominant at a distance of 110 m. The following Figure 2.11 shows an excess attenuation plot of both inhomogeneous wind and lapse temperature profile.

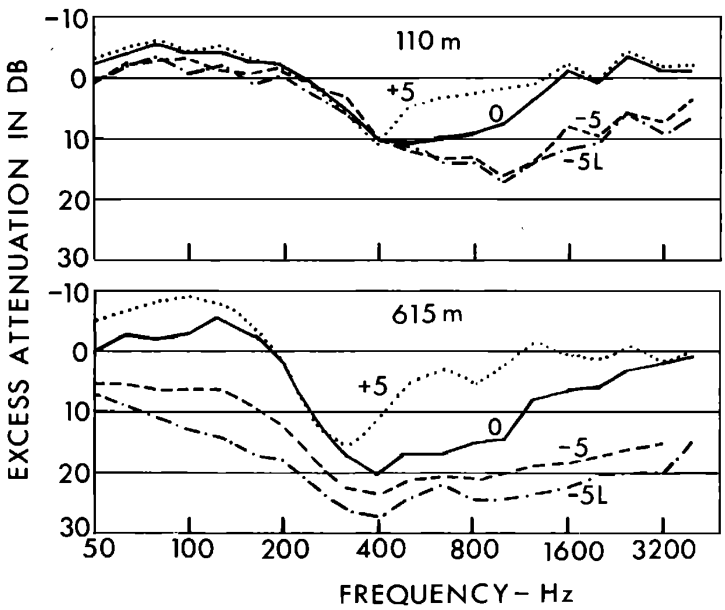

Figure 2.11: Observed attenuation of aircraft noise in a ground-to-ground configuration under a variety of weather conditions. Calculated losses from atmospheric absorption and spherical spreading have been subtracted from the attenuation measured in 1/3 octave bands for distances of 110 m and 615 m. The numbers on the curves indicate the vector component of the wind velocity in the direction of propagation in m/s. All curves are for neutral conditions of temperature except for those marked L, which are for lapse. [Piercy et al., 1977]

It can be seen in Figure 2.11 that the refraction effect at a distance of 110 m starts at 400 Hz. The reason that sound enters the shadow zone is not fully understood, but one theory is that the shadow boundary wave is diffuse and therefore a significant amount of sound energy enters the shadow zone by turbulent air flow. In a non-turbulent atmosphere condition the SPL inside the shadow zone is attenuated well more than 30 dB SPL. Close to the ground, the atmosphere condition is always turbulent because of ground friction. The turbulence wind diffuses the sound wave and changes the direction of propagation. The wave that enters the shadow zone is considered as a creeping wave while turbulent air flow is present. The creeping wave will by them self also be refracted and therefore parallel to the other refraction waves. [Embleton, 1996]

Oblique- and crosswind The effect of oblique- and crosswind on acoustical wave propagation in inhomogeneous atmospheric conditions are rarely studied. The author in [Piercy et al., 1977] explain that the refraction is directly zero when only crosswind is present, and increase progressively as the direction of propagation deviate from the angle of crosswind. The author of [Crocker, 1998] support this theory for inhomogeneous atmospheric condition.

Since the effect of oblique wind on a line source array speaker is rarely studied, a measurement in windy condition is performed. The measurement is performed over mown grass in a large open area used for football. The used measurement technique is done according to [Gunness, 2001] where more than one impulse response is measured, and average by alining the impulse response. The wind was considered as healthy for an outdoor concert. The wind speed was measured to 14 m/s doing the full measurement. The measurement was done with a four element line source array 1.1 m above the ground. There were used two microphones, where both were situated 25 m from the speaker in the first measurements and 23 m from the speaker in the last measurements. While changing the distance, the angle to the speaker was changed. The frontal direction of the speaker was placed orthogonal to the wind direction, and the microphone was placed on both side of the speaker as shown in Figure 2.12

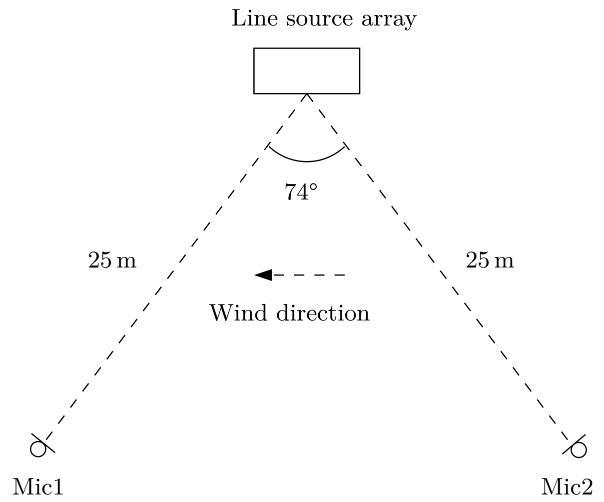

Figure 2.12: The figure shows the microphone position versus the position of the line source array angle of main lobe

The measurement was done with sine swept and according to the description in Appendix A. The measurement was performed with two microphone positions, two measurements where the microphone are within the speaker high frequency directional angle and three outside the speaker high frequency directional angle. The first measurement is shown in Figure 2.13. The other four measurement result can be seen in Appendix A. They show the same tendency, but the difference between the measurements are more drastically in the measurement where the microphone are situated outside the high frequency directional angle.

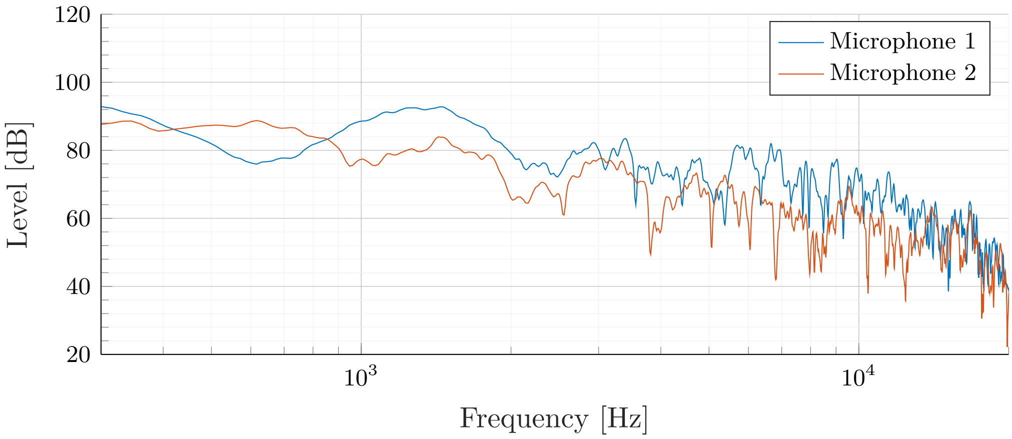

Figure 2.13: The graph shows the first transfer function measurement within the high frequency directional angle. The L_{eq} SPL different between the microphones is 4.41 dB SPL (IR_3)

It can be seen in Figure 2.13 that the general SPL is higher for microphone 1. Furthermore, microphone 1 also shows the typical downwards refraction ground reflection interference in the frequency response which is very similar to the calculated ground reflection interference in [Piercy et al., 1977]. Microphone 2 does not have the same strong interference in the low frequency and the general SPL is lower than microphone 1. This difference indicates upwards refraction in the direction of microphone 2 with only a small amount of ground reflection. The resulting L_{eq} SPL difference for all measurement is shown in Table 2.1.

Table 2.1: The table shows the measured L_{eq} SPL for all measurement and the difference between the microphone

Measurement number	Mic 1 L_{eq}	Mic 2 L_{eq}	Difference
Measurement 1 Figure A.4	71.82 dB SPL	66.33 dB SPL	5.49 dB SPL
Measurement 2 Figure A.5	69.09 dB SPL	64.69 dB SPL	4.40 dB SPL
Measurement 3 Figure A.6	67.67 dB SPL	63.44 dB SPL	4.23 dB SPL
Measurement 4 Figure A.7	68.10 dB SPL	63.69 dB SPL	4.41 dB SPL
Measurement 5 Figure A.8	68.44 dB SPL	63.62 dB SPL	4.81 dB SPL
Average	69.02 dB SPL	64.35 dB SPL	4.67 dB SPL

As it is shown in Table 2.1, the L_{eq} SPL is higher for microphone 1 in all measurement. Moreover the average L_{eq} SPL difference is 4.67 dB SPL while for A-weighted L_{Aeq} SPL the average difference is 6.17 dB SPL.

With respect to the intelligibility frequency range, a weighting filter is designed to observe the SPL differences in the critical intelligibility frequency range. The filter is based on the founded intelligibility frequency range in [Letowski and Scharine, 2017]. It is shown in [Letowski and Scharine, 2017] that the critical intelligibility frequency range lays between 1.0 kHz and 4.0 kHz. The designed intelligibility weighting filter is an 8^{th} order bandpass filter with lower crossover frequency at 1.0 kHz and higher crossover frequency at 4.0 kHz. The resulting average difference is 7.88 dB SPL and the maximum difference is 9.95 dB SPL.

Turbulent Turbulence is an atmospheric condition where the wind eddies. It often starts with large eddies and progressively brakes down like a cascade effect to smaller and smaller eddies which only depend on the local region. When the eddies are as small as 1 mm the energy disappears in viscosity and thermal conduction. A statistical distribution of the eddies is defined as turbulence. The turbulence wind flow is, therefore, a chaotic and stochastic process by nature and is present all the time. It can occur because of change in landscape, stage and blockage, but can also be a process of flow speed increase in the wind, which make the wind to refract on itself. Turbulence is often high on a windy afternoon day and low under the inverse of lapse. Turbulence also often occurs near the ground because the ground surface slows down the speed of wind by the friction to the ground. The effect of turbulence on sound is known to make phase and amplitude fluctuation of pure tone. The fluctuation increases with distance until the standard divination of the phase fluctuation is comparable to 90° [Piercy et al., 1977]. At this point the phase correlation for each sound path is uncorrelated

Chapter 3

Summary of Problem Analysis

The analysis started addressing the generally used method for a live concert. It is founded that live concert today use line source array system to cover the audience area with sound. The line source array is flown above the audience at the main stage, and the delay speaker covers the back audience at a large concert. The line source array is constructed of many identical speakers attached to each other in a vertical line. Moreover, the distance from the speaker to the individual audience depends on the audience position. The analysis founded that a homogeneous SPL among all audience might not possible but the SPL among all audience can be optimised by knowledge of the condition of the atmosphere and gain up for the spreading lose. The author observes that the wind does have a frequency and distance-dependent effect on sound propagation, for example at high frequency the high frequency attenuate audibly in the crosswind. The high frequency blows away for periods and comes back again. The analysis of sound from a line source array started by the ideal geometric spreading loss. Here it is founded that the sound propagation of the line source array highly depends on the hight of the source. The line source array propagates differently with respect to frequency. At a certain hight of the line source array the propagation is a cylindrical propagation until a certain distance from the source where it starts propagating as a spherical source. In the cylindrical propagation, the sound field is defined as near-field while in the spherical propagation the sound field is defined as far-field. In the non-ideal scenario, the line source array propagates in inhomogeneous atmospherical condition. To cover the inhomogeneous atmospherical condition, the local homogeneous atmospherical condition is analysed. In the homogeneous atmospherical condition, it is founded that the temperature, humidity, pressure and wind influence the sound field. The effect of temperature and humidity is close coupled on sound propagation. When the temperature is high, and the humidity is low the air has a significant high frequency absorption whereas when the temperature and humidity follow each other, the absorption is less. The second effect the temperature and humidity have on sound propagation is the speed of sound. The higher the temperature is, the higher the sound of speed. The humidity affects the speed of sound the same way as the temparature, but the increase is negligible compared to the temperature. The effect of wind seems to have a sparse effect on the sound propagation when and only when the wind is homogeneous. It is founded that the speed of wind affects the speed of sound. If the wind moves in the direction of the sound propagation the wind speed is an addition to the speed of sound. In the opposite wind case, the speed of sound is lowered. In the case of oblique- or cross-wind, the effect seems to be unclear for high frequencies. One author has simulated a low frequency spherical source and founded that the only effect is the time of arrival to the audience. The impact of the atmospheric pressure is small, and the pressure close to the ground is so high that other limitations of wave propagation limit the SPL before the negative amplitude riches vacuum in the condensation. When the wave compresses the air, the wave travels faster such that the received wave at the audience is a sawtooth wave. The effect produces harmonic distortion where some of the harmonic energy is attuned be the viscous losses. The harmonic distortion is present in SPL lower than 120 dB SPL but is not as critical as the distortion created by the construction of the speaker enclosure. The audience area is assumed to have high absorption in frequency above 1.0 kHz, while frequency in octave band 31.5 Hz is assumed to have low absorption of the audience.

In the inhomogeneous atmospherical condition, it is founded that refraction of the sound wave is one of the biggest challenges for an outside sound concert. The refraction occurs because of inhomogeneous speed which is present in both inhomogeneous wind and temperature. It is further founted that the refraction is frequency dependent and distance dependent. The effect, however, is low at a distance lower than 50 m with a wind speed of 5 m/s. Depending on the atmospheric condition two kinds of refraction was founded, upwards and downwards. Upwards refraction produces a shadow zone where turbulent atmospheric condition makes creeping wave intro the shadow zone. For the case of oblique and crosswind the effect of high frequency, the refraction might be zero at direct crosswind but increases progressively as the direction of propagation deviate from crosswind. One measurement was done to research the effect of crosswind on a line source array. It was founded that the average L_{Aeq} SPL at microphone 1 was 6.17 dB SPL higher than microphone 2. Therefore it can be concluded that the crosswind with respect to the speaker coverage area does affect.

Chapter 4

Problem statement

Based on the knowledge founded in chapter 2 and the conclusion drawn in chapter 3 a problem statement can be made. For the rest of this theses, the following will be the focus.

Is it possible to control the speaker directivity such that the average SPL over the speaker coverage area is more homogeneous in cross- and obliquewind condition

4.1 Delimitation

The following delimitations are made for the rest of the project:

- It is chosen to work with mono line source array since the number of line source array element is limited to six pieces.
- Due to the amount of needed audience to the research, the homogeneous SPL is searched over mown grass without the audience.

Part II

Test Design

Chapter 5

Preknowledge of outside measurement

5.1 Measuring in inhomogeneous atmosphere

This section aims to gain pre-knowledge about outdoor measurement, such that effecting inhomogeneous condition doing measurement is controlled. Outdoor measurement has two primary sources of disturbing, which is present at concert area distances. At a concert, the area might be surrounded by buildings or other non-horizontal reflection surfaces. Those surfaces are excluded in this explanation. The first primary sources of measurement disturbing are ground reflection. The ground reflection is covered as the first part of the chapter. The second sources for measurement disturbing are wind noise, which has to be controlled doing the measurement to gain measurement of the line source array and not the wind noise. The explanation starts with the former.

5.2 Ground reflection

Ground reflection is a reflection of the sound by the ground surface. The ground reflection is present while the source is above the ground or downwards refraction is present. In a measuring system with a microphone, the ground reflection is present at the microphone while the microphone is lifted from the ground or downwards refraction is present. A ground reflection of sound gives a time receiving difference at the microphone of the same signal while the direct sound path is different from the ground reflected sound path. The following Figure 5.1 shows a block diagram of the sound path with the presence of ground reflection.

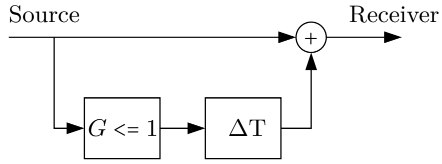

Figure 5.1: The figure shows a block diagram of ground reflection from the source to the receiver

As shown in the block diagram in Figure 5.1, the delivered SPL to the receiver depends on the delta time between the sound path and the ground reflection attenuation of the sound. The case where $G = 1$ is never true because it requires that the reflecting surface is 100 % reflecting and the source is an infinity high and wide source such that the attenuation concerning the path distances is zero. In the ideal case ground reflection can at a maximum give the double of power or 6 dB SPL or the sound can entirely be cancelled. The cancelling occurs when the sound path of the ground reflection is half the wavelength longer, one half the wavelength, and so on. The maximum amplification occurs while the sound path from the ground reflection is one wavelength longer, then two wavelengths longer, and so on. Since the wavelength is proportional to the frequency, then if the ground reflects all frequency, the ground reflection gives a comb filter in the frequency response. To calculate the wavelength extension factor with respect to a given path difference in meter, the following Equation 5.1 is used.

$$\text{fac} = \frac{m \cdot f}{v} \tag{5.1}$$

Where:

fac	is the factor of the wave length it gets longer at the given path distance and frequency	[1]
f	is the frequency	[Hz]
m	is the path differences	[m]
v	is the speed of sound	[m/s]

While calculating the factor of the wavelength that its get longer by a given sound path differences, it is seen that the frequency dependent maximum attenuation is present for at all odd doubling frequency above the first maximum attenuation. In the maximum amplification, it is all the even doubling of the first frequency.

5.3 Wind noise

Wind noise is noise produced by pressure fluctuation in turbulence wind flow [Wilson, 2003]. The frequency spectrum of the wind noise is pink. Therefore, the highest frequency component is in the low frequency range. The wind noise, therefore, might not produce any headroom problem in the frequency where refraction occurs, since this is in the middle and high frequency range. The problem with wind noise doing measurement is that the wind noise pressure level in the low frequency can be as high as the microphone or preamp overload. An overload of the microphone or preamp produces distortion in the measurement. Distortion from the preamp is present in all output frequency since the output signal is at the output rail voltage on the preamp. While the maximum rail voltage is attained, the output becomes squared. Microphone distortion is as speaker distortion, The membrane excites its linear excursion range, and the output curve is squeezed. To handle the wind noise, a windscreen can be used. All measurement while the wind is present in this thesis is performed where the microphone is covered with the original belonging windscreen.

Chapter 6

Proposal solution

6.1 proposal of solution to the wind problem

This section aims to propose a solution to the problem founded in the crosswind measurement section 2.3.1 and the problem statement in chapter 4. To be able to find a solution to the problem, the optimal condition is defined in section 6.2. Then a proposed solution to the crosswind is defined in section 6.3 and lastly a proposed solution to the parallel wind is defined in section 6.4

6.2 Optimality condition

To be able to search for a solution and design a test to research if the proposed solution has the which effect on the coverage area, the optimal condition is defined in this section. The optimal condition is as simple as the SPL coverage in the coverage area of the speaker without wind. In other words, the line source array has a frontal horizontal directional angle defined as the -6 dB SPL limit of the main pressure lobe. The line source array main lobe is given in the horizontal degree as an addition of the main lobe from the frontal direction to both side and can both be symmetric and asymmetric, depending on the line source array element. The following Figure 6.1 shows an illustration of the main lobe.

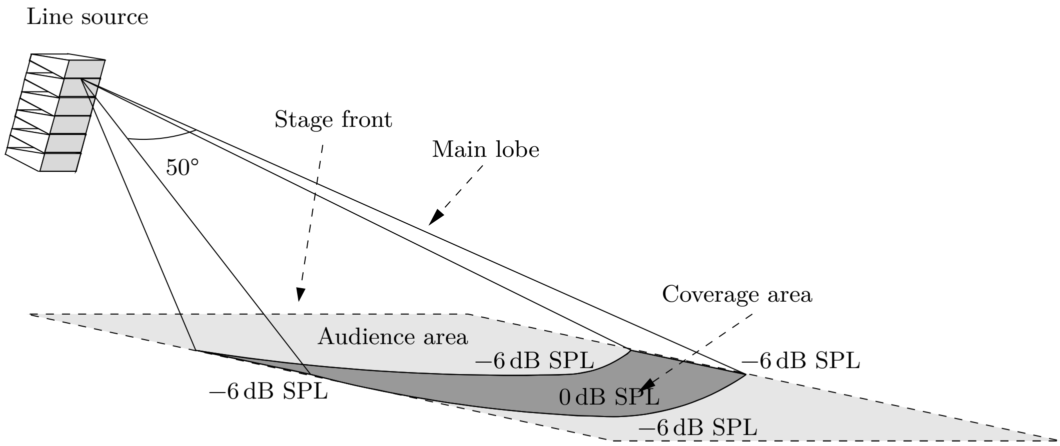

Figure 6.1: The figure shows the pressure limit which defined the main lobe of the line source array and the coverage area without wind

As illustrated in Figure 6.1 the coverage area is a parabolic surface which is limited as the −6 dB SPL coverage limit of the line source array. This is the coverage area with no wind effect and is the coverage area which is defined as the optimal condition. The solution to the crosswind and the parallel wind, therefore, is a way to be able to adjust the coverage area such that the line source array can eliminate the effect of the wind and cover the area as without wind. To be able to eliminate the wind effect at the audience area, audience area have to be defined To defined the audience area, a questioner is made among the large sound rental company in Denmark which ask for audience area to a concert. The questioner is founded in Appendix Q. The gold of the questioner is to find the highest coverage distance from the line source array. The founded maximum distances before delay tower is approximate 60 m, and furthermore, the wind might be stronger than 5 m/s to a concert but wind above 10 m/s to 12 m/s will stops the concert. Therefore the defined coverage area as shown in Figure 6.1 is 60 m from the stage front.

6.3 Proposal solution to crosswind

The crosswind problem is shown in section 2.3.1 to highly modified the coverage area. Agents the wind the upwards refraction is shown to attenuate the sound more than 6 dB SPL A-weighted at a distance of only 25 m and a mean wind strange of 14 m/s. Furthermore, it is founded that the shadow zone SPL depends on the SPL in the sound path, because the wind eddies, eddies the sound into the shadow zone. It is then researched if adding more power into the upwards refraction direction also ads more power into the shadow zone by the wind eddies. The following Figure 6.2 illustrate the eddies theory in upwards refraction.

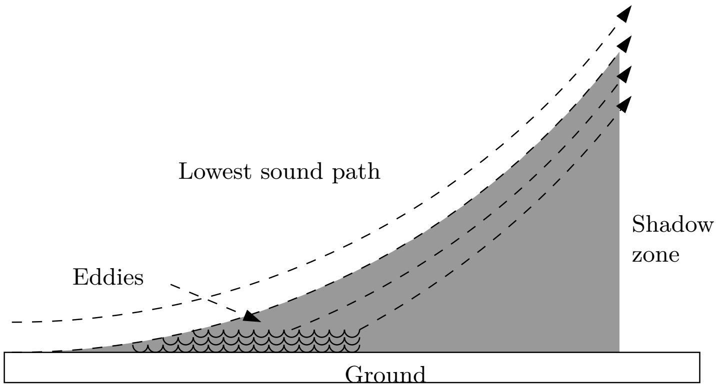

Figure 6.2: The figure shows the sound path above the zhadow zone and inside the shadow zone produced by the eddies

The proposed solution is then to steer more power into the direction of upwards refraction and less power into the front and in the direction of downwards refraction to research the eddies theory shown in Figure 6.2. The following Figure 6.3 shows a graphical illustration of the proposed solution to archive a more homogeneous SPL in the coverage area of the line source array with the wind.

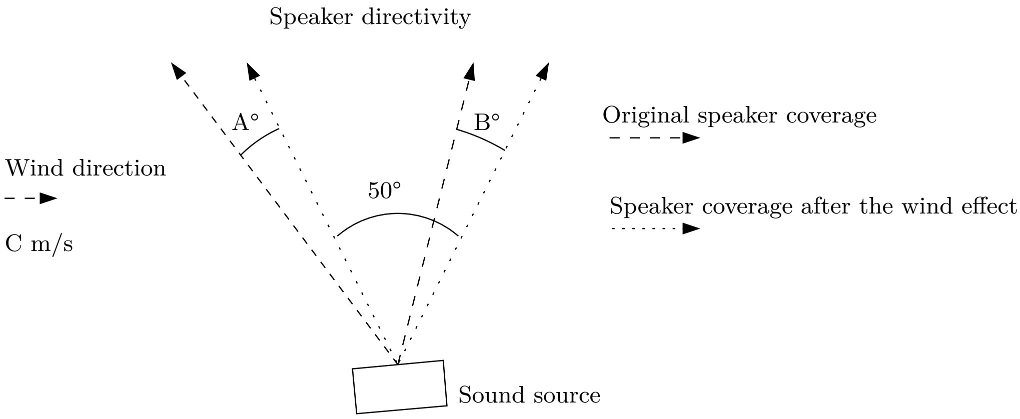

Figure 6.3: The figure shows the wanted direction of the sound coverage area after the effect of crosswind. C is the speed of wind in cross direction of the frontal direction of the speaker. A and B is the main lobe angle that needs to be founded. On the figure the angle are equal but that might not be true

The gold is then to search A° and B° based on wind speed C m/s and the optimal coverage area as shown in Figure 6.3 such that the SPL coverage differences is optimized. As founded in section 2.3.1 the refraction is frequency dependent, therefore, finding the optimal A° and B° might not be possible for all frequency. Furthermore the refraction in the low frequency is nearly zero for the distance present at the concert.

6.4 Proposal solution to parallel wind

The above proposal solution deals with the crosswind problem. When the wind direction change such that the wind comes from the back audiences to the stage, or in other words, is parallel with the frontal direction of the speaker, another theory is research than the eddies theory. The resand to search for another solution is that using the eddies theory in parallel wind require that the power from the line source array is raised. The proposed solution is then to move the shadow zone instead of raising the power in the shadow. To be able to move the shadow zone, the idea is to change the vertical angle of the main lobe, such that the upper speaker ether point more downwards or upwards for upwards refraction or downwards refraction respectively. Therefore if the upper speaker points more downwards the energy from the speaker might arrive at the ground where else if the line source element is pointing parallel to the ground, the energy never enters the ground surface. The following Figure 6.4 shows the proposal solution to parallel wind refraction.

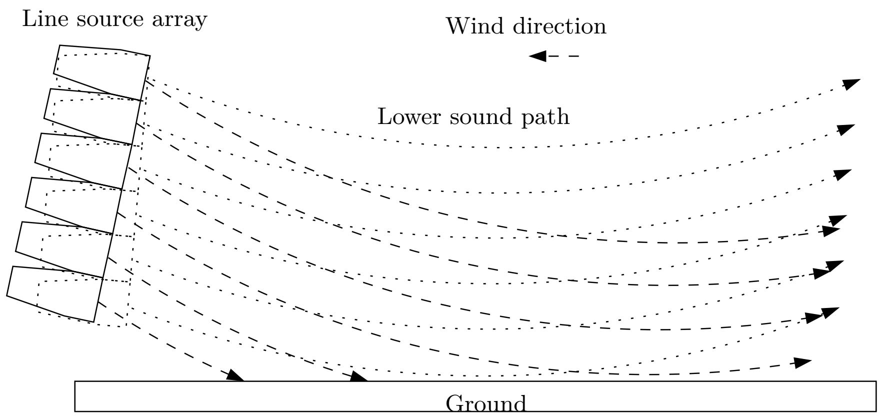

Figure 6.4: The figure shows the proposal solution to the upwards refraction. The non tilted line source array figure shows the lower vertical main lobe ray while the array is orthogonal to the ground where the tilted line source array shows the lower vertical main lobe ray while the line array is angled more downwards

The shadow zone distance is depending on the hight of the line source array from the ground within the limited hight of flying points on the stage. As higher the line source array is flown, as higher the distance is before the shadow zone is present while the vertical angle is optimised to the audience area.

Chapter 7

Test of Proposal Solution

7.1 Test of proposal solution

This chapter aims to design the measurement for the proposed solution. The measurement is based on an L-acoustics KUDO line source array, which is described as the first part of this chapter. Afterwards, the measuring setup for both crosswind and parallel wind is designed based on the used line source array and concert conditions. The second part of this chapter deals with the wind noise challenge in outdoor measurement. The end of this chapter design the measurement software and the needed sensors.

7.2 Description of the used line source array

The description of the used line source array starts with an introduction to the line source element, where the frequency response of the single element is measured as well as the directional characteristics. In the end, the horizontal directionally control, and the vertical directionally control is explained.

The line source elements which is used to test the proposed solution is an L-Acoustics KUDO line source array. This line source array is a legacy long throw variable curvature speaker. This speaker is today renewed and renamed to L-acoustics K2. The line source array can be flown as a vertical line with a maximum of 21 elements. The maximum number of an element is due to the safety limit on the flying tools. One single element have a frequency response from 50 Hz to 18 kHz with a approximatly deviation of ± 3 dB SPL and have a maximum SPL of 140 dB SPL at 1 m. The following Figure 7.1 shows a frequency response measurement of a single KUDO line source element in 50° horizontal angle.

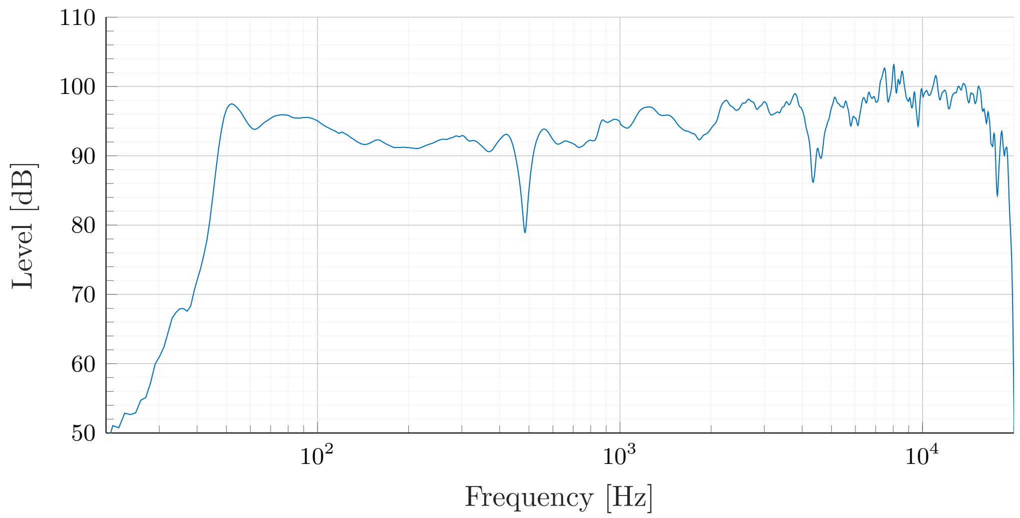

Figure 7.1: The graph shows the frontal frequency response in 50° horizontal angle

This measurement in Figure 7.1 is done in the anechoic chamber at Aalborg University as well as the following measurement in this section. The measurement is explained in Appendix J. The horizontal coverage angle of the L-Acoustics KUDO can be controlled individually on every line source element. The line source element allows both symmetric horizontal coverage and asymmetric coverage. The angle from the frontal direction to the outer main lobe −6 dB SPL is either 25° or 55°. By this two angle for both sides, four coverage angle of the speaker is possible, 110°, 50° and 80° ether to the left or the right. To obtain a better resolution that only the −6 dB SPL the directionality characteristics is measured in all settings. The measurement can be founded in Appendix J . The interesting settings while rotating the line source array is 25° / 25° and 25° / 55° which is shown in Figure 7.2 and Figure 7.3 respectivly.

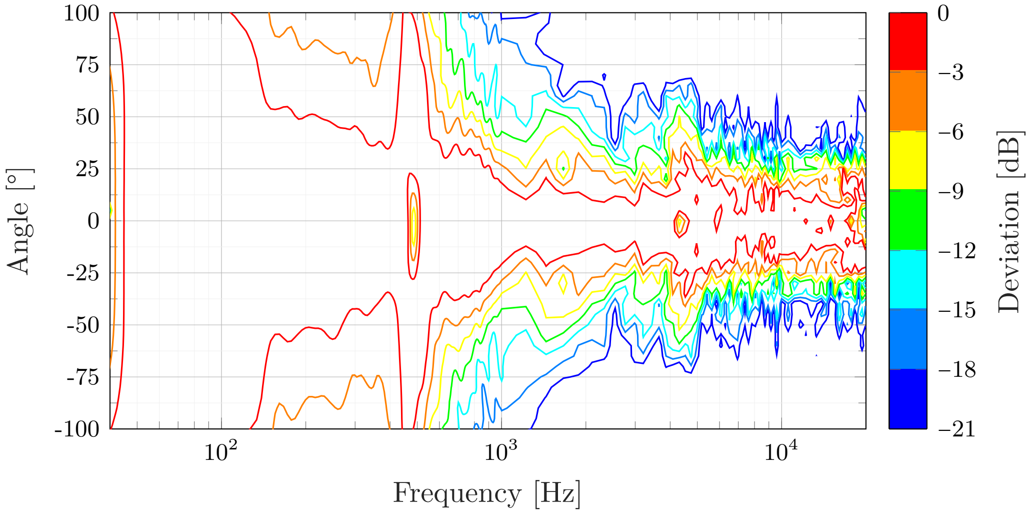

Figure 7.2: The graph shows a contour plot with 3 dB SPL step of the directionally of the L-acoustics KUDO with 25° / 25° settings. The lower black contour line indicate the dBdirectionality for the maximum rotation of the speaker

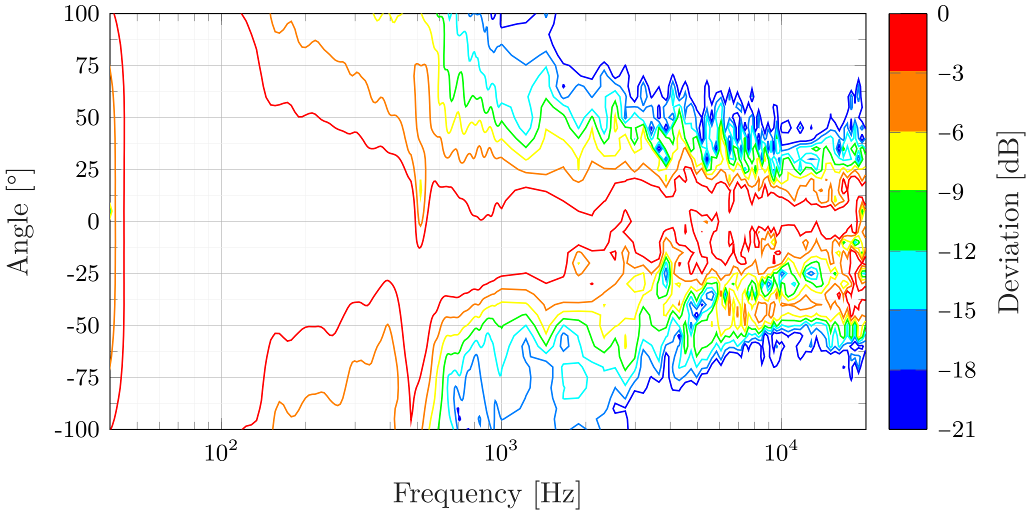

Figure 7.3: The graph shows a contour plot with 3 dB SPL step of the directionally of the L-acoustics KUDO with 25° / 55° settings. The lower black contour line indicate the dBdirectionality for the maximum rotation of the speaker

The mechanical directional characteristics solution in the L-acoustics KUDO as well as other line source array element is not made for wind challenge but for neighbouring disruptions and higher SPL in the main lobe of the high frequency. All solution used today is only possible to be changed by hand and is not electrically controlled. The method for changing the horizontal directivity in the L-Acoustics KUDO line source element is two plexiglass plate fixed to the front grill. The fixing mechanism can be adjusted sidewise by realising two splits on both plexiglass plates. The plate can then be slid along the grill to change the mouth of the speaker output. The following Figure 7.4 illustrate the principle.

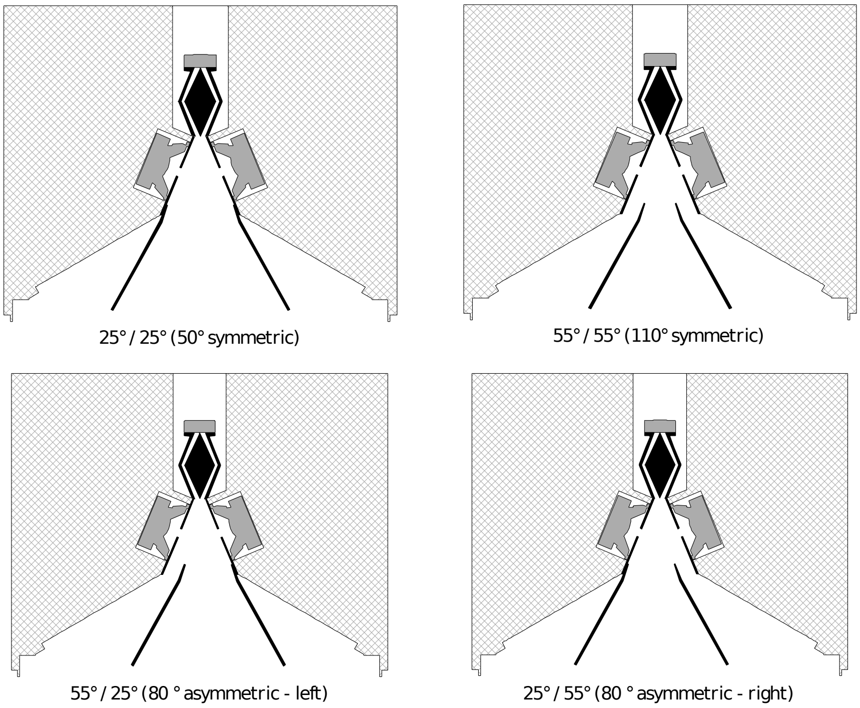

Figure 7.4: The figure shows how the horizontal directivity is controlled on a L-Acoustics KUDO line source array element [L-Acoustics, a].

While the plexiglass plates are in 55° mode as shown in Figure 7.4, the wider directionallity is obtained by soundwave reflection on the plexiglass plate.

The line source array vertically coverage area can be controlled from 0° to 10° with 1° step size. To be able to control the vertical main lobe of the line source array, the mechanical solution is the angle between the line source element. This means that the vertical coverage control cannot be controlled on the individual line source element as the horizontal coverage. To be able to control the vertical coverage, the speaker is trapeze designed such that the high frequency horn throat stays together while the angle between the elements is adjusted in the back of the element. The following Figure 7.5 shows how the line source element are angled vertically.

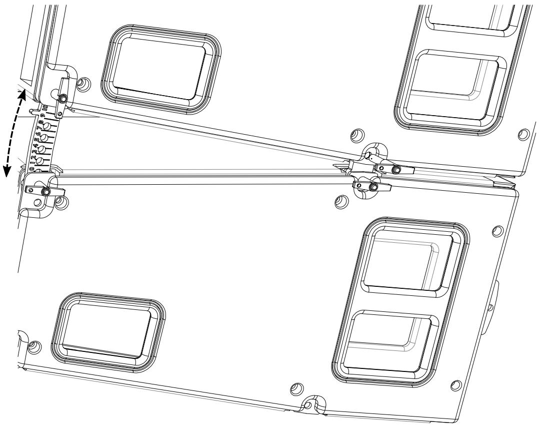

Figure 7.5: The figure shows how the vertical directivity is controlled on a L-Acoustics KUDO line source array element [L-Acoustics, b].

To be able to fix the vertical coverage on the L-acoustics KUDO, the upper left rigging pin shall only be placed into the line source element rig when the angle shown on the metal pease shows the desired vertical coverage angle between two line source element.

7.3 Designing the measurement

This section aims to design a measurement based on the proposed solution section 6.1 and the properties of the used line source array founded in the previous section. The first part of this section gives a general overwrite of the measuring setup. Afterwards, the independent measurement structure is designed for the crosswind and the parallel wind, respectively.

7.3.1 General measuring setup

The line source measurement setup is designed such that the proposed solution can be tested without mechanical change of the line source array. The test setup, therefore, do not change the speaker directionality along with the measurement. Furthermore, the amount of available line source array for the measurement is limited to six line source element. The following Figure 7.6 shows the line source speaker setup and start vertical angling for both the crosswind and side wind measurement.

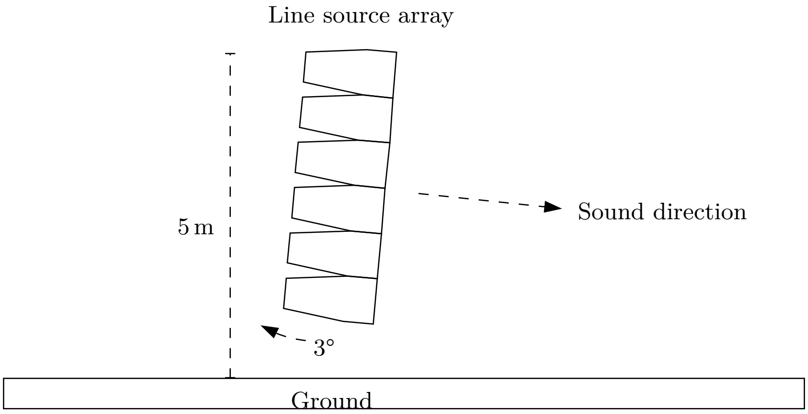

Figure 7.6: The figure shows test setup for both beasurement

The vertical angle between the line source elements is 0° between all element for both the crosswind and parallel wind.

7.3.2 Crosswind line array settings

The idea is to measure the SPL coverage while playing in the frontal direction, and then measure the SPL coverage while the line source array is rotated against the wind. The search is then for the least SPL differences in the coverage area. To be able to ensure that the rotation of the line source array keeps the SPL in the downwards refraction direction as much as possible, this section designs the directional characteristics settings of the line source array doing the crosswind measurement.

It is founded in section 2.3.1 that downwards refraction raises the SPL by downwards reflection but the amplification is much less than the attenuation in upwards refraction and is therefore assumed negligible for directionally chose. Therefore, to decide on the horizontal directionally settings is compared in different settings. The comparison uses the founded characteristics directionally of the line source array in section 7.2 and the crosswind measurement in section 2.3.1

As seen in Figure 7.2, when the speaker is rotated 25° up against the wind, which is the rotation where the maximum SPL is pointed into the outer −6 dB SPL coverage angle of the line source array, the downwards direction is lowered from approximately −6 dB SPL to approximately −18 dB SPL. This rotation occurs an attenuation of 12 dB SPL, which might be too high. While comparing with Figure 7.3 instead, the line source array rotation of 25° only attenuation the SPL in the downwards direction with 6 dB SPL.

To decide on a mechanical solution an example is calculated based on the directionality measurement in section 7.2 and the crosswind measurement in section 2.3.1. The example is based on the optimal rotation for both directionality characteristics, where the difference between the upwards side and the downwards side is smallest. The following paragraph explains and shows the example.

Example The example shows four cases of the L-Acoustics KUDO line source array. One case where the data from the datasheet is used, one case where the measurement in section 2.3.1 is used. Then two examples where the differences in SPL is calculated from an rotation of 20° for 25° / 55° settings and a rotation of 10° for 25° / 25° settings and added to the measurement. The following Figure 7.7 shows the example.

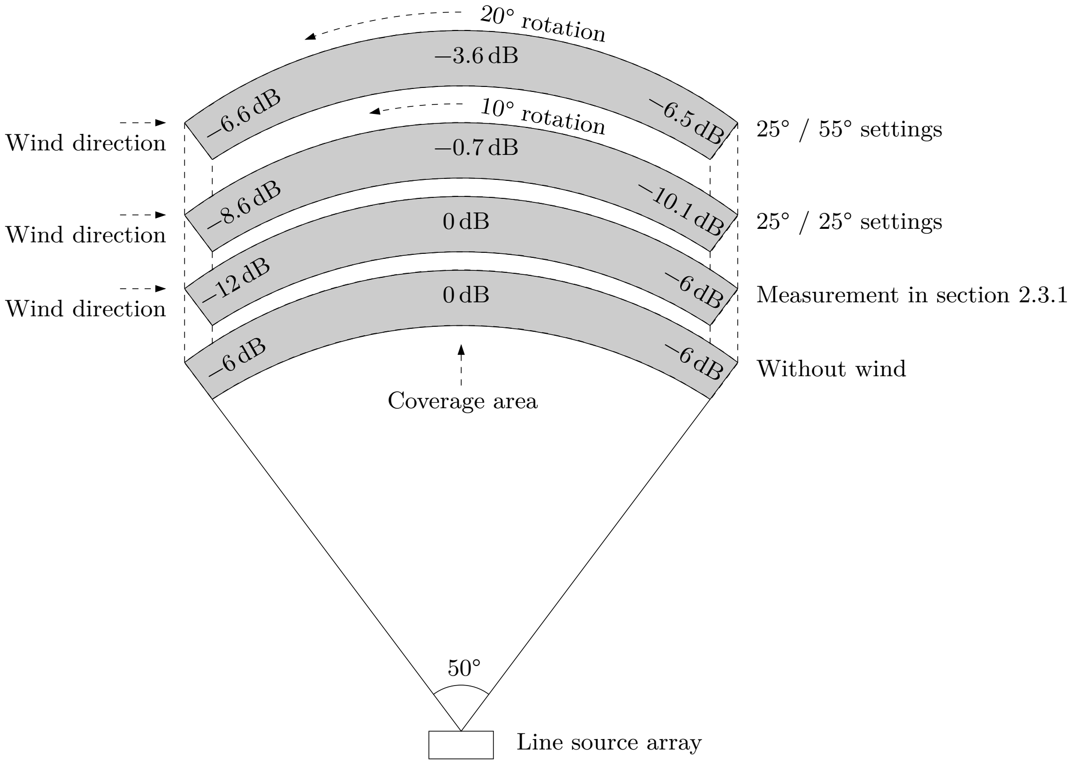

Figure 7.7: The figure shows the main lobe coverage area without rotation in the two lower and with rotation in the two upper

The centre SPL in the measurement in Figure 7.7 was not measured doing the measurement, the stated value is a prediction based on [Piercy et al., 1977] which indicate that the energy addition at short distances because of downwards refraction is small compared to the energy loss with upwards refraction.

As seen in Figure 7.7, a rotational of 20° gives a more homugenius SPL while the line source array is in 25° / 55° settings compare the the symetric settings. The diviation from the frontal direction is approximately 3 dB SPL. In the other case while the rotation is only 10° and the settings is 25° / 25° the SPL is also approximately evently spredt but the divination to the frontal direction is much higher. Based on the calculated example, the chosen directionally settings is 25° / 55° for the measurement. The following Figure 7.8 shows the speaker angle settings for the crosswind measurement as a top wiev.

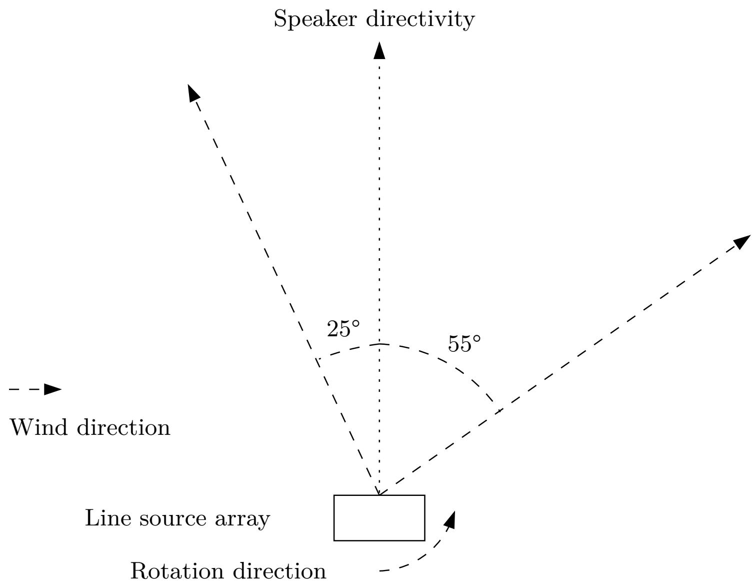

Figure 7.8: The figure shows the line source array setup for the measurement.

The Figure 7.8 shows the speaker settings versus the wind direction.

7.3.3 Parallel wind line array settings

The idea is to have horizontal symmetric coverage while changing the vertical angle for every measurement. The array is tilted some degree until the optimal angle is measured. The optimal angle is the angle where the shadow zone is pushed as far back as possible concerning the wind speed and the hight of the speaker array.

7.3.4 Microphone position at crosswind

The microphone position highly depends on the coverage area of the line source element. The line source element which is flown highest covers the back audience, while the line source element which is closest to the ground cover the frontal audience. Therefore, the distance from the speaker to the microphone has to be found based on the knowledge of coverage distance and the minimum distance before refraction. The distances from the stage to the back audience depends on the size of the concert. For a small concert, the main stage covers the full area where for large concert delay tower helps the coverage. Delay tower is often used for a concert where the distances from the stage to the audience is above 50 m and sometimes up to 73 m as Roskilde festival Appendix Q. The general founded maximum distances from the main stage to the first delay tower is founded to be 73 m for a huge concert, 50 m for a large concert and 30 m for small concert Appendix Q. Concerning the refraction distances it is shown in Table 2.1 that refraction occur at a distance of 25 m with 13 m/s. Base on the knowledge of the maximum distances founded in Appendix Q and the refraction distance, the coverage distances are chosen to be 50 m for the test, since the used line array flying tools is not able to fly the line array as high as the asked companies, and Roskilde festival is an extreme case concerning the size. The flying height of the line source array in the questioner is about 12 m to 16 m where the flying height of the used test setup is only up to 5 m. The hight of the microphone has to be decided based on the audience experience to a concert. To be able to simulate an audience packed area doing the measurement, the following describes the predicted ground reflection characteristics at a concert and how to be able to reproduce it in a measurement.

Along with a concert, the audience head is assumed to be the new ground plane for high frequency. This assumption is based on the high frequency absorption of the audience founded in section 2.2.4. Moreover, it is assumed that reflection occurs at low frequency since the audience absorption drops below 250 Hz. Based on the assumed audience sound reflecting experience, the microphone hight shall optimally be approximately 1.70 m above the ground with a mechanism which blocks for the high frequency reflection. In section 7.3.9 a windscreen is designed with high frequency reflection blockage and wind noise reduction. This method is tested before the final test to ensure that the reflection blockage work as described. Otherwise, the microphone is situated on the ground to eliminate the ground reflection at high frequency. The microphone is placed with an angle of ± 25° from the frontal direction of the speaker as shown in Figure 7.9.

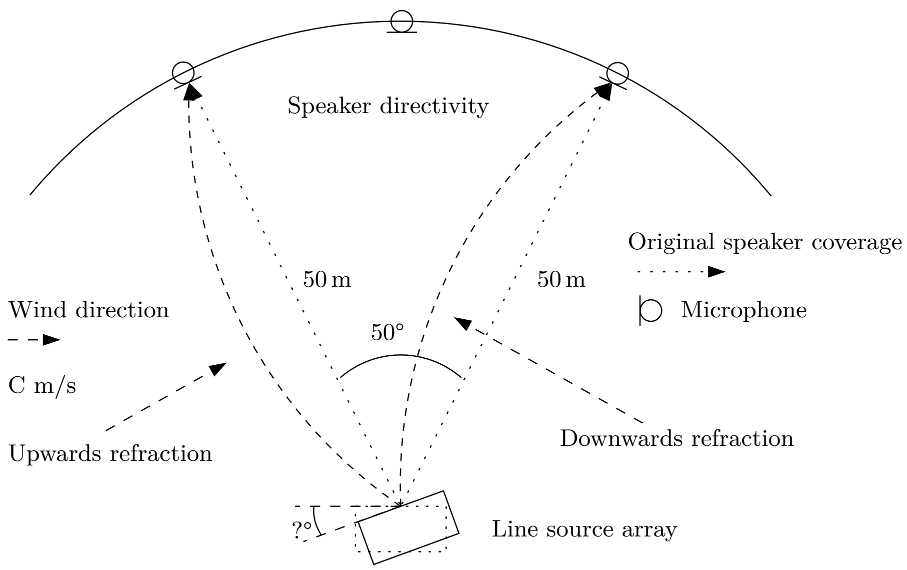

Figure 7.9: The figure shows the measurement setup

This angle is chosen such that the outer main lobe coverage area is measured and because it is the given directionality angle of the speaker at the narrow-angle settings.

7.3.5 Microphone position at parallel wind

The microphone position of the parallel wind measurement depends on the shadow zone position. It is wanted to measure in the shadow zone to explore if it is possible to move the shadow zone backwards by tilting the line array. Therefore, two measuring scenarios are designed. The first is based on a realistic tilt angle to a concert, where the coverage area of the line source array covers the microphone position. The second is based on a tilt angle where the coverage area of the line source array is in front of the microphone. The two scenarios are defined as scenarios one and scenarios two, respectively. By these two methods, the shadow zone is predicted to be present in scenarios one, while the line source array plays against the wind, and in scenarios two the wind refracts the sound wave to the microphone. The following Figure 7.11 shows scenario two.

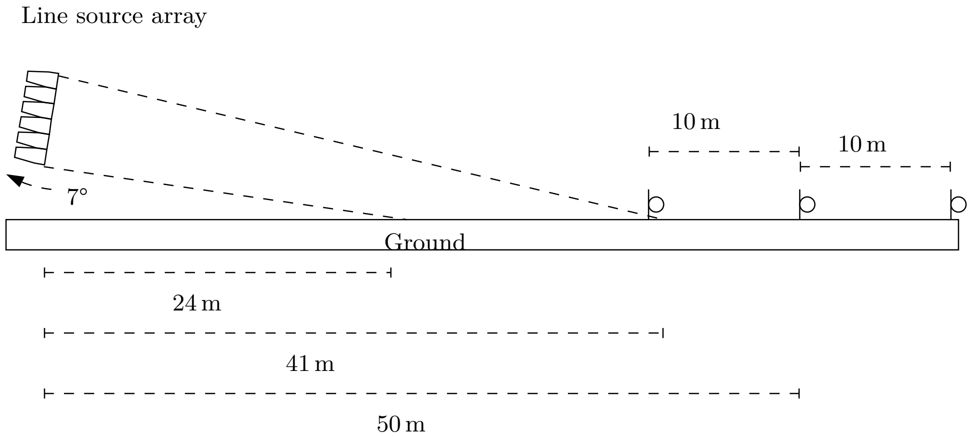

Figure 7.10: The figure shows the measurement setup while the line source array is tilted 7° forward

As seen in Figure 7.10, the main lobe of the line source array is assumed to be near-field, which only held for high frequencies. At a distances of 40 m this illustration covers frequencies above 6.0 kHz, frequencies below will be wider as the frequency drops section 2.1. The illustration illustrates that the highest power of the line source array is within the centre of the main lobe in the frequency of interest due to the directionality characteristics of the line source array. In this case, the microphone should be outside the main lobe while no refraction is present, but as the wave refract, the microphone becomes inside the main lobe.

The following Figure 7.11 illustrate Scenario one.

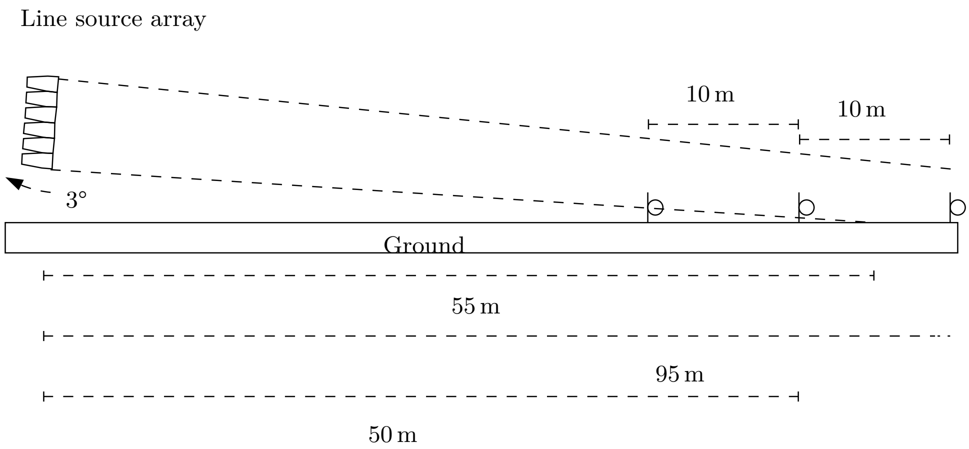

Figure 7.11: The figure shows the measurement setup while the line source array is tilted 3° forward

In the test case shown in Figure 7.11 more SPL is delivered to the centre and back microphone compare to the test case in Figure 7.10 while no refraction is present. While upwards refraction is present, the proposed solution in section 6.4 indicate that the refraction refracts the sound wave such as the SPL distribution is vice versa. The upwards refraction refract the sound wave in Figure 7.10 above the microphone and the refraction of the soundwave in Figure 7.11 refract the soundwave to the microphone. In this test case, the microphone is situated on the ground such that the microphone is as deep in the shadow zone as possible. In other words, as shown in Figure 6.2, while the microphone is positioned in the same distance from the line source array, while the microphone is on the ground compare to lifted above the ground, the shadow zone is most present at the ground. If more SPL is present in the Figure 7.10 compare to Figure 7.11 the shadow zone distance might be able to be optimised.

7.3.6 Sensors and its position

Doing the measurement, the temperature, the humidity and the wind direction and speed is measured. All measurement is done syncronised along with the impulse response measurement. The wind is measured into position since the wind condition is dynamic concerning the area. The wind measurement is done close to the speaker and at the centre microphone both in the crosswind measurement and in the parallel wind measurement. The temperature and humidity are only measured in one position near the line source array since the temperature and humidity are assumed to stable and identical at the measuring area.

Before the measuring system is built, the wind direction is measured to ensure a perfect angle of the speaker. To decide to set up the angle of the measuring system, the wind is measured visually by the directional fan on the anemometer. After the measuring system is built, the anemometer is positioned such that the output angle is ether 90° or 270°. A headroom of 90° before the anemometer goes to ether 0° or 359°. The reason to have the headroom is that the cross point between 0° and 359° is a cross point of the measuring potentiometer where it jumps from maximum value to minimum value. The anemometer is further explained in section 7.4.2

7.3.7 Rotation of the line source array

This section aims to design the turning method for the line source array and ensure that the speaker point in the desired angle. A mechanical solution is chosen for both rotation of the line source array and measuring the rotational angle of the line source array. The mechanical solution to rotate the line source array with a long piece of truss connected to the back of the flying tools of the line source array. By this method, a person can move the other end of truss and stabilise the angle by placing the end of the truss on the ground. Moreover, to ensure that the rotation is as at the specified angle, two laser pointer is attached beneath the line source array — one in the vertical rotation axis and one behind the vertical rotational axis. The one on the vertical rotational axis is then the reference to the back laser pointer. The laser points onto a plate where a rotational angle is given. The following Figure 7.12 illustrate the solution.

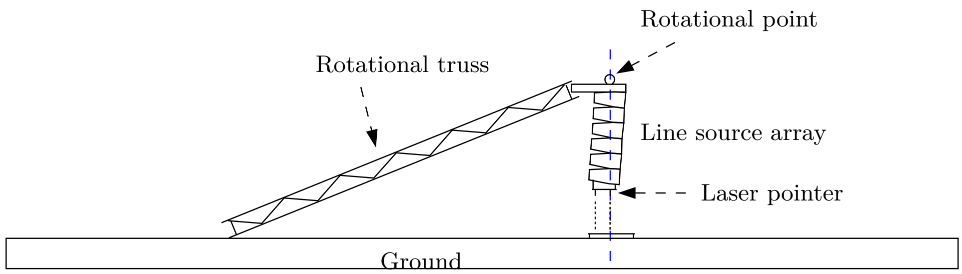

Figure 7.12: The figure shows the rotational mechanic where the blue dashed line illustrate the vertical rotational axis.

In Figure 7.12 the rotation is achieved by moving the ground position of the rotational truss towards the reader or away from the reader. The laser pointer holder and plate for measuring the angle is shown in the following Figure 7.13 and Figure 7.14.

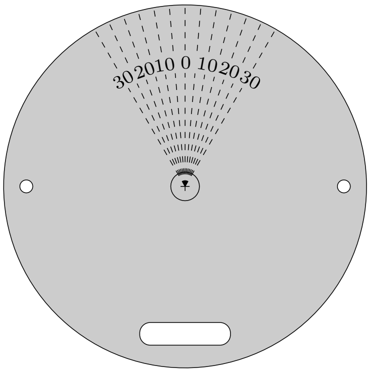

Figure 7.13: The figure shows the angle plate.

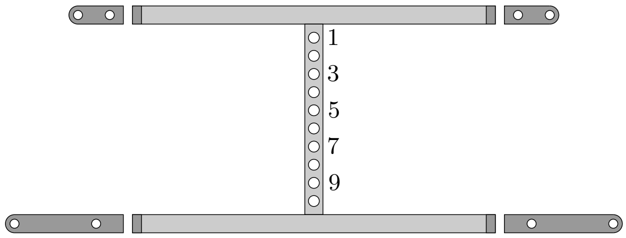

Figure 7.14: The figure shows the laser holder.

The reference laser is guided intro hole 1 in Figure 7.14, which is at the rotational axis while the line source array is tilted 3°. The back laser is guided into hole 10 such that the highest distance between the laser is achieved. The measuring angle plate is then placed on the ground with the reference laser pointing at the centre and the back laser pointing at the 0° angle while the line source points directly forward. By rotating the line source array, the laser point in the back laser is rotated and gives the rotation of the line source array.

In the parallel wind measurement, the reference laser is used to measure the tilting angle. While the line source array is in the 3° general position, the laser pointer point directly down. The backwards movement of the laser point is calculated to be 44 cm from the general position to 7° downwards tilting.

7.3.8 Measuring area and condition

The measurement is achieved in a flat area with mown grass. The optimal area is without any building or trees, but this optimal area is not possible doing the measurement in this thesis. The second best measuring area is a flat area where only a few building is present, and with no forest but three is allowed in a small number of pieces. The mown grass area beside Tryvej 13, 9320 Hjallerup is chosen because it fits the second best description, and the author has a close relation to the owner of the area.

To keep the wind speed realistic for measurement at concert situation, while refraction is present, the wind speed doing the measurement is limited in the range for average 5 m/s to 10 m/s. Less average wind speed than 5 m/s is avoided to ensure the measurable effect of the wind on sound propagation. The higher limit of the 10 m/s is chosen to ensure that the speaker tower is safe at the hight of 5 m. The limited size of the line source array tower setup, makes it wind sensitive. Moreover, no rain is allowed to be present in the measuring day.

7.3.9 Design of windscreen

It is founded in section 5.3 that wind effect the measurement by pink noise. This noise might not affect the measurement headroom in the refraction frequency range, but an overload of the microphone or preamp by the low frequency noise produces distortion which shall be avoided. Secondly, the signal to noise ration shall be sufficiently high in the frequency range of refraction. Therefore, to be able to control the wind noise, this section design the preferable microphone windscreen configuration for the measurement based on the available equipment in the acoustics lab.

Only two outside measuring microphone system with two microphones in all is available in acoustics lab, and therefore a windscreen is designed such three identical windscreens can be made. A research of wind speed attenuation, wind noise and frequency effect is done on serval windscreen concept, which is founded in Appendix B. All windscreen is an addition to the original windscreen which always is present on the microphone.

Based on the finding in Appendix B, the final windscreen optimises the stability of the founded windscreen in Appendix B with a PVC foam mounted on a circular wood plate instead of the Rockwool bat. This configuration shows the best performance in lowering the wind speed near the microphone. Moreover, it is chosen that the microphone shall be at the hight of the ear. Therefore, the wood plate is an additional ground plan added to the bottom of the windscreen to block for ground reflection. The following Figure 7.15 illustrate the windscreen

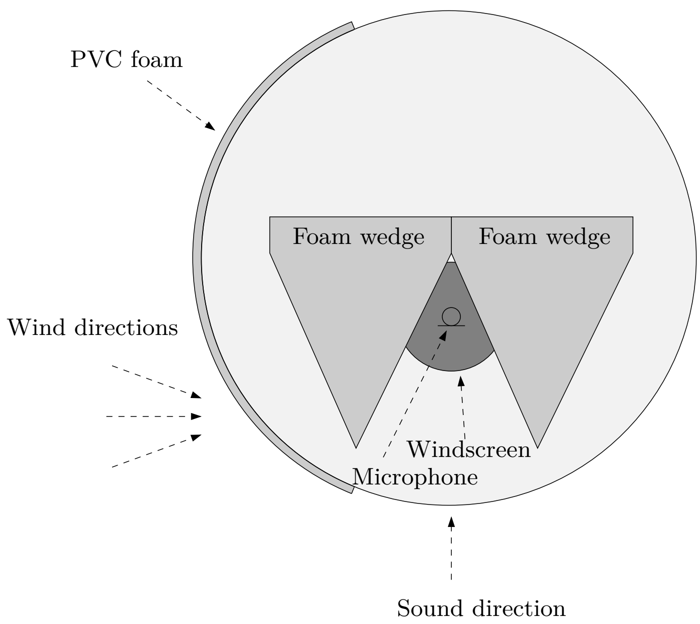

Figure 7.15: The figure shows the final designed windscreen for the measurement

The change from Rockwool bat to PVC foam is made based on the better stability of PVC foam and that the foam wedge is assumed to cancel the reflection from the

PVC foam. While adding the wood plate the original windscreen to the microphone is lifted by 4.5 cm from the wood plate which might result in sound reflection from the wood plate. To eliminate the sound reflection from the wood plate, the technique from wind turbine measuring setup is used, where the windscreen is cut. In the wind turbine microphone setup, the cut is done such that half of the microphone is cut down into the wood plate. In the designed windscreen no hemispheres are available, therefore this cut is not suitable. The cut is therefore made 2 mm to 3 mm beneath the microphone opening of the original windscreen such that the original windscreen fully covers the microphone. The cut is illustrated in the following Figure 7.16.

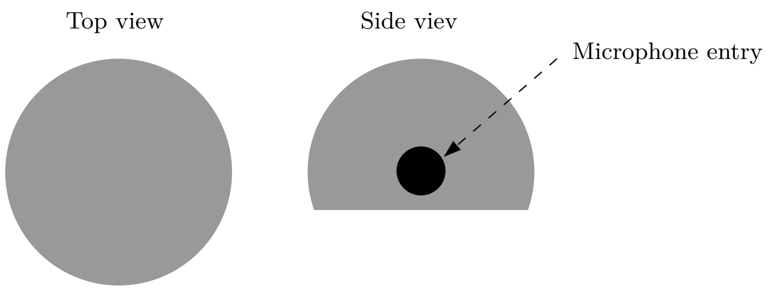

Figure 7.16: The figure shows the modified original windscreen

7.3.10 windscreen wind noise attenuation

This section aims to research the wind noise attenuation produced by the windscreen in real condition to ensure that the wind noise does not overload the microphone. The measurement is done both with and without the designed windscreen to decide if the windscreen works in a real scenario with high speed and directionality changing of the wind. The measurement is furthermore done both in the ear hight and on the ground to research if one position has a better signal to noise ration. The first performed measurement is a series of two measurements, one in the ear hight and one on the ground. Both measurements are performed with the designed windscreen.

The measurement is done in the same vertical, and horizontal angle in two step, first in ear hight then at the ground with the same windscreen. The measurement is done 10 times at each position, such that to measurement with nearly the same wind speed can be compared. The windscreen is placed 90° against the wind, which means that the windscreen is placed in its optimal position where the wind blows directly onto the wide PVC foam plate. The following Figure 7.17 shows the result. Measurement, where the windscreen is rotated is also performed and can be founded in Appendix N.

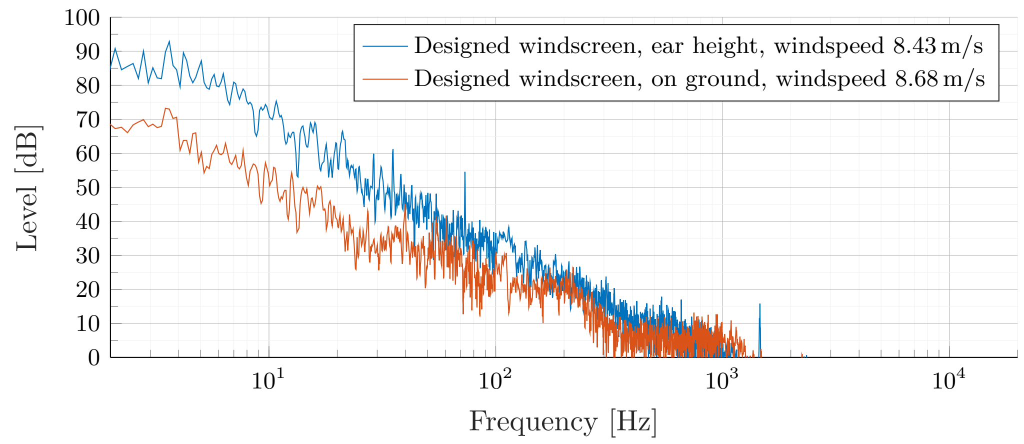

Figure 7.17: The graph shows the frequency content of the measurement with the windscreen in the hight of the ear and on the ground

As it is seen in Figure 7.17, the wind noise highly depends on the hight of the windscreen position. By lowering the windscreen from the ear hight, down to the ground surface, the wind noise is lowered with approximately 20 dB SPL in the low frequency range, which is the frequency area where the wind noise is highest. Furthermore, it is research if the designed windscreen has higher wind noise attenuation compared to only the modified original windscreen. The following Figure 7.18 shows the result.

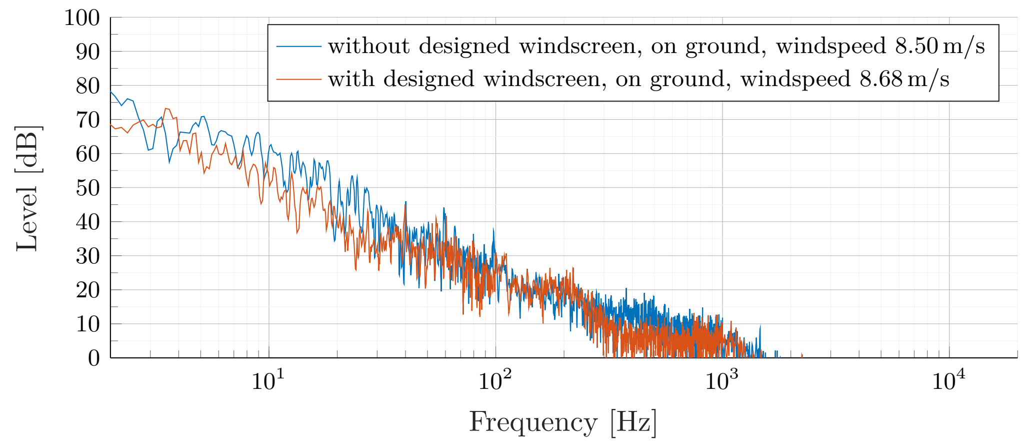

Figure 7.18: The graph shows the frequency content of the measurement with and without the windscreen

As seen in Figure 7.18, the windscreen have generally a 5 dB SPL to 10 dB SPL wind noise attenuation. The measurement description is founded in Appendix N.

7.4 Data logging system

This section aims to explain the measuring software and electronic hardware designed for the measurement. To be able to measure the weather condition, measuring hardware has to be chosen and designed. To be able to transfer data from the weather sensors to the measuring software, a small microprocessor is programmed to read sensor data and transfer the data to the measuring software. This section starts to explain the measuring software and its requirements to the weather data transfer protocol. Then the weather sensors are chosen and firmware is designed to a microprocessor. In the end, the hardware is designed.

7.4.1 Software

This section gives a short overview of the MATLAB®software used for the measurement. The overview does not include any code but only the method of measuring the impulse response and get nearly synchronised data from the serial bus. This section starts explaining the data transfer between the sound card and the computer and the weather hardware to the computer. Both part are connected via Universal Serial Bus (USB) connection. Afterwards, the impulse measuring method is explained.

The data transfer rate between the soundcard and weather hardware to the computer is decided by the buffer length of the audio signal. The audio signal is not allowed to lack while measuring the impulse response. MATLAB®transfer a buffer with audio to the sound card and gets a buffer back with measured signal. The played and recorded signal is syncronised. After the buffer is received MATLAB®have a short period to do calculations, but the calculation shall be finish, and the next audio buffer shall be sent between two samples. The chosen buffer size between MATLAB®and the soundcard is 4096 sample. The following Figure 7.19 illustrate the data transfer protocol.

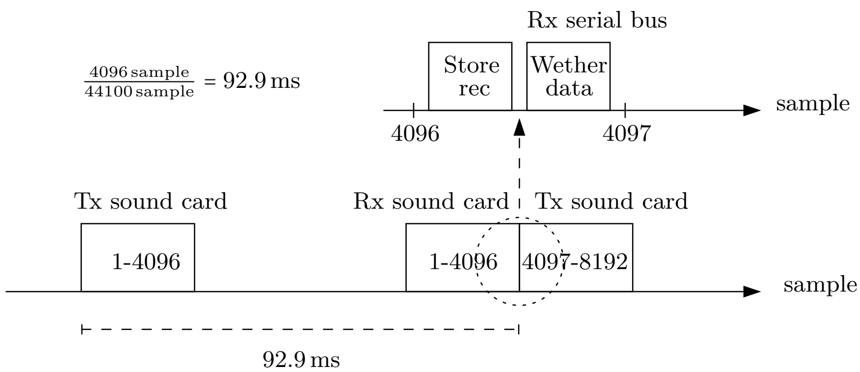

Figure 7.19: The figure shows the transferring samples between the sound card and computer and between the serial bus and the computer. The length of the buffer boxes is just an illustration, the actual length is not measured.

As seen in Figure 7.19, the length of the buffer size limits the amount of weather data. The sound sweep measurement which is explained next is chosen to be 5 s long. This gives 55 weather data measurement point doing the impulse response measurement. All weather information and sound information is stored into a mat file after every measurement such that the analysis can be done offline.

The impulse response is measured with sine sweep according to [Müller and Massarani, 2001]. The method is to deconvolute the measured signal by the reference signal which produces the impulse response of the speaker. In the measuring software, the deconvolution is done in the frequency domain, because it speeds up the calculation. A hanning window windows both the measured signal and the reference signal. To exclude the influence of the sound card, the reference signal is played through one output channel and measured by one of the microphone input. It is assumed that the characteristic of every output and input is equal. To be able to make calibrated impulse responses, the measured reference signal is related to the microphone sensitivity by the following Equation 7.1

$$\mathrm{ref}_s = \mathrm{ref}_m \cdot \frac{\mathrm{mic}_{\mathrm{sen}}}{rms(\mathrm{ref}_m)} \tag{7.1}$$

Where:

ref_s	is the calibrated reference signal	[1]
ref_m	is the measured reference signal	[1]
$\mathrm{mic}_{\mathrm{sen}}$	is the rms sensitivity of the microphone in digital number at one pascal rms	[1]

After the reference signal is related to the measured signal, deconvolution is calculated by calculating the Fast Fourier Transform (FFT) for both signal, divide the measured signal by the reference signal and calculate the Inverse Fast Fourier Transform (IFFT). The result is an impulse response where the amplitude corresponds to a calibrated pascal value of the played time signal. By the impulse response both the l_{eq} and the frequency response can be calculated. The calibrated frequency response is calculated with the MATLAB®function `freqz`. The l_{eq} is calculated with the following Equation 7.2.

$$L_{\mathrm{eq}} = 10 \cdot log10\left(\frac{1}{T} \cdot \frac{\int IR^2}{20\mu^2}\right) \tag{7.2}$$

Where:

L_{eq}	is the calibrated equivalent sound pressure level	[dB]
IR	is the impulse response	[Pa]
20μ	is the hearing threshold level reference	[Pa]
T	is the measured time period. In this case while it is an impulse response, the time period is always set to 1 no matter how long the sine sweep is designed to be	[s]

As an example, if the played signal is from 20 Hz to 20 kHz and it is measured that all frequency is 94 dB SPL, the L_{eq} gives 94 dB SPL.

The measuring software is founded in Appendix I

7.4.2 Sensor and microprocessor

The microprocessor for weather measurement is based on an Arduino UNO. The chose of an Arduino is made because code for both the temperature and humidity sensor and the used anemometer is available on the internet.

The chosen temperature and humidity sensor are an AM2302 because it is available as a component at Aalborg University and it covers relative humidity from 0 % to 100 % and a temperature range from −40 °C to 80 °C which is more than enough of the measurement. The data sheet of the sensor is founded in [AOSONG].

The chosen anemometer is a Davis Vantage Pro2 anemometer. This anemometer is chosen because the connection is direct to the wind speed sensor and the wind direction sensor. The direction sensor is a 20 kΩ 360° potentiometer, where the speed sensor is a contact which makes one short circuit to ground for every rotation. The directional sensor can, therefore, be connected to an analogue input port where the speed sensor is connected to a digital input. The data sheet for the anemometer is founded in [Davis]

7.4.3 Firmware

The firmware is designed to support two anemometers, one temperature sensor and one humidity sensor. The temperature and humidity sensor is one unit and communicates digitally to the Arduino. The communication is done through the dht.h Arduino library. The data is then called from a function of the library, and the author has not designed the digital connection. The anemometer both measure the wind direction and wind speed. The wind direction is an analogue voltage from 0 V to 5 V while the angle goes from 0° to 359°. The rotational angle from the direction sensor increases while the directional goes from south to west, therefore it works in the same direction like a compass. The analogue voltage is measured with the build in 10 bit Analog to Digital Converter (ADC) which gives a digital number from 0 to 1024. This measured number is transferred directly to the com bus without angle correction. The conversion to angle is done in MATLAB®.

The wind speed measurement sensor gives a pulse for every rotation. According to the datasheet of the wind anemometer, one rotation of the wind speed sensor over a time period of 1 s correspond 1.0058 m/s. To be able to measure the wind speed in a higher resolution that 1.0058 m/s the pulses is time average over a defined period. To be able to measure over a period a First In First Out (FIFO) buffer is designed for the pulses as shown in the following Figure 7.20

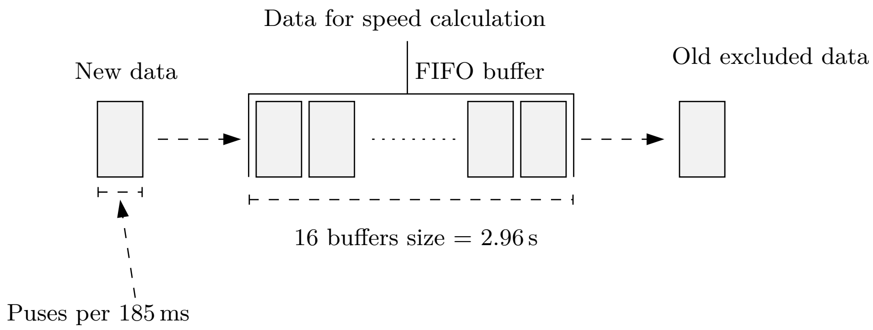

Figure 7.20: The figure shows the FIFO buffer system for wind speed measurement

As seen in Figure 7.20, the update time is for every 185 ms and the buffer contains 16 pieces of 185 ms which gives an average time over 2.96 s. This buffer size gives a wind speed resolution of 339.8 mm/s.

The update time is slower than the data transfer time interval between the Arduino and MATLAB®. This resolution is decided to be sufficient since the mechanic of the speed sensor by itself average the wind speed.

The firmware is synchronised with MATLAB®by adding a delay in the main loop and not tricking on a timer. Therefore, the program runtime is only stable down to ± 3 ms precision with a mean update time for the firmware of 92.3 ms. The mean update time is based on five time measurement with 80 samples in each. The negative shift of the firmware update doing the 55 weather update transferred to MATLAB®gives a lack of −38.8 ms after end measurement. The lack of −38.8 ms is much less than the update of −92.3 ms, which indicate that the time synchronisation lack is less than one sample and no time shift is present. Since the update sometimes is above 92.9 ms the weather updates sample to MATLAB®can be the same twice. This issue is only present in the first 5 samples. After those samples, the lack in synchronisation does that 96 ms is an update before the MATLAB®is ready to receive data from the serial bus.

Based on the above explanation, the following weather data is present in the impulse response measurement, where it shall be noted that within the first few samples, an repetition can occur. This repetition is considered as indifferent, since the first 500 ms is a starting silence period of the sine sweep and frequency below 40 Hz and, therefore, is removed from the data analysis.

- The wind direction is updated for every weather sample.
- The wind speed is updated for every second weather sample.
- The temperature and humidity are updated for every weather sample.
- The MATLAB®software ask in total for 55 weather samples doing one impulse response measurement.

The data transfer is done through the serial bus vis USB connection. The following Figure 7.21 shows a snapshot of the serial bus delivered by the Arduino.

Speed 1	Direc 1	Speed 2	Direc 2	Temp	Hum
5.44	790	6.12	884	21.90	68.90
5.44	791	6.12	882	21.90	68.90
4.42	790	5.78	863	21.90	68.90
4.42	791	5.78	832	21.90	68.90
3.74	790	5.44	820	21.90	68.90
3.74	790	5.44	827	21.90	68.90
3.40	791	5.10	831	21.90	68.90
3.40	790	5.10	832	21.90	68.90

Figure 7.21: The figure shows a snapshot of the serial bus. The first vertical line, which is the left vertical data line is the wind speed of the first anemometer. The second vertical line is the wind direction of the first anemometer. The third vertical line is the wind speed of the second anemometer. The fourth vertical line is the wind direction of the second anemometer. The fifth vertical line is the temperature and the last vertical line is the humidity.

The firmware is founded in Appendix H

7.4.4 Hardware

To be able to connect both the two anemometers and the temperature and humidity sensor to the Arduino UNO an Arduino shield is designed. The shield is designed such that is can be plugged directly onto the Arduino. The following Figure 7.22 shows the schematic of the shield and the Printed Circuit Board (PCB)

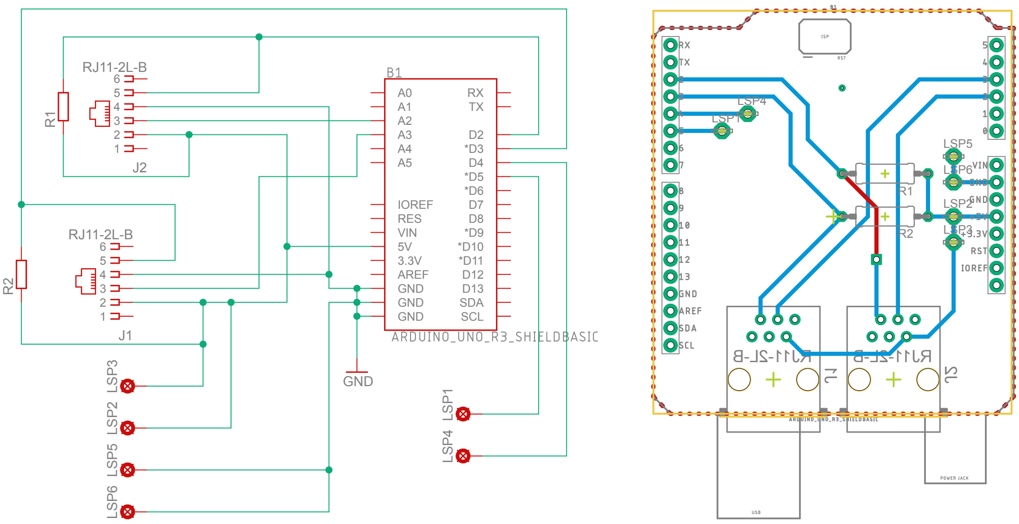

(a) The figure shows the schematic of the shield

(b) The figure shows the PCB layout of the shield

Figure 7.22: Ardouino shield design

The to resistors in Figure 7.22 R1 and R2 is pull-up resistors for the wind speed contact with a resistance of $4.7\,\mathrm{k\Omega}$. While the contact in the anemometer is not shorted, the voltage at the input pin on the Arduino is $5\,\mathrm{V}$. While the contact is shorted the voltage is $0\,\mathrm{V}$. The two RJ11 connectors are for the Anemometer connection. The six test point is soldering connection to the temperature and humidity sensor.

All hardware can be seen in Appendix O

Chapter 8

Test of measuring design

8.1 Test of measuring design

This section aims to test the design measurement in a windy day, to outsource problem and error in the measuring design. The test is done in full scale with all six line source array element and in the designed hight. The test is intended to both test the crosswind measuring design and the parallel wind measuring design, but the wind condition only allowed for crosswind test. After the crosswind measuring design was tested the wind speed dropped to beneath 1 m/s. In the crosswind measuring design, three problems and one code error are observed. The code error is a data save bug, where only the direction of the wind at the line source array tower is saved. The wind direction data at the microphone position is overwritten by the wind direction data at the line source array. The code bug is fixed for the final measurement. The following three section 8.1.1, section 8.1.2 and section 8.1.3 explain the observed difficulties or design failure and propose a solution to them. The first difficulty which is discovered is major ground reflections in the measurement. The second problem seems to be frequency response differences while using the windscreen, where the third error is the angle of the line source array while measuring in the hight of the ear. The explanations is based on the measurement as seen in Figure 8.1 which shows the frequency response on all three microphones at 0° rotation.

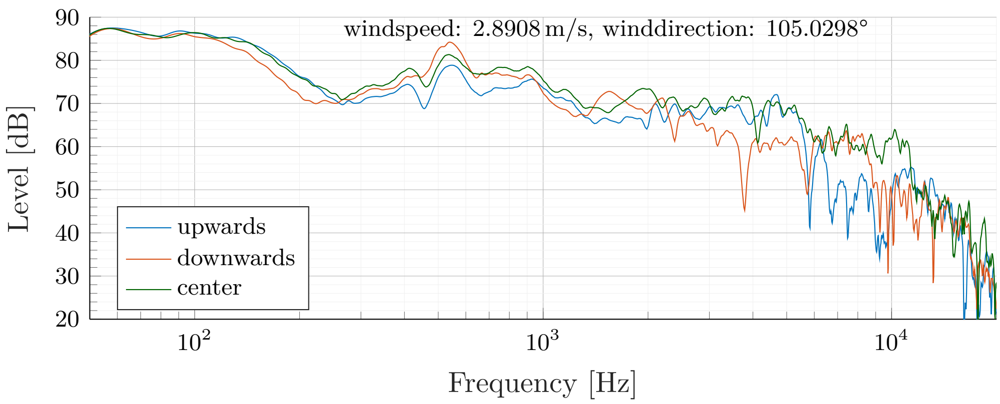

Figure 8.1: The graph shows the mean frequency response of 10 measurement for all three microphone while the speaker is not rotated. The mean is calculated in the time domain by aligning the impulse response with the help of cross-correlation. The wind speed and wind direction is also the mean of the 10 measurements.

To be able to differentiate between the microphone in the explanation, the microphone is named according to the position and the wind direction. In the upwards refraction direction, the microphone is named upwards microphone, in the downwards refraction direction the microphone is named downwards microphone, and the centre microphone is named centre microphone. The following Figure 8.2 illustrate the microphone position versus the wind direction.

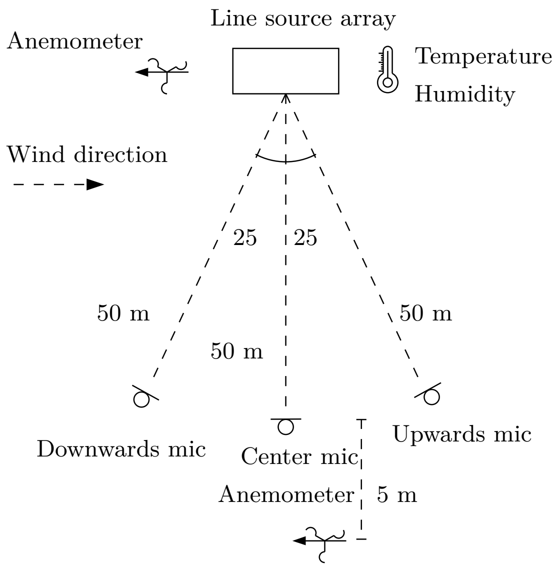

Figure 8.2: The figure shows the microphone position versus the position of the line source array, while the line source array is 0° rotated

In Figure 8.2, the position of the anemometer temperature and humidity sensor is given at its position doing the measurement. Ensure that the measurement is a measure of the transfer function and not the wind noise, a signal to noise measurement is performed as the first part. The signal to noise ration is measured in two ways, one where the wind noise is measured and one where transfer function is measured at high SPL level whereafter the output level of the speaker is lowered by 10 dB SPL, and the transfer function is measured again. While the frequency response in the hole frequency range is lowered by 10 dB SPL, the headroom is at least 10 dB SPL. The noise floor is pink with 70 dB SPL as the maximum at 2 Hz at all microphone position with a wind speed of 5 m/s. All measurement is done with signal to noise ration of more than 10 dB SPL. The signal to noise ratio was visually checked by plotting the measuring result in MATLAB®. The signal to noise ratio measuring is not saved as a file in the test measurement but is in the final measurement.

8.1.1 Ground reflections

One intended outcome of the windscreen is to block for the ground reflection by the circular wood plate, such that the measuring position can be in the hight of the ear, as explained in section 7.3.2. This part of the windscreen fails in blockage all ground reflections in the frequency above 250 Hz as seen in Figure 8.1. The measured depth is not the same as in the directionality measurement of the speaker in Figure 7.3. The centre microphone does not have that high peaks and deeps, but the upwards and downwards microphone seems to suffer from a ground reflection in the high frequency, which makes the refraction comparison between the microphone position difficult. One thing that might cause the reflection is the position different from 0° vertical of the windscreen with respect to the ground. If the plate is tilted forward, there might be some reflection reaching the microphone. A calculation of the reflection might have helped to justify the ground reflection theory, but since the source is a line source array and not a point source, the ground reflection is not as easy to calculate. There might be thousands of sound path from the line source to the microphone where the sound path length is half the wavelength longer. The following Figure 8.3 illustrate the path calculation difficulties and the forward tilted windscreen.

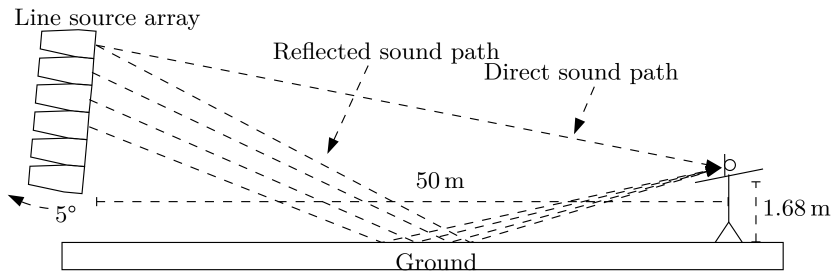

Figure 8.3: The figure shows an illustration of the measured setup and some soundpath

To be able to make a qualified considering to decide if the peaks and depth are due to ground reflection, the measurement is compared to a measurement where the microphone windscreen is situated on the ground and the frequency characteristics in the measuring direction in Figure 7.3. It has to be noted that the windscreen has a speaker stand connector mounted underneath, which lift the centre of the designed windscreen such that the windscreen cannot lay flat on the ground but is tilted forward. The windscreen was tilted forward by a maximum of 8° or less doing all measurement on the ground in all microphone position. The following Figure 8.4 shows a frequency response at all three microphones position of the line source array, where the windscreen is placed on the ground and with a non-rotation line source array.

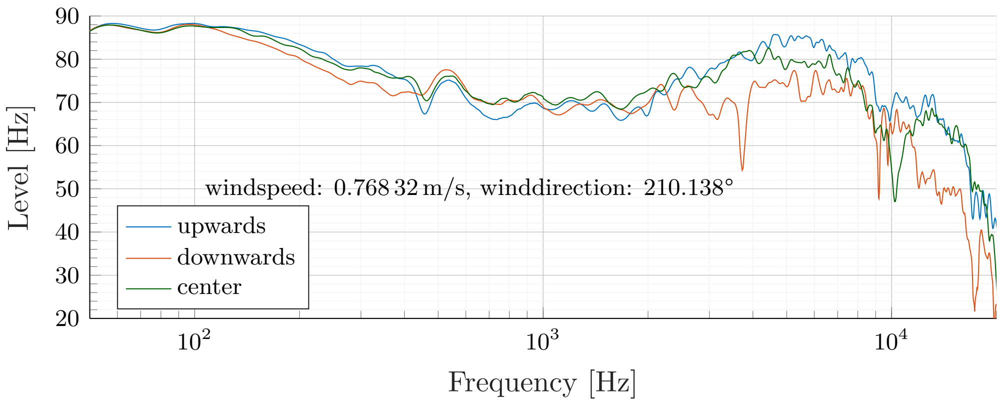

Figure 8.4: The graph shows the measuring result along with all three microphones, while the microphone is in the windscreen and the windscreen is on the ground. The graph is a mean of three measurements for the upwards and downwards microphone and one measurement for the centre microphone. The mean calculation is done in the time domain where all impulse responses are aligned with cross-correlation

The frequency depth seen at 3.7 kHz in the downwards direction is due to the directionality characteristics of the line source array and can also be seen in Figure 7.3. The same applies to 9.2 kHz and 10 kHz

Comparing the measurement where the windscreen is lifted 168 cm from the ground in Figure 8.1 and the measurement in Figure 8.4, it is seen that the first ground reflection comes around 250 Hz depending on the microphone. This ground reflection is dB wise even for all microphone position and might, therefore, be due to sound wave travels through the windscreen bottom plate. The following arriving ground reflection depends on the microphone position and then might be due to the vertical angle of the designed windscreen. For the upwards microphone, there seems to be highly reflections in the frequency area from 5.5 kHz to 9.5 kHz where comb filtering is present. Another common response on all microphone while the windscreen lays on the ground is depth around 10 kHz. This depth might be due to the lift of the microphone while it is within the modified original windscreen or that the windscreen is tilted forward. Based on the founding in the measurement, ground reflection occurs in the measurement.

8.1.2 Frequency differences

Doing the measurement, a frequency differences between 2.0 kHz and 10 kHz is observed in some measurement and is researched in this section. The frequency differences are observed while the microphone is laying on the ground with and without the windscreen. Furthermore, the wind doing the measurement is less than 1 m/s and therefore, refraction is assumed to be low. A comparison measurement is done, where the windscreen is removed from the centre microphone since the wind stopped at the end of the measurement. The following Figure 8.5 shows the measurement result for all three microphones with windscreen and two measurements where the windscreen is removed from the centre microphone.

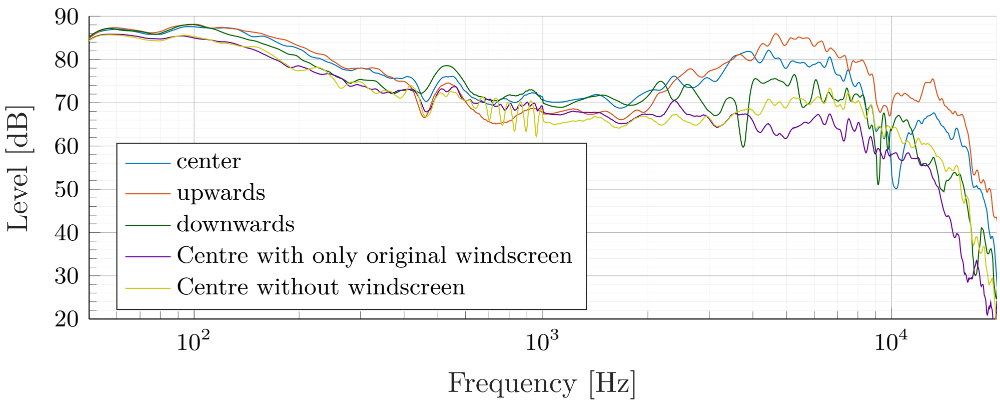

Figure 8.5: The graph shows the measuring result along all three microphones, where one of the measurements for the centre microphone is done with designed windscreen setup and two measurements is done without the design windscreen setup. While the microphone is in the designed windscreen, the designed windscreen is on the ground. While the microphone is outside the design windscreen, the microphone lays on a wood plate with the same size as the designed windscreen.

It is seen in Figure 8.5 that the depth at 10 kHz is gone for the centre microphone without the designed windscreen, but the frequency response at the centre and upwards position is generally higher than the other three measurement. The measurement is done with less than 1 m/s of wind speed, and therefore, refraction is assumed to be excluded as a factor of differences. This means that the differences in the windscreen setup might influence the frequency response. Three mechanical differences are observed on the windscreen setup doing the measurement. The first is the vertical angle of the windscreen, which was different along with all designed windscreens doing the measurement because the ground is uneven. The ground unevenness is measured afterwards to a maximum of 8°. Secondly, the rotational angle of the designed windscreen was also different, along with all designed windscreen. The rotational angle is defined to be 0° to the line source array while the line source array points directly into the centre of the windscreen opening, as shown in Figure 8.6.

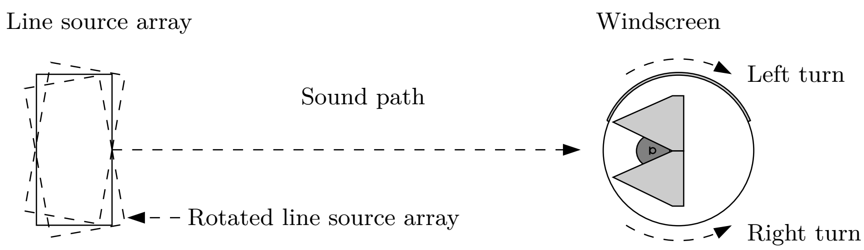

Figure 8.6: The figure shows an illustration the windscreen vertical 0° angle

As illustrated in Figure 8.6 no matter the tournament of the speaker, the opening shall point directly to the speaker. In the measurement, the opening was not pointing directly to the speaker. The vertical angle was adjusted with depends on the wind direction, this means that the windscreen at downwards direction is turned left, where the windscreen at upwards direction is turned right.

The last differences were the placement of the foam on the plate. In the downwards direction the foam is placed more inwards to the centre of the plate while the foam on the other two designed windscreen was placed as shown in Figure 8.6

8.1.3 Speaker angle

The angle of the line source array was calculated while the measurement setup was built. In the calculation, the wrong microphone reference point was used. The microphone position which was used in the calculation was while the microphone on the ground and not in the ear hight and therefore, higher tilt angle was calculated. The measuring angle should have been the given angle in section 7.3.1 where the near-field covers both at the ground position and the ear hight position in the distance of 50 m but the angle was calculated to 5.7° and the line source array was tilted to 5°. The following Figure 8.7 shows the microphone positions.

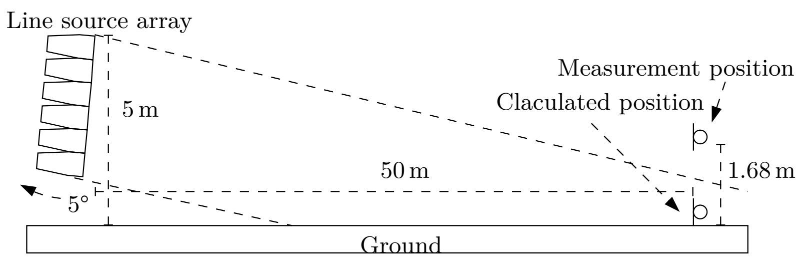

Figure 8.7: The figure shows the microphone position doing the calculation of the line source array tilting and the measurement

While using the 5° tilt angle doing the measurement, the hight before the microphone exit above the near-field of the line source array coverage main lobe is calculated to be 63 cm. Therefore, since the microphone was placed 1.68 m above the ground, the microphone is fare above the near-field. Comparing the Figure 8.1 and Figure 8.4 it is clearly seen that the microphone is outside the near-field of the high frequency. Above 2.0 kHz, the SPL is more than 10 dB SPL lower in the ear measuring hight compare to the ground position with the same distances to the speaker.

8.1.4 Measuring result

While all error and difficulties are described and is known to disturb the measurement, the measurement indicates that raising the power in the upwards direction, also raising the power in the shadow zone. Comparing the microphone against each other is difficult since the differences in the frequency response between the microphone as described above. Therefore, to extract useful data, the frequency response on the same microphone is compared for 0° of tournament, 10° of tournament and 20° of tournament. The first microphone which is compared is the microphone in the upwards direction. The following Figure 8.8 shows the frequency response for every tournament.

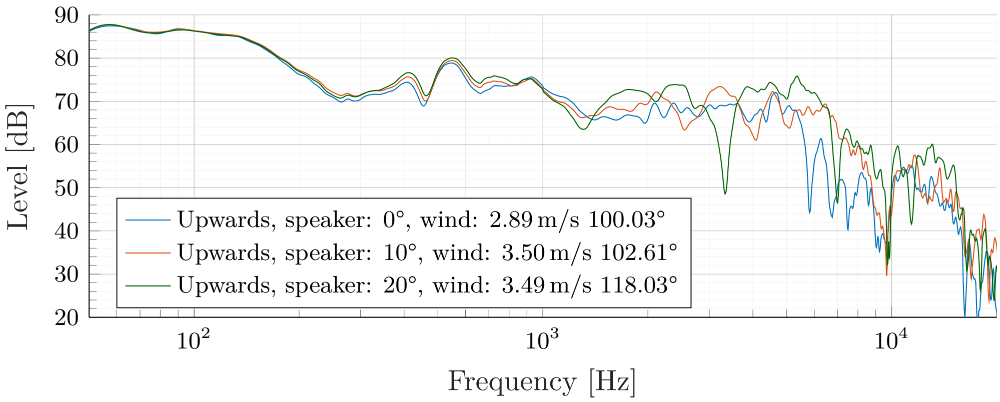

Figure 8.8: The graph shows the measuring result for the upwards microphone in three line source array rotation, while the microphone is in the windscreen and the windscreen is in the hight of the ear. The graph is a mean of 10 measurements in all three angles. The mean calculation is done in the time domain where all impulse responses are aligned with cross-correlation

As seen in Figure 8.8, while the speaker is turned towards the upwards microphone, the SPL is raised. The peaks and depth are not at the same frequency, which makes the visually evaluation difficult, but it visually shows that turning the speaker raises the SPL in some frequency area, especially above 1.0 kHz. The following Table 8.1 shows the single number SPL both non weighted and A-weighted.

Table 8.1: The table shows the measured L_{eq} and $L_{\mathrm{A_{eq}}}$ SPL for the upwards microphone

Speaker angle	0°	10°	20°
L_{eq}	66.64 dB SPL	67.46 dB SPL	68.70 dB SPL
$L_{\mathrm{A_{eq}}}$	63.90 dB SPL	65.19 dB SPL	67.27 dB SPL

The second microphone which is compared is the microphone in the downwards direction. The following Figure 8.9 shows the frequency response for every tournament.

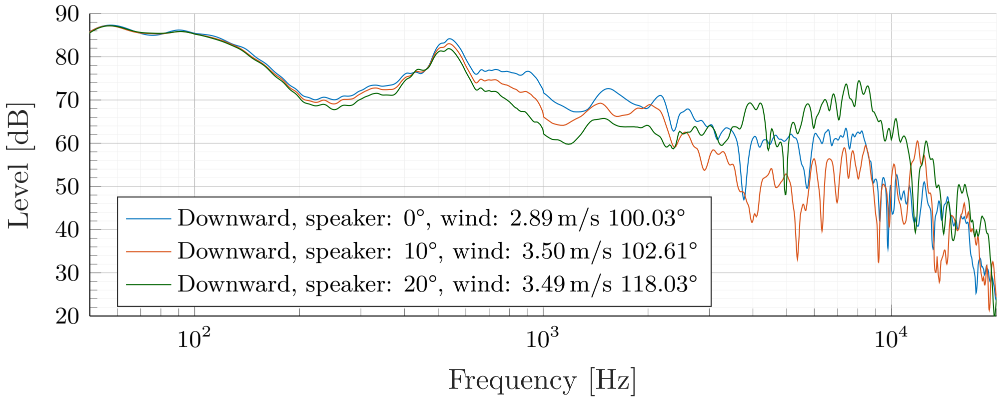

Figure 8.9: The graph shows the measuring result for the downwards microphone in three line source array rotation, while the microphone is in the windscreen and the windscreen is in the hight of the ear. The graph is a mean of 10 measurements in all three angles. The mean calculation is done in the time domain where all impulse responses are aligned with cross-correlation

As seen in Figure 8.9, while the speaker is turned, the SPL is lowered unless the 20° above 2.5 kHz. The raise in power comes from the directionality characteristics of the line source array as seen in Figure 7.3. The peaks and depth is ether not at the same frequency which make the visually justment difficult but it is observed i generally that turning the speaker lower the SPL from 0° to 10° above 650 Hz. The following Table 8.2 shows the single number SPL both non weighted and A-weighted.

Table 8.2: The table shows the measured L_{eq} and $L_{\mathrm{A_{eq}}}$ SPL for the downwards microphone

Speaker angle	0°	10°	20°
L_{eq}	66.86 dB SPL	65.46 dB SPL	67.12 dB SPL
$L_{\mathrm{A_{eq}}}$	64.24 dB SPL	61.59 dB SPL	64.36 dB SPL

The third microphone, which is compared, is the microphone in the centre direction. The following Figure 8.10 shows the frequency response for every tournament.

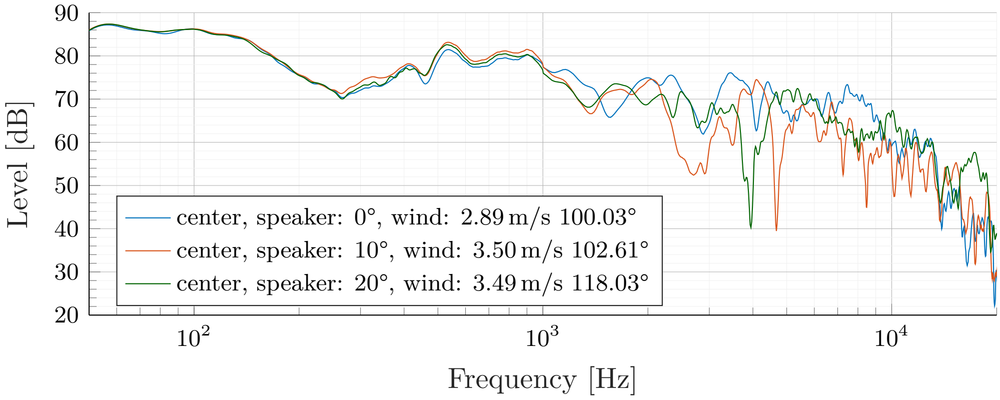

Figure 8.10: The graph shows the measuring result for the centre microphone in three line source array rotation, while the microphone is in the windscreen and the windscreen is in the hight of the ear. The graph is a mean of 10 measurements in all three angles. The mean calculation is done in the time domain where all impulse responses are aligned with cross-correlation

As seen in Figure 8.10, the frequency response does not ether raise or fall markebly while the speaker is turned. The large depth between 2.0 kHz and 5.0 kHz comes from the frequency characteristic of the line source array as seen in Figure 7.3. The following Table 8.3 shows the single number SPL both non weighted and A-weighted.

Table 8.3: The table shows the measured L_{eq} and $L_{\mathrm{A_{eq}}}$ SPL for the center microphone

Speaker angle	0°	10°	20°
L_{eq}	69.72 dB SPL	68.79 dB SPL	68.77 dB SPL
$L_{\mathrm{A_{eq}}}$	68.64 dB SPL	67.07 dB SPL	67.00 dB SPL

8.2 research of the problems

To be able to decide the last few details of the final measurement based on the test and data analysis performed in section 8.1, the frequency response of the designed windscreen is founded in free field condition while rotating and tilting. Secondly, the final windscreen hight is decided. In section 8.2.1, the frequency response of the windscreen is founded where the windscreen is rotated and tilted.

8.2.1 windscreen frequency response

This section aims to research the frequency response of the designed windscreen. It is observed in section 8.1.2 that the measurement with the designed windscreen in the centre and downwards direction has a higher frequency response between 1.0 kHz and 10 kHz compare to two measurements without the designed windscreen at the centre. Therefore it has to be founded if the windscreen by itself have differences in frequency response while the windscreen is rotated or tilted. The windscreen is measured in the anechoic chamber both with tilting and with rotation to research the effect of differences of the windscreen. The measurement is founded in Appendix M. It is observed in the measurement that the windscreen does not have a frequency differences more than ±2 dB SPL while the windscreen is not rotated and not tilted. Furthermore, small forward tilting up to 9° only have an attenuation effect above 10 kHz due to plate reflection. A rotation of 30° ether to the left of to the right does attenuate in the frequency range of 1.0 kHz to 4.0 kHz. The frequency response of the windscreen is also measured while removing the foam wedge, but in this configuration produces high reflection in the frequency response. Generality the designed windscreen only change the frequency response up to 2 dB SPL while the designed windscreen points within ± 10° to the line source array and with tilting beneath 3°. The following measurement Figure 8.11 shows the different while the microphone only is required with the original modified windscreen and with the designed windscreen

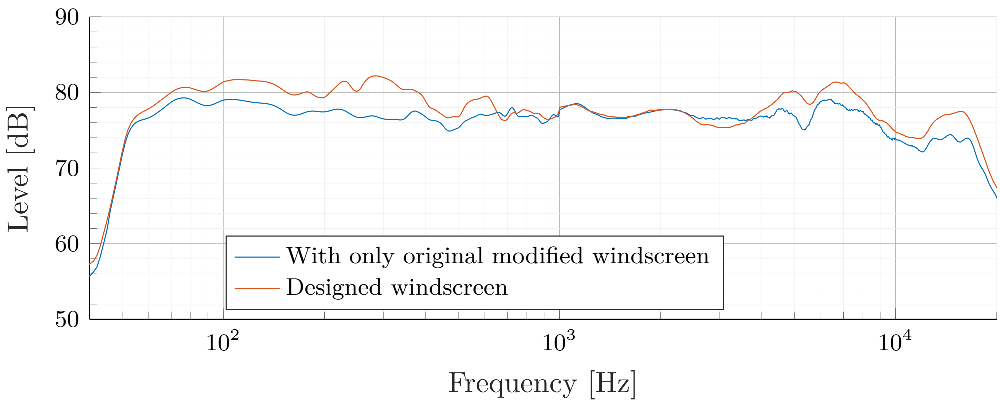

Figure 8.11: The graph shows frequency response of the speaker measured without windscreen and with the designed windscreen with no rotation and no tilting

8.3 Update to the final measurement

In the final measurement, the designed windscreen is used as it is designed. It is founded that the windscreen does not have any frequency differences more than 2 dB SPL in the high frequency and small differences in the position make no difference. It is founded that high tilting and high rotation does have an effect of the frequency response and shall be avoided to the final measurement. In the end, the differences between the speaker characteristics with asymmetric make it challenging to compare the side microphone since the 55° directionality characteristics have a boost in the higher frequency at 45°, as seen is Figure 7.3. Therefore the following points describe the update to the final measurement.

Update	Argumentation
The windscreen is positioned at the ground surface hight and not in the ear hight.	This requirement is made according to the founded ground reflection in section 8.1.1 and that the ground reflection shall be minimised such that the microphone might be able to compared among each other. Secondly, it is known from the design of the windscreen that the wind noise is 20 dB SPL lower near the ground section 7.3.10. Finally, it is assumed in section 7.3.10 that the reflection is low in the high frequency while the area is full of the audience which supports that the ground reflection in the high frequency has to be minimised in the measuring point.

Update	Argumentation
The windscreen shall lay flat on the ground without tilting higher than 6° and point 0° to the line source array	This requirement is made according to the founded frequency response change in section 8.2.1 while the windscreen is tilted and rotated.

Update	Argumentation
The speaker shall have symmetric directionality characteristics with a beamwidth of 50°	This requirement is made according to the founded in the measuring result section 8.1.4, where the differences in directionality characteristics make it difficult to compare the upwards microphone and downwards microphone since the line source array has a SPL boost in the 45°

Part III

Measurement

Chapter 9

Measurement

9.1 The measurement

In this chapter, the measuring result from the final measurement is shown. In the first part of this chapter, the wind noise measured at the start of the measurement is shown. Secondly, the signal processing of filtering the wind noise from the impulse response is explained. The second part covers the measurement versus the wind direction. Only the measurement where refraction occurs according to the designed measurement is a successful measurement. All other measurement is excluded. The third part covers the measurement done in the crosswind. The fourth part covers the measurement done in the parallel wind.

9.2 Wind noise doing measurement

Wind noise is present in all measurement and has to be addressed before the impulse response is analysed. As the first part of the final measurement, the wind noise is measured and visualised to ensure optimal signal to noise ratio. The wind noise is measured for all three microphones twice at a different time and wind speed above 5 m/s. The wind noise measurement is only done this two time of every microphone on the measuring day. The following Figure 9.1 shows the wind noise at all three microphone position, including the wind speed.

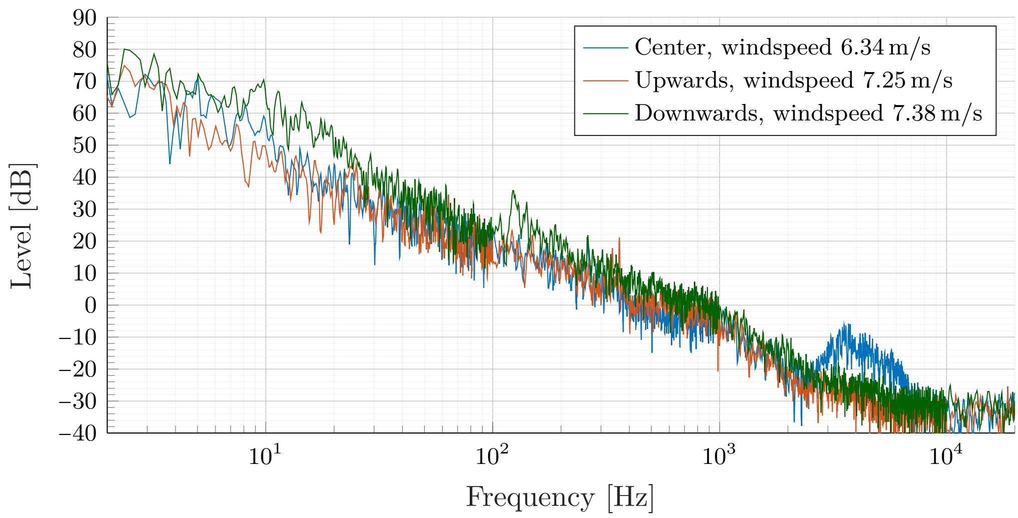

Figure 9.1: The graph shows the wind noise in all three measurement microphone at the exact position which is used for the crosswind measurement

The measurement Figure 9.1 shows that the wind noise is pink and therefore most present in the low frequency. This low frequency wind noise is filtered in two steps. First, the impulse responses are filtered by a second order high pass filter at 40 Hz. The 40 Hz is decided based on the lowest cut frequency of the line source array. The cut off is due to an internal filter in the Digital Signal Processor (DSP) settings of the line source array controller and the physical construction of the line source element. As the second filter, the impulse responses are windowed to remove wind noise component present along the impulse response time. The wind noise is present as a delayed signal in the impulse response because the wind noise is present under the full sine sweep measuring period. The following Figure 9.2 shows one impulse response measured doing the final measurement.

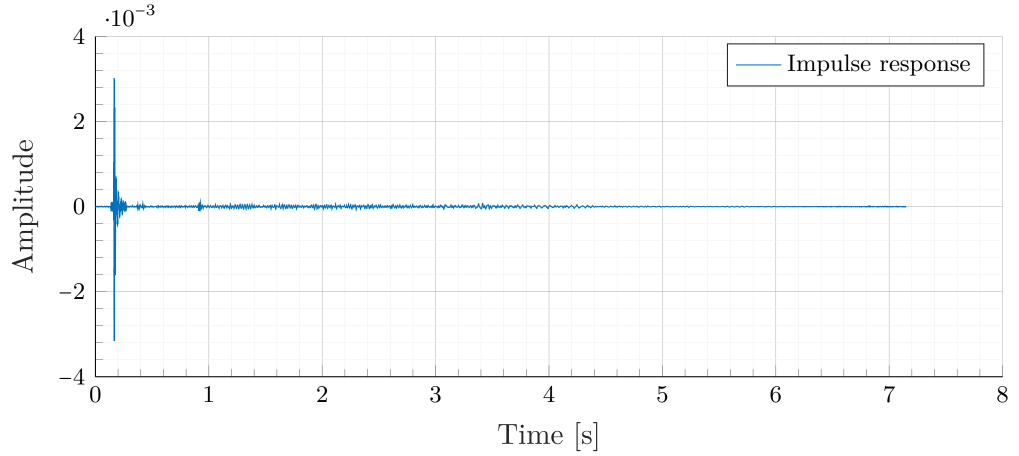

Figure 9.2: The graph shows one impulse response measurement of the upwards microphone where the line source array is not rotated

As seen in Figure 9.2, the noise is present along the impulse response timeline. This wind noise is not interesting for the analysis and is therefore windowed by a custom made window. The following Figure 9.3 shows the same impulse response as before while it is filtered and windowed with the custom made window.

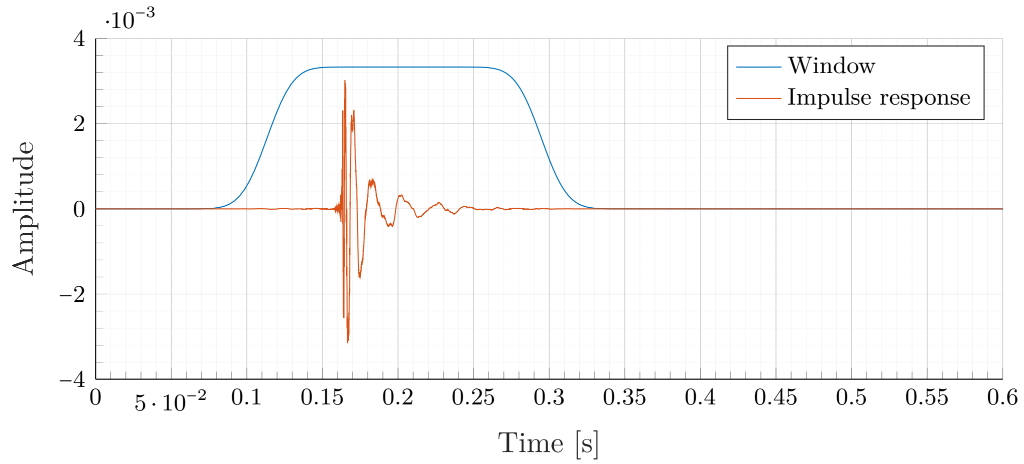

Figure 9.3: The graph shows one impulse response measurement of the upwards microphone where the line source array is not rotated and the designed window. The window is scaled down in amplitude in the graph.

The window function in Figure 9.3 is an amplitude wise scaled version. The window is only scaled such that both the impulse response and the window is visible in the same plot. The window for the calculation has a unity gain in the maximum amplitude. In Figure 9.3, it is seen that the window passes the impulse response without change, while the delayed wind noise is filtered. Both filtering method is applied for both the crosswind analysis and the parallel wind analysis.

9.3 Accepted measurement

The measurement for the crosswind is more sensitive to wind direction fluctuation that the parallel wind measurement. In the parallel wind measurement setup, the wind direction shall turn 90° from parallel to the frontal sound direction, before the upwards refraction change to downwards refraction. Unless that the crossover is at 90°, the upwards refraction effect decay along with the change in wind direction in both positive and negative direction from parallel. Therefore, the average wind direction for the parallel wind is limited to be within ±25°. In the crosswind measurement, the wind divination is more critical. The criticality of wind direction divination is illustrated in Figure 9.5

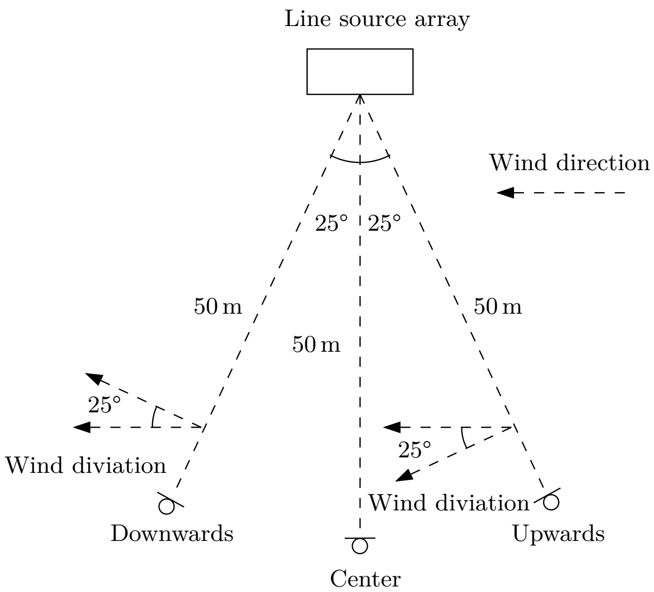

Figure 9.4: The figure shows the measurement setup and the nearest critical angle before the refraction direction flips.

As seen in Figure 9.5, the refraction crossover point is at 25° in the right rotation for the downwards direction and 25° in the left rotation for the upwards rotation. Therefore together they limit the wind direction to be within ±25° before the refraction condition change on one of the microphones. Therefore, for the crosswind measurement, the average wind direction is limited to be between ±20°.

9.4 Crosswind measurement

This section is presenting the final measurement which is done according to the crosswind measurement design description in chapter 7 including the update described in chapter 8. The measurement appendix is founded in Appendix P. The measurement setup is nearly identical to the measurement in chapter 8 unless that the wind direction is turned 180°, the anemometer at the microphone position is placed 5 m to the right of the centre microphone instead of 5 m to the back of the centre microphone and the anemometer at the line source array is moved to the right side. The measurement is done from 0° to 30° in step of 10° towards the upwards direction. The measurement setup is illustrated in Figure 9.5.

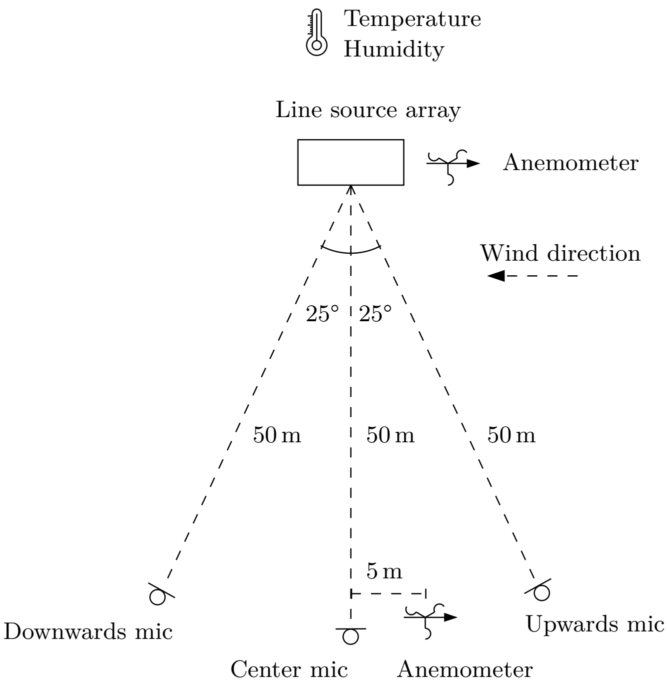

Figure 9.5: The figure shows the microphone position versus the position of the line source, while the array is 0° horizontal turned

While analysing the upwards refraction to the downwards refraction, it is interesting to analyse at which frequency the refraction starts. This analysis is done on the measurement done in the final measurement with wind speed between 5 m/s and 10 m/s. The refraction knowledge is used to decide which frequency range that has to be analysed. The frequency range that shows no or less than 3 dB SPL refraction is excluded from the analysis. The desition of 3 dB SPL deviation is based on audible differences and wind turbulence. The refraction is analysed by calculating frequency response for all measurement with wind speed above 5 m/s and compared between the three microphones position. The comparison between measurement is done visually by plotting the frequency response for all measurement. One measurement which shows the general refraction phenomena is shown in Figure 9.6

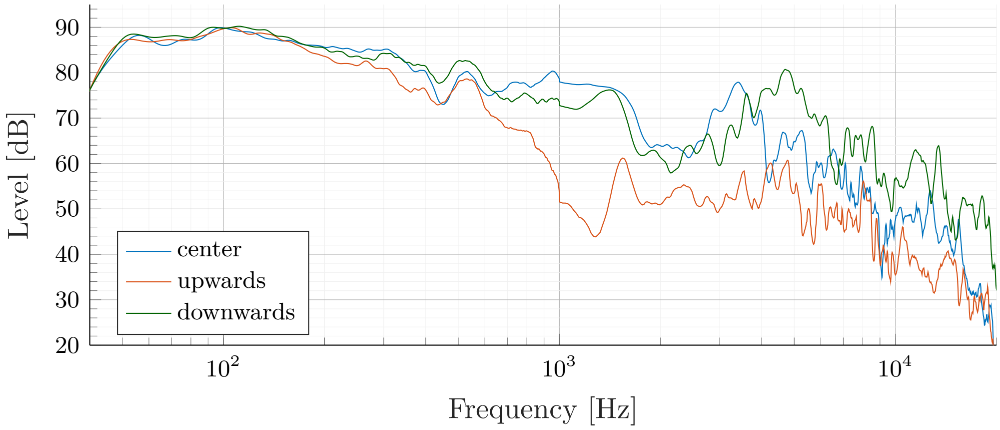

Figure 9.6: The graph shows one measurement while the line array is not rotated and the wind speed is measured to be 8.00 m/s

As seen in Figure 9.6, the refraction starts at 150 Hz and gets above 3 dB SPL in the frequency range above 600 Hz. The measurement is done at least 10 times for every angle and based on the amount of data, one graph for every angle is shown where the rest of the result is shown in L_{eq} octave separation above 600 Hz afterwards. The graph only includes upwards measurement and downwards measurement. The centre microphone measurement is given in the L_{eq} to keep the plot visual manageable. In all chosen measurements, the wind speed is above 8 m/s. The following four measurement shows the frequency response with the given line source array rotation.

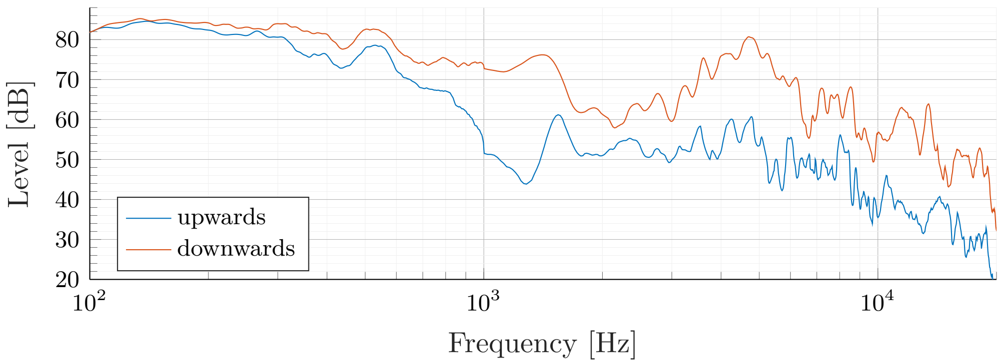

Figure 9.7: The graph shows the frequency response measured by the upwards microphone and the downwards microphone with line source array rotation of 0°

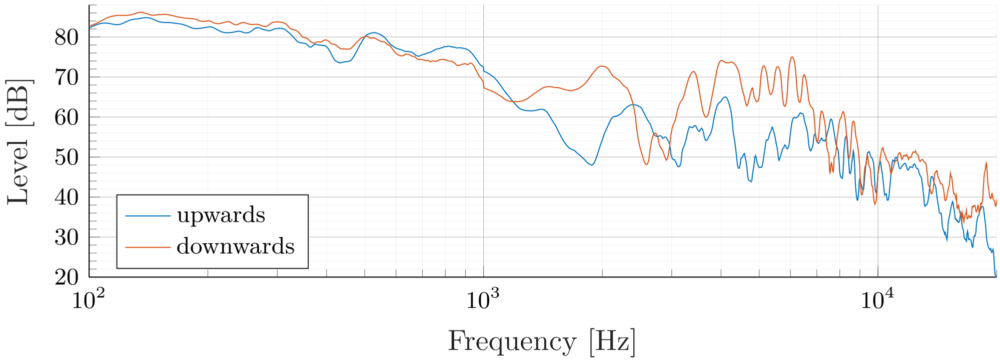

Figure 9.8: The graph shows the frequency response measured by the upwards microphone and the downwards microphone with line source array rotation of 10°

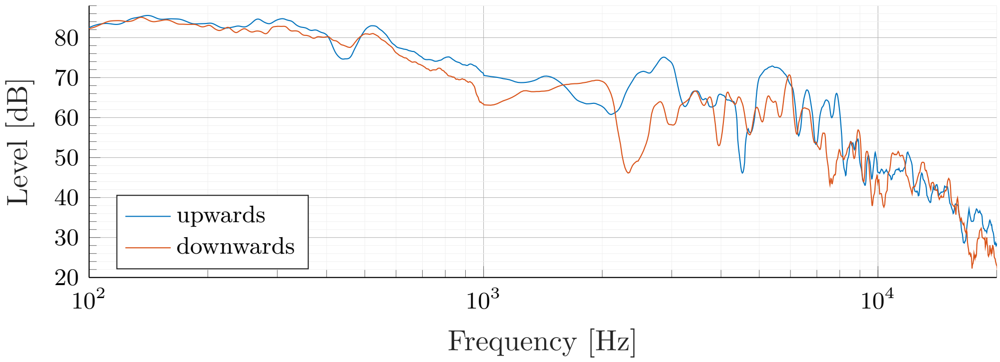

Figure 9.9: The graph shows the frequency response measured by the upwards microphone and the downwards microphone with line source array rotation of 20°

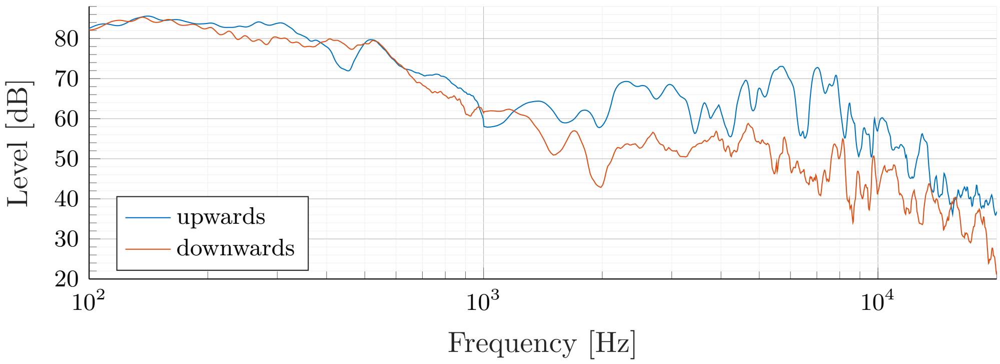

Figure 9.10: The graph shows the frequency response measured by the upwards microphone and the downwards microphone with line source array rotation of 30°

In the analysis, the measurement is split into groups depending on the wind speed with a step of 1 m/s. Furthermore, all measurement in the analysis is between ±20° from crosswind to the speaker. Crosswind to the speaker is defined as 90° and therefore, angle between 70° to 110° is the acceptable. All measurement deviates from this range is excluded. Moreover, measurement with wind speed beneath 5 m/s is also excluded. From those limitations, the following Table 9.1 shows the amount of measurement for each wind speed step.

Table 9.1: The table shows the number of measurement which is between 65° to 115° in the given m/s interval

Speaker angle	0°	10°	20°	30°	Total
[5 m/s, 6 m/s[	0	2	4	4	10
[6 m/s, 7 m/s[	2	6	5	5	18
[7 m/s, 8 m/s[	5	3	4	4	16
[8 m/s, 9 m/s[	6	1	2	1	10
[9 m/s, 10 m/s[	1	2	4	0	7
Total	14	14	19	14	61

It is seen in Table 9.1 that 61 measurement is available and the most is within wind speed of 6 m/s to 10 m/s.

The measurement is calculated into octave band, to be able to compare the measured result in frequency bands. The measurement result is divided into wind speed groups with the same interval as in Table 9.1. For every octave band in every group, the l_{eq} is calculated and rounded to the nearest integer. The dB is left out in the table such that the table fits within one page. Every measurement is given by a 'm' with a following number. The letter 'm' stands for measurement where the number specifies the actual played measurement number; for example, the firth measurement in a row is named m4. For every new speaker angle, the number is reset and started with the number 1. In every measurement group, the average of the measurements is calculated for every octave band. Every group contain information for each microphone, and the average is calculated for each microphone separately. The upwards microphone information is named U, the centre microphone information is named C, and the downwards microphone information is named D. Furthermore the average difference between the upwards microphone and the downwards microphone is calculated and given as Dif in the table. In the end, the absolute differences between the centre microphone and the upwards microphone are calculated and added to the absolute differences between the centre microphone and the upwards microphone. This value gives the absolute differences between the outer main lobe to the centre. This value is named Cdif and is referred to as the absolute difference between the centre and the side microphone. All calculation is done without rounding, only the number in the table is rounded. The following Table 9.2, Table 9.3, Table 9.4, Table 9.5, Table 9.6 shows the measured result in the given wind speed interval.

Table 9.2: The table shows the measurement in in octave band and within the interval [5 m/s, 6 m/s[with the given line source array angle

freq	1k			2k			4k			8k			16k			Wind	
Mic	U	C	D	U	C	D	U	C	D	U	C	D	U	C	D	μ	σ
10°																	
m1	61	60	55	54	58	55	53	58	56	46	53	53	36	45	47	109°	17°
m13	54	50	55	48	51	50	55	65	57	50	61	54	42	49	47	109°	10°
avg	58	55	55	51	54	52	54	61	57	48	57	53	39	47	47	109°	14°
Dif	−2.50 dB			1.41 dB			3.10 dB			5.28 dB			7.93 dB				
Cdif	2.80 dB			5.86 dB			11.94 dB			12.56 dB			8.61 dB				
20°																	
m4	64	60	56	64	58	56	57	61	59	50	57	58	40	46	46	86°	22°
m8	56	58	53	51	46	47	54	51	55	52	48	53	42	39	41	83°	11°
m15	52	52	54	50	48	49	59	51	48	56	53	45	43	44	39	95°	10°
m17	63	60	55	56	55	52	54	52	55	53	49	52	41	44	43	92°	14°
avg	59	58	55	55	52	51	56	54	54	52	52	52	42	43	42	89°	14°
Dif	−4.06 dB			−4.39 dB			−1.89 dB			−0.29 dB			0.39 dB				
Cdif	4.06 dB			4.39 dB			2.71 dB			1.39 dB			2.36 dB				
30°																	
m3	50	53	46	44	41	37	49	47	42	48	42	39	42	33	33	98°	11°
m14	59	53	46	52	46	43	56	56	49	52	51	45	43	41	38	91°	18°
m15	56	55	48	50	43	39	56	48	44	55	43	39	47	33	32	107°	21°
m17	52	51	51	50	44	45	57	53	52	55	46	44	46	37	38	97°	19°
avg	54	53	48	49	44	41	55	51	47	53	46	42	45	36	35	98°	17°
Dif	−6.62 dB			−7.95 dB			−7.98 dB			−10.93 dB			−9.50 dB				
Cdif	6.62 dB			7.95 dB			7.98 dB			10.93 dB			9.50 dB				

Table 9.3: The table shows the measurement in in octave band and within the interval [6 m/s, 7 m/s[with the given line source array angle

freq	1k			2k			4k			8k			16k			Wind	
Mic	U	C	D	U	C	D	U	C	D	U	C	D	U	C	D	μ	σ
0°																	
m14	53	52	62	42	52	61	53	57	62	48	53	58	36	51	51	88°	13°
m17	49	59	59	40	52	56	49	54	59	45	53	56	35	44	46	107°	13°
avg	51	56	61	41	52	59	51	55	61	46	53	57	35	48	49	97°	13°
Dif	9.62 dB			17.67 dB			9.76 dB			10.75 dB			13.40 dB				
Cdif	9.62 dB			17.67 dB			9.76 dB			10.75 dB			13.40 dB				
10°																	
m5	54	52	51	45	50	44	52	55	54	51	53	51	41	45	45	96°	12°
m6	56	60	58	47	64	64	53	67	66	51	66	65	43	54	53	78°	9°
m8	56	61	60	48	54	60	51	58	61	52	51	55	43	47	50	100°	13°
m9	55	60	57	54	52	49	52	54	53	49	57	51	40	51	43	89°	6°
m11	57	58	55	43	60	48	48	64	56	49	56	54	47	49	51	107°	17°
m12	63	59	58	58	60	58	56	66	63	51	61	59	44	48	48	95°	11°
avg	57	58	56	49	57	54	52	60	59	50	57	56	43	49	48	94°	11°
Dif	−0.39 dB			4.82 dB			6.77 dB			5.38 dB			5.44 dB				
Cdif	3.44 dB			9.98 dB			10.10 dB			7.86 dB			7.12 dB				
20°																	
m2	66	58	57	53	53	51	56	55	58	52	48	50	45	41	42	73°	17°
m6	56	56	55	49	47	49	48	54	53	47	52	48	38	42	38	87°	10°
m9	53	52	54	47	49	48	54	52	54	51	45	51	49	36	38	104°	12°
m19	54	53	54	52	45	51	61	51	49	60	47	47	47	39	41	98°	17°
m20	57	50	52	56	46	46	61	59	50	59	56	50	53	47	43	93°	15°
avg	55	54	55	51	48	49	56	54	53	54	50	49	46	41	40	91°	14°
Dif	−0.84 dB			−2.32 dB			−3.13 dB			−4.67 dB			−5.68 dB				
Cdif	2.05 dB			3.77 dB			3.13 dB			4.67 dB			5.68 dB				
30°																	
m4	58	58	47	55	47	37	54	49	46	53	45	44	41	41	38	100°	14°
m6	48	47	48	50	43	44	55	55	46	58	48	40	50	41	33	86°	13°
m8	56	54	54	51	44	46	59	48	52	54	49	46	49	42	39	87°	11°
m13	56	53	47	54	45	42	61	50	45	59	47	38	49	37	32	103°	14°
m19	48	54	45	55	42	44	64	46	47	61	43	41	50	37	37	88°	8°
avg	53	53	48	53	44	43	59	50	47	57	46	42	48	39	36	93°	12°
Dif	−4.98 dB			−10.22 dB			−11.60 dB			−14.99 dB			−12.14 dB				
Cdif	5.77 dB			10.22 dB			11.60 dB			14.99 dB			12.14 dB				

Table 9.4: The table shows the measurement in in octave band and within the interval [7 m/s, 8 m/s[with the given line source array angle

freq	1k			2k			4k			8k			16k			Wind	
Mic	U	C	D	U	C	D	U	C	D	U	C	D	U	C	D	μ	σ
0°																	
m10	53	59	60	44	53	52	51	56	57	47	53	59	39	50	52	102°	12°
m15	53	60	58	39	59	51	46	67	56	44	64	57	37	51	47	90°	17°
m18	57	51	59	49	46	52	50	50	57	45	48	55	34	43	49	101°	13°
m20	47	47	58	42	48	55	47	55	58	46	54	56	39	47	49	99°	10°
m22	40	45	59	44	53	49	49	56	63	48	56	66	39	45	52	96°	11°
avg	50	53	59	44	52	52	49	57	58	46	55	59	38	47	50	97°	13°
Dif	8.74 dB			8.19 dB			9.24 dB			12.66 dB			12.39 dB				
Cdif	8.74 dB			8.19 dB			9.24 dB			12.66 dB			12.39 dB				
10°																	
m2	46	59	54	42	56	51	46	65	62	45	56	59	38	51	50	80°	17°
m3	54	55	57	47	59	53	54	61	61	52	56	55	41	46	47	104°	12°
m15	58	59	56	47	56	56	49	56	61	48	60	59	40	53	45	97°	10°
avg	53	58	55	46	57	53	50	61	61	48	58	57	39	50	47	94°	13°
Dif	2.56 dB			7.39 dB			11.68 dB			8.90 dB			7.83 dB				
Cdif	7.93 dB			14.75 dB			11.68 dB			9.25 dB			13.28 dB				
20°																	
m3	58	58	53	55	53	45	63	54	48	54	46	47	41	40	40	104°	19°
m5	53	60	56	45	51	53	53	55	56	53	54	51	41	44	41	77°	8°
m10	55	57	51	47	47	43	50	51	49	48	49	49	41	39	41	93°	9°
m14	53	55	52	47	49	48	55	53	48	51	53	42	41	48	36	99°	12°
avg	55	58	53	48	50	47	55	53	50	51	50	47	41	43	39	93°	12°
Dif	−1.96 dB			−1.16 dB			−4.91 dB			−4.16 dB			−1.52 dB				
Cdif	7.56 dB			4.49 dB			4.91 dB			4.16 dB			5.35 dB				
30°																	
m9	51	51	49	54	46	43	58	53	46	60	48	43	49	38	38	85°	13°
m11	63	49	47	60	46	40	53	53	47	50	47	41	42	40	37	92°	10°
m12	54	58	55	54	48	41	58	52	49	58	46	44	48	37	41	103°	8°
m18	51	53	51	57	48	44	64	55	45	72	48	42	59	42	36	91°	15°
avg	55	53	50	56	47	44	58	53	47	60	47	43	49	39	38	93°	12°
Dif	−4.63 dB			−12.21 dB			−11.61 dB			−17.48 dB			−11.25 dB				
Cdif	4.63 dB			12.21 dB			11.61 dB			17.48 dB			11.25 dB				

Table 9.5: The table shows the measurement in in octave band and within the interval [8 m/s, 9 m/s[with the given line source array angle

freq	1k			2k			4k			8k			16k			Wind	
Mic	U	C	D	U	C	D	U	C	D	U	C	D	U	C	D	μ	σ
0°																	
m9	49	54	58	46	47	52	53	53	55	47	52	52	42	42	49	83°	16°
m11	52	58	60	49	58	54	50	62	59	44	67	54	35	56	49	84°	11°
m12	55	64	59	49	62	59	54	59	57	50	58	61	35	49	56	88°	10°
m13	49	56	61	42	51	63	45	54	63	45	53	58	34	50	50	86°	9°
m16	47	63	59	43	59	56	47	62	67	43	52	60	35	43	53	104°	11°
m19	48	57	57	38	58	51	47	62	59	45	58	62	34	53	52	89°	10°
avg	50	59	59	45	56	56	49	59	62	46	57	59	36	49	51	89°	11°
Dif	8.93 dB			11.23 dB			10.74 dB			12.53 dB			15.42 dB				
Cdif	8.92 dB			11.23 dB			10.74 dB			12.53 dB			15.42 dB				
10°																	
m10	55	54	51	48	52	49	56	64	53	52	63	52	39	50	49	97°	10°
Dif	−3.77 dB			1.11 dB			−2.85 dB			0.15 dB			9.30 dB				
Cdif	3.77 dB			8.46 dB			19.00 dB			21.68 dB			11.88 dB				
20°																	
m11	50	53	52	49	47	43	59	54	50	56	54	44	47	42	37	95°	9°
m16	57	59	54	57	57	54	60	56	55	57	50	53	43	44	41	98°	15°
avg	54	56	53	53	52	49	60	55	53	57	52	48	45	43	39	97°	12°
Dif	−0.18 dB			−4.58 dB			−6.80 dB			−7.77 dB			−5.76 dB				
Cdif	5.22 dB			4.58 dB			6.80 dB			7.77 dB			5.76 dB				
30°																	
m7	53	56	48	59	48	46	65	55	50	61	52	45	47	46	35	97°	9°
Dif	−5.07 dB			−13.06 dB			−15.90 dB			−15.60 dB			−11.15 dB				
Cdif	10.44 dB			13.06 dB			15.90 dB			15.60 dB			11.15 dB				

Table 9.6: The table shows the measurement in in octave band and within the interval [9 m/s, 10 m/s[with the given line source array angle

freq	1k			2k			4k			8k			16k			Wind	
Mic	U	C	D	U	C	D	U	C	D	U	C	D	U	C	D	μ	σ
0°																	
m21	53	51	50	50	55	46	62	67	57	54	63	60	44	51	53	100°	9°
Dif	−2.57 dB			−4.00 dB			−5.10 dB			5.98 dB			8.46 dB				
Cdif	2.57 dB			13.76 dB			14.76 dB			11.48 dB			8.46 dB				
10°																	
m4	44	54	54	47	51	52	47	52	55	41	50	54	37	40	49	95°	11°
m7	55	54	54	50	53	50	53	56	60	51	50	55	42	41	45	103°	13°
avg	49	54	54	48	52	51	50	54	57	46	50	55	40	41	47	99°	12°
Dif	4.94 dB			3.10 dB			7.69 dB			8.55 dB			7.64 dB				
Cdif	4.94 dB			4.61 dB			7.69 dB			8.55 dB			7.64 dB				
20°																	
m1	53	57	49	50	51	49	54	51	55	53	50	48	44	45	40	76°	7°
m7	56	53	56	52	47	50	58	55	51	55	53	49	47	45	44	81°	12°
m12	55	57	55	53	49	59	59	58	56	55	53	51	43	43	42	97°	15°
m13	56	52	56	52	49	55	56	54	58	57	51	52	47	42	41	89°	11°
avg	55	55	54	52	49	53	57	54	55	55	52	50	45	44	42	86°	11°
Dif	−0.79 dB			1.44 dB			−1.93 dB			−5.15 dB			−3.73 dB				
Cdif	1.39 dB			7.01 dB			3.04 dB			5.15 dB			3.73 dB				

9.5 parallel wind measurement

This section is presenting the final measurement which is done according to the parallel wind measurement design description in chapter 7 including the update described in chapter 8. The measurement appendix is founded in Appendix P. The line source array setup is identical to the measurement in section 9.4 unless that the line source array is rotated 90° up against the wind. Furthermore, the microphone is moved according to the description in section 7.3.5. The foam wedge is rotated 90° on the plate such that the PVC foam plate is covering for the wind from the back. The windscreen setup is as following Figure 9.11

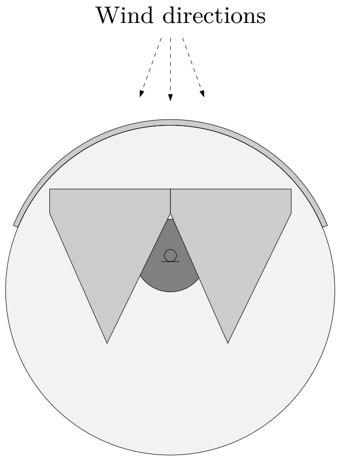

Figure 9.11: The figure shows the setup of the windscreen while parallel wind measurements

The anemometer at the microphone position is placed 5 m to the left of the centre microphone and the anemometer at the line source array is placed in the hight of the line source array and in the left side of the line source array. Both the back and front microphone is placed 10 m from the centre microphone. The measurement is done in 3° downwards tilting and in 7° downwards tilting. The measurement setup is illustrated in Figure 9.12 as a top view.

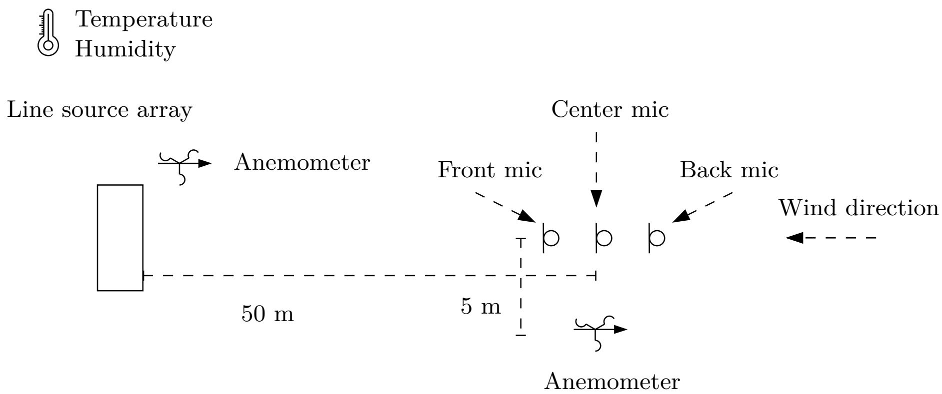

Figure 9.12: The figure shows the measuring setup for parallel wind measuring as a top view.

To be able to compare the result from each microphone, while the microphone is placed with different distance to the line source array, the distance and viscosity dependency between the microphones is removed from the measurements. It is decided to norm the distance to 50 m which is the centre microphone based on the maximum distances before delay tower. Calculating the distance dependency loss is not as simple for a line source array as for a point source, since the SPL loss at doubling of distance depends on the wavelength, distance and hight of the line source array section 2.1. Furthermore, the loss also depends on the viscosity of the air section 2.2.1. To be able to remove those factor from the measurement, the frequency versus near-field limit have to be founded. The graph in Figure 2.2 shows the limiting distance where the near-field change to far-field for the used line source array with 6 line source element. From the graph, the following Table 9.7 shows the near-field, far-field relation versus distances.

Table 9.7: The table shows the frequency range versus distances there the SPL loss is ether in near-field or in far-field and not in between

	far-field	near-field
40 m - 50 m	0 Hz - 5.8 kHz	7.2 kHz - 20 kHz
50 m - 60 m	0 Hz - 7.2 kHz	8.7 kHz - 20 kHz

It is seen in Table 9.7 that a part of the frequency range is neither in near-field or far-field within the distance between the microphone and cannot be calculated with the normal distances calculation for near-field and far-field. Therefore, to calculate the losses in SPL the area expansion is calculated for every frequency with distances step from 1 m to 60 m. The differences between 40 m to 50 m and 50 m to 60 m in dB is shown in the following Figure 9.13

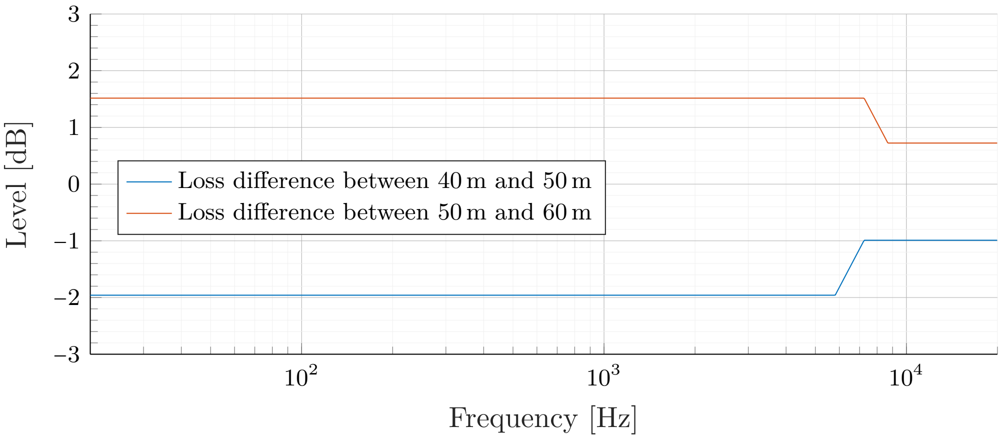

Figure 9.13: The graph shows the distance dependent loss from the center microphone to the front and back microphone. The loss is negative between 40 m to 50 m because the the front microphone is closer to the line source array then the center microphone

The Figure 9.13 shows the distances dependency filter. The upper filter illustrated as a red line is added to the back microphone where the lower filter illustrated as a blue line is added to the front microphone. The next filter which is designed is the frequency versus absorption filter. Absorption depending on humidity and temperature, to calculate the loss at 10 m of distances, the formula in standard [ISO 9613-1:1993] is used with the measured data for every measurement. The atmospherical pressure is not measured doing the measurement, and therefore, the reference

101.325 kPa is used as pressure. All 30 measurement is done with short time differences and therefore, the temperature and humidity only change with a fraction. Unless that the temperature and humidity only change with a fraction, the filter is recalculated for every measurement. For every measurement, 55 sample is available for both temperature and humidity, the average of the 55 samples is calculated and used for the filter calculation. One filter example is given in Figure 9.14 with 12 °C and 48 % humidity. The example temperature and humidity are from one of the measurement.

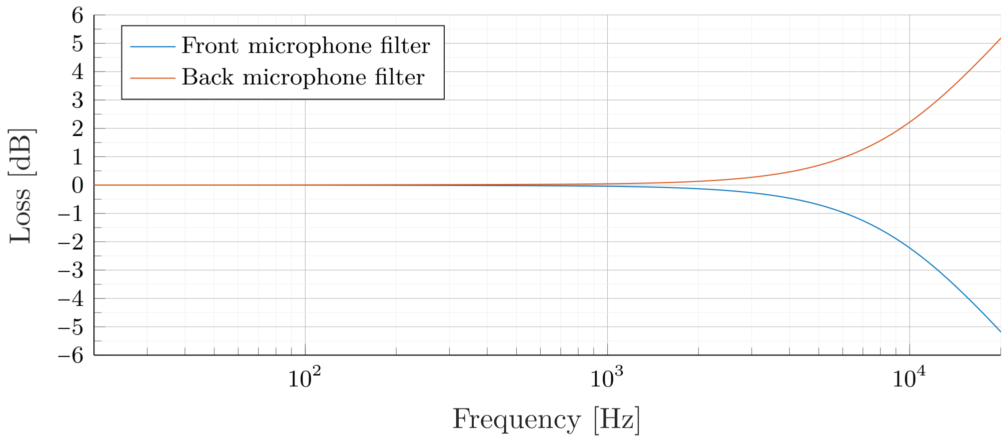

Figure 9.14: The graphs shows the viscosity loss in a distance of10 m. The blue graph is negative because the front microphone is closer to the line source array than the centre microphone

The frequency response in Figure 9.14 is used to compensate the viscosity in the air.

To apply the filters, the FFT is calculated for all measurements and the filter Figure 9.13 and Figure 9.14 is applied to the signal in both the positive and negative frequency domain in linear scale. Afterwards, the result is transferred back to time domain via IFFT for signal analysis. The measurement is done at least 10 times for every angle and based on the amount of data, one graph for both tilt angle is shown where the rest of the result is given in L_{eq} octave separation above 150 Hz in a table. In all chosen measurements, the wind speed is approximately 7 m/s. The following two measurement shows the frequency response with the given line source array downwards tilt angle.

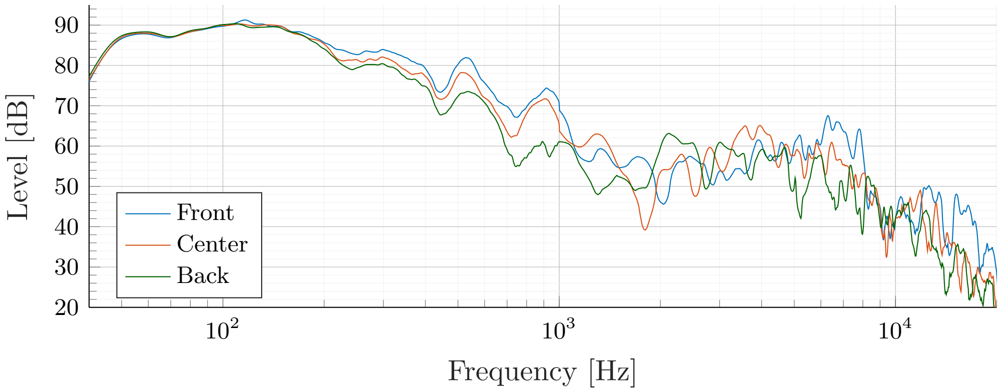

Figure 9.15: The graph shows one frequency response measurement where the line source array is tilted 3°

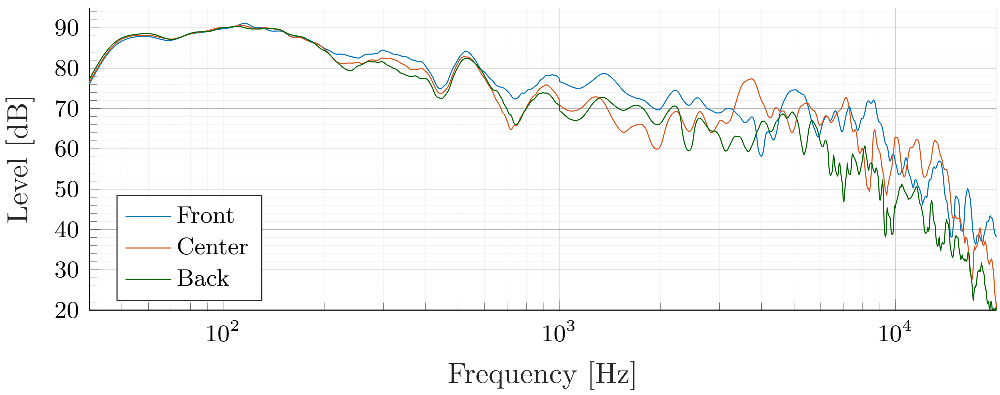

Figure 9.16: The graph shows one frequency response measurement where the line source array is tilted 7°

In the analysis, the measurement is split into groups depending on the microphone position. The reason that the group is microphone wise and not wind speed interval is that the amount of data is small. Furthermore, all measurement in the analysis is between ±25° from parallel wind to the speaker. All measurement deviates from this range is excluded. Moreover, measurement with wind speed beneath 5 m/s is also excluded, and measurement above 7 m/s is excluded because only a few measurements are available. From those limitations, the following Table 9.8 shows the amount of measurement for each tilt angle.

Table 9.8: The table shows the number of measurement which is between −25° to 25° in the given m/s interval

Speaker angle	3°	7°	Total
[5 m/s, 7 m/s[	3	5	8

The measurement is calculated to into octave band, to be able compare the measured result in frequency band. The measurement is divided into three groups shown in, one for every microphone. For every octave band in every group the l_{eq} is calculated and rounded to nearest integer. The dB is left out in the table to make the data more manastible. Every measurement is given by a m with a following number. The letter m stands for measurement where the number specify the actual played measurement number, for example the firth measurement in a row is named m4. In every group the average of the measurements is calculated for every octrave band and for every microphone. The nearest microphone to the line source array is named F for front, the centre microphone is named C and the back microphone is named B. Futhermore the average difference between the the two tilt angle is calculated and is given as Dif in the table. All calculation is done without rounding, only the number in the table is rounded.

The following Table 9.9, shows the measured result in the given wind speed interval.

Table 9.9: The table shows the measurement in in octave band and within the interval [5 m/s, 7 m/s[with the given line source array angle

freq	125 Hz		250 Hz		500 Hz		1.0 kHz		2.0 kHz		4.0 kHz		8.0 kHz		16 kHz	
deg	3°	7°	3°	7°	3°	7°	3°	7°	3°	7°	3°	7°	3°	7°	3°	7°
F																
m1-3	66	66	64	64	63	63	57	59	53	55	54	54	58	53	48	45
m5-4	67	66	65	63	64	61	60	57	58	54	57	55	58	58	51	49
m6-6	66	66	63	63	60	62	54	62	44	61	60	61	54	61	42	51
m7	N	66	N	64	N	64	N	64	N	68	N	73	N	68	N	59
m10	N	66	N	64	N	64	N	61	N	60	N	63	N	63	N	49
avg	66	66	64	64	62	63	57	60	52	59	54	61	57	61	47	51
Dif	-0.6		-0.47		-0.55		3.31		7.57		7.59		4.25		3.39	
C																
m1-3	66	66	63	63	61	61	57	58	53	61	58	67	53	58	45	44
m5-4	67	65	64	62	60	60	59	58	56	58	59	62	56	55	44	44
m6-6	66	66	62	62	57	61	52	57	44	56	52	63	48	60	38	52
m7	N	65	N	63	N	62	N	60	N	62	N	63	N	60	N	46
m10	N	65	N	63	N	61	N	57	N	53	N	57	N	56	N	51
avg	66	65	63	62	60	61	56	58	51	58	56	63	52	58	42	47
Dif	-0.64		-0.43		1.44		2.16		6.65		6.19		5.56		5.04	
B																
m1-3	66	66	63	63	61	61	60	58	58	58	55	63	55	54	43	42
m5-4	67	65	63	61	60	55	57	57	54	51	54	55	53	53	42	46
m6-6	65	65	61	61	54	60	44	57	47	57	48	57	44	52	35	41
m7	N	65	N	62	N	60	N	53	N	46	N	50	N	52	N	42
m10	N	65	N	63	N	60	N	53	N	51	N	62	N	60	N	49
avg	66	65	62	62	59	59	54	56	53	52	52	57	51	54	40	44
Dif	-0.79		-0.57		0.82		1.90		-0.66		4.66		3.73		3.76	

Table 9.10: The table shows the average wind direction and deviation within the wind speed interval [5 m/s, 7 m/s[

3° tilt angle	Direction	σ
m1	2°	14°
m5	8°	17°
m6	8°	10°

7° tilt angle	direction	σ
m3	15°	15°
m4	17°	14°
m6	$-22°$	14°
m7	3°	9°
m10	3°	8°

Chapter 10

Results

10.1 Data analysis

This chapter aims to analyse the data obtained in the final measurement shown in chapter 9. The analysis is done in two parts, on part for crosswind and one part for parallel wind. The analysis starts with the former.

10.2 Crosswind data analysis

The crosswind data analysis is only based on the approved data shown in the five tables in section 9.4. Furthermore the number of data point in the individual measurement angle in the interval of [8 m/s, 9 m/s[and [9 m/s, 10 m/s[is generally small with only one or no data in some line source angle. Therefore, those two interval is combined to one interval [8 m/s, 10 m/s[of the data analysis. The analysis analyses the difference between the upwards microphone versus the downwards microphone and the absolute difference between the centre microphone versus the side microphone in all four wind speed intervals. The analysis is done in octave band as the shown data, then from octave band 1.0 kHz to octave 16 kHz. The analysis between the upwards and downwards microphone calculates the linear least square fit between the calculated octave value. While a point excites 3 dB SPL from the fit, the weather information at the exact time is analysed. As the secondary analysis, all data is analysed as one combination of all octave band to find the optimal angle for every wind speed interval. The last part analysis the absolute difference between the centre microphone and the upwards and downwards microphone. While the line source array angle is positive, the speaker is rotated towards upwards refraction direction, and while the line source angle is negative, the line source array is rotated towards downwards refraction direction. The following Figure 10.1 is the 1.0 kHz octave band.

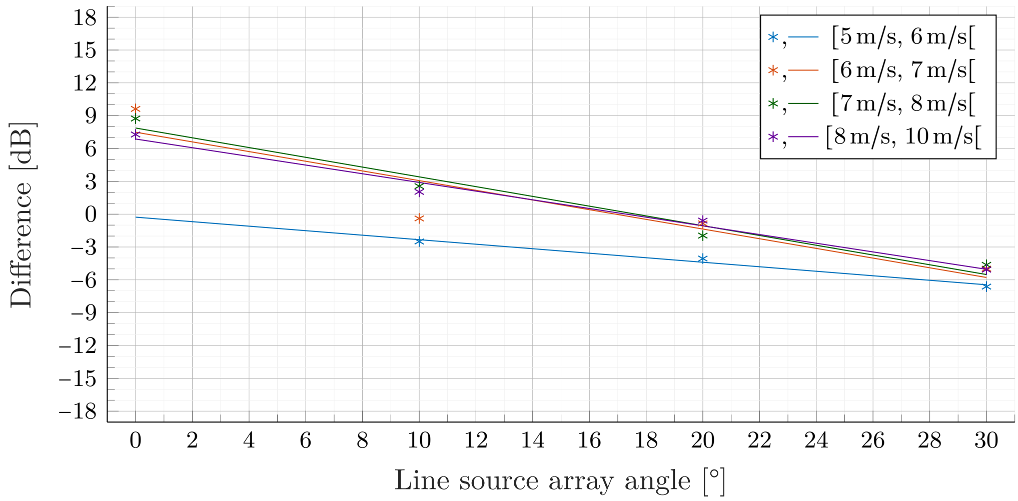

Figure 10.1: The graph shows the average 1.0 kHz octave band dB differences between the upwards and downwards microphone position calculated in section 9.4 in the given wind speed interval as a point. While the points is in the positive part of the graph, the dBis highest in the downwards microphone position. It moreover gives the linear least square fit of every wind speed interval as a line.

The dots in Figure 10.1 correspond to the measured data, where the line is the linear least square fit. The interval from [6 m/s, 10 m/s[shows that the optimal angle for the 1.0 kHz octave band is nearly the same. The refraction effect on the 1.0 kHz octave band does not change much in this interval. Only the measuring point in the interval [6 m/s, 7 m/s[at 10° is more that 3 dB SPL from the fitted line. The average wind angle at speaker angle 10° is 96.7° with wind speed of 6.4 m/s in the 1.0 kHz octave band frequency limit. All other measuring points in the same interval is also analysed with respect to wind speed and direction and shows no deviation from the limits.

At the interval [5 m/s, 6 m/s[no data is measured in 0° speaker angle and the average wind angle at speaker angle 10° is 1° from the limit, with only 2 data measurement. The average wind angle at speaker angle 10° in the 1.0 kHz is 113.4° with wind speed of 5.4 m/s. The 113.4° angle should give higher upwards refraction on to the upwards refraction microphone and nearly no downwards refraction on the downwards refraction microphone. This wind measuring point, in this case, might not be representable to the wind direction between the speaker to the microphone or turbulence in the air disturb the measurement. The average wind angle at speaker angle 10° in the 1.0 kHz is 92.9° with wind speed of 5.4 m/s. This measurement seams untrustable according to the refraction theory.

The following Table 10.1 gives the calculated angle based on the least square fit.

Table 10.1: The table shows the angle where the least square fit crosses the 0 dB differences between the upwards microphone and the downwards microphone in the 1 kHz octave band in the given wind speed interval

1.0 kHz

Interval	Angle
[5 m/s, 6 m/s[	−1.3°
[6 m/s, 7 m/s[	17.0°
[7 m/s, 8 m/s[	17.6°
[8 m/s, 10 m/s[	17.3°
Average	12.7°

The following graph Figure 10.2 shows the result for the 2.0 kHz octave band.

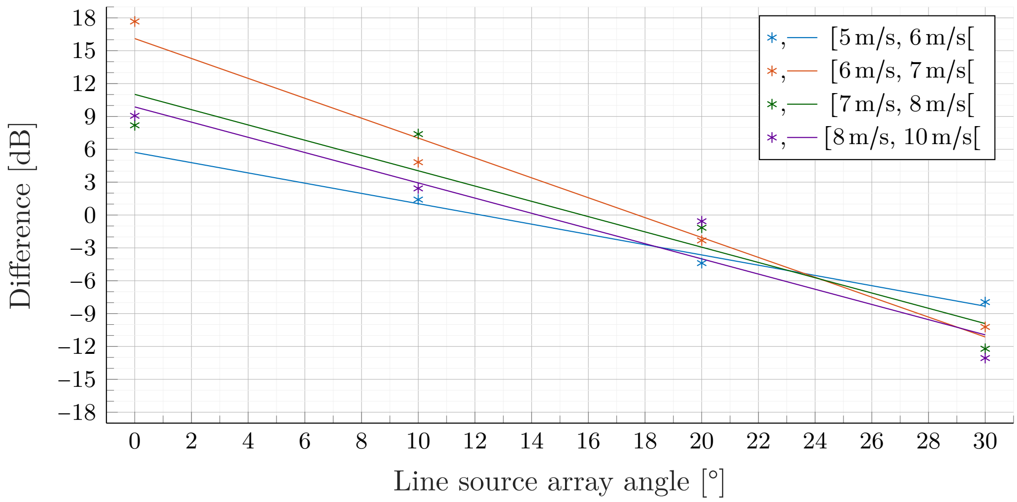

Figure 10.2: The graph shows the average 2.0 kHz octave band dB differences between the upwards and downwards microphone position calculated in section 9.4 in the given wind speed interval as a point. While the points is in the positive part of the graph, the dBis highest in the downwards microphone position. It moreover gives the linear least square fit of every wind speed interval as a line.

One measuring point in the interval [8 m/s, 10 m/s[at 20° is more that 3 dB SPL from the fitted line. The average wind direction at speaker angle 20° is 87.0° with wind speed of 9.1 m/s in the 2.0 kHz octave band frequency limit. All other measuring points in the same interval are also analysed with respect to wind speed and direction and show no deviation from the limits. Nothing indicated that these measuring points are a non-trustable measurement. In the interval [7 m/s, 8 m/s[one points excite 3 dB SPL from the fit. The average wind direction at speaker angle 10° in the 2.0 kHz is 91.8° with wind speed of 7.6 m/s. All other measuring points in the same interval are also analysed with respect to wind speed and direction and show no deviation from the limits. Nether in this measurement, the measured wind speed or wind direction is the reason that the point excites the fit by 3 dB SPL.

The following Table 10.2 gives the calculated angle based on the least square fit.

Table 10.2: The table shows the angle where the least square fit crosses the 0 dB differences between the upwards microphone and the downwards microphone in the 2 kHz octave band in the given wind speed interval

2.0 kHz	
Interval	Angle
[5 m/s, 6 m/s[	12.2°
[6 m/s, 7 m/s[	17.7°
[7 m/s, 8 m/s[	15.8°
[8 m/s, 10 m/s[	14.2°
Average	15.0°

The following graph Figure 10.3 shows the result for the 4.0 kHz octave band.

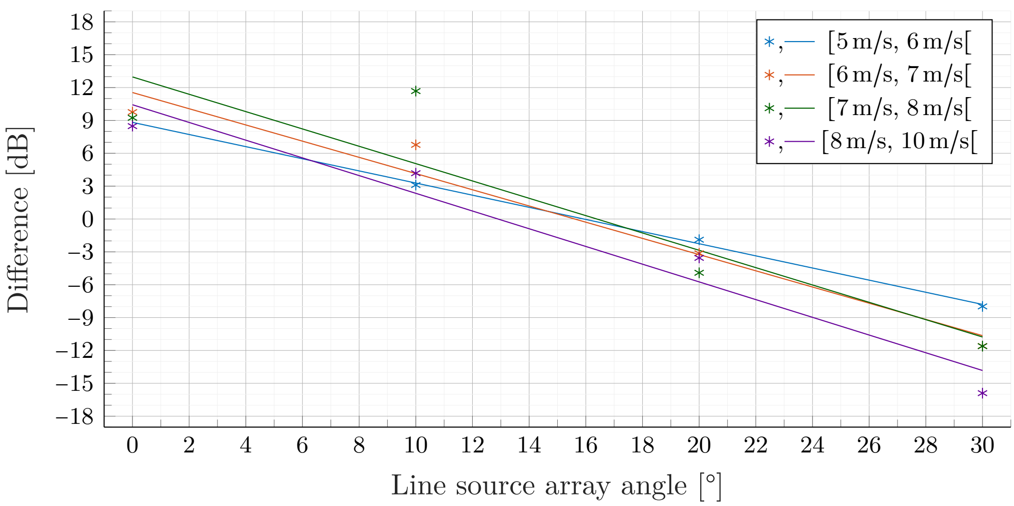

Figure 10.3: The graph shows the average 4.0 kHz octave band dB differences between the upwards and downwards microphone position calculated in section 9.4 in the given wind speed interval as a point. While the points is in the positive part of the graph, the dBis highest in the downwards microphone position. It moreover gives the linear least square fit of every wind speed interval as a line.

One measuring point in the interval [7 m/s, 8 m/s[at 20° is more that 3 dB SPL from the fitted line. The average wind angle at speaker angle 10° in the 4.0 kHz is 90.1° with wind speed of 7.8 m/s. All other measuring points in the same interval are also analysed with respect to wind speed and direction and show no deviation from the limits. In the interval [7 m/s, 8 m/s[one points excite 3 dB SPL from the fit. The average wind direction at speaker angle 0° in the 4.0 kHz is 98.3° with wind speed of 7.8 m/s. Nether in this measurement, the measured wind speed or wind direction is the reason that the point excites the fit by 3 dB SPL.

The following Table 10.3 gives the calculated angle based on the least square fit.

Table 10.3: The table shows the angle where the least square fit crosses the 0 dB differences between the upwards microphone and the downwards microphone in the 4 kHz octave band in the given wind speed interval

4.0 kHz	
Interval	Angle
[5 m/s, 6 m/s[	16.0°
[6 m/s, 7 m/s[	15.6°
[7 m/s, 8 m/s[	16.4°
[8 m/s, 10 m/s[	12.9°
Average	15.2°

The following graph Figure 10.4 shows the result for the 8.0 kHz octave band.

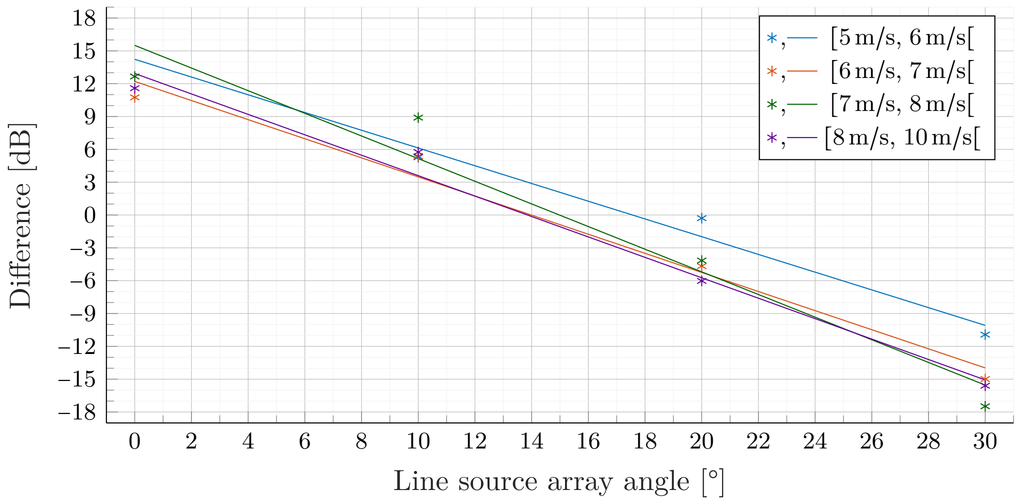

Figure 10.4: The graph shows the average 8.0 kHz octave band dB differences between the upwards and downwards microphone position calculated in section 9.4 in the given wind speed interval as a point. While the points is in the positive part of the graph, the dBis highest in the downwards microphone position. It moreover gives the linear least square fit of every wind speed interval as a line.

All data points in the graphs except of one point in the interval [7 m/s, 8 m/s[have less than ±3 dBSPL deviation from the least square fit. The average wind direction for this point with speaker angle 10° in the 8.0 kHz is 92.4° with wind speed of 7.7 m/s. All other measuring points in the same interval are also analysed with respect to wind speed and direction and show no deviation from the limits. Nether in this measurement, the measured wind speed or wind direction is the reason that the point excites the fit by 3 dB SPL.

The following Table 10.4 gives the calculated angle based on the least square fit.

Table 10.4: The table shows the angle where the least square fit crosses the 0 dB differences between the upwards microphone and the downwards microphone in the 8 kHz octave band in the given wind speed interval

8.0 kHz	
Interval	Angle
[5 m/s, 6 m/s[	17.5°
[6 m/s, 7 m/s[	14.0°
[7 m/s, 8 m/s[	15.0°
[8 m/s, 10 m/s[	13.8°
Average	15.1°

The following graph Figure 10.5 shows the result for the 16 kHz octave band.

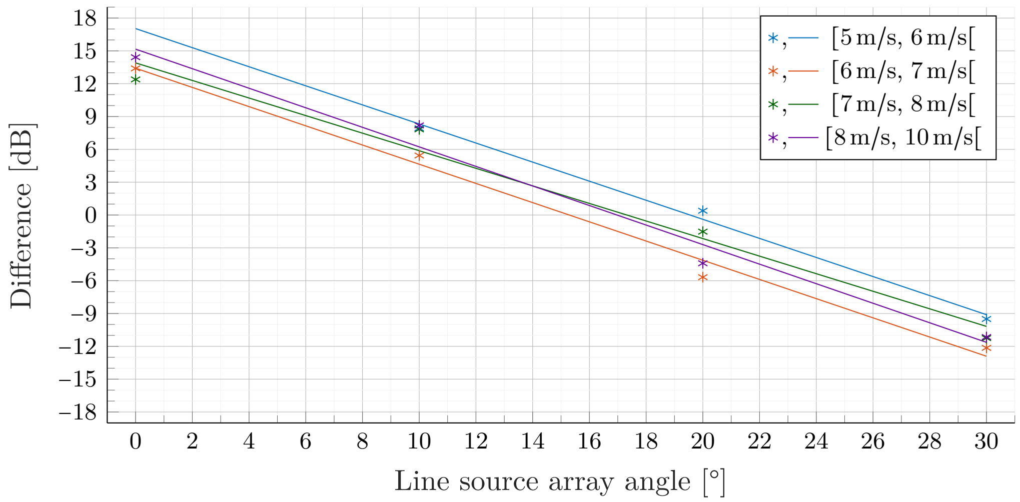

Figure 10.5: The graph shows the average 16 kHz octave band dB differences between the upwards and downwards microphone position calculated in section 9.4 in the given wind speed interval as a point. While the points is in the positive part of the graph, the dBis highest in the downwards microphone position. It moreover gives the linear least square fit of every wind speed interval as a line.

All data points in the graph have less that ±3 dBSPL deviation from the least square fit.

The following Table 10.5 gives the calculated angle based on the least square fit.

Table 10.5: The table shows the angle where the least square fit crosses the 0 dB differences between the upwards microphone and the downwards microphone in the 16 kHz octave band in the given wind speed interval

16 kHz

Interval	Angle
[5 m/s, 6 m/s[	19.6°
[6 m/s, 7 m/s[	15.3°
[7 m/s, 8 m/s[	17.3°
[8 m/s, 10 m/s[	17.0°
Average	17.3°

The mean angle for every interval is then as following Table 10.6

Table 10.6: The table shows the average optimal line source array angle between all octave band in the given wind speed interval

The angle

Interval	Average	σ	Average (discart −1.3°)	σ (discart −1.3°)
[5 m/s, 6 m/s[	12.8°	8.3°	17.3°	0.3°
[6 m/s, 7 m/s[	15.9°	1.5°	15.9°	1.5°
[7 m/s, 8 m/s[	16.4°	1.1°	16.4°	1.1°
[8 m/s, 10 m/s[	15.0°	2.0°	15.0°	2.0°
Average	15.0°		16.15°	

The former analysis is based on the least square fit for the individual octave band. One angle in the 1.0 kHz octave band shows irregular result based on all other measurements and the refraction theory. By discarding this measurement, the analysis showed a line source array angle between 12.2° to 19.6°. The average line source array angle between the octave band from each wind speed interval is shown to be between 15.0° to 17.3°. Nothing indicates that the angle is highly correlated with the wind speed in the wind speed interval from [5 m/s, 10 m/s[. As a static interval based on this calculation, the average line source array angle for all wind speed interval is 16.15°.

The following analysis of the crosswind is based on the least square fit of the data, while all data point form the octave band in one wind speed interval is used to generate one least square fit. The wind speed interval is as the former analysis. The following Figure 10.6 shows the least square fit with a box plot in the measured angle.

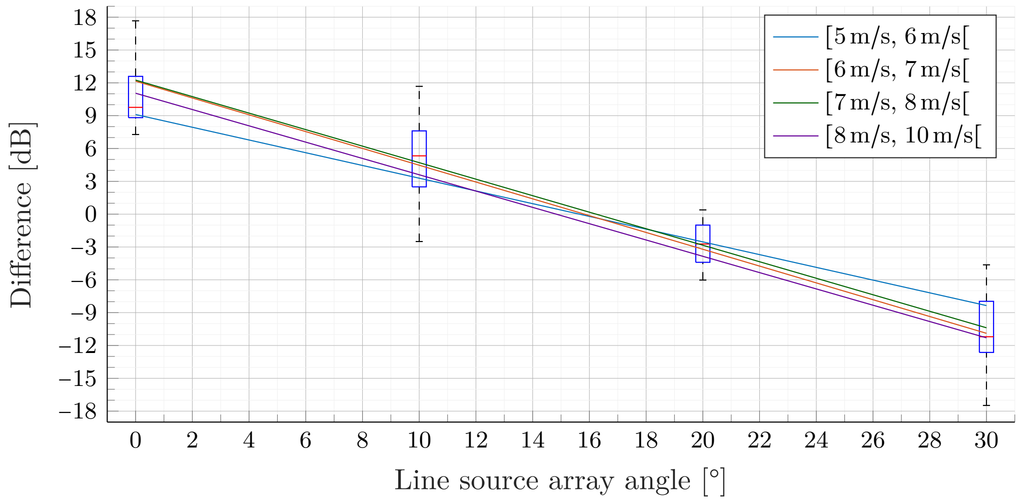

Figure 10.6: The box plot include all average dB differences of all octave band between the upwards and downwards microphone position calculated in section 9.4. The graph shows the linear least square fit of every wind speed interval as a line.

The boxes in Figure 10.6 indicate the 25th and 75th percentiles where the Whisker indicate the 99.3 % or 2.7σ of the measuring point. The red line indicates the median. It is seen that generally, the 50 % for the measurement is within an interval equal or less than 5 dB SPL and all least square fit shows a similar tendency. The 0 dB difference crosses for the optimal angle is between 14.8° to 16.2° and the differences between the upwards microphone and the downwards microphone is similar in the measured wind speed intervals, unless the [5 m/s, 6 m/s[which show slightly less slope. The lowest deviation is founded at the measured 20° angle. The following Table 10.7 shows the calculated optimal angle for every wind speed interval based on the least square fit with all octave band measurement points.

Table 10.7: The table shows the optimal line source array angle calculated as a linear square fit, while all measuring point for every wind speed interval is used

The optimal angle

Interval	Angle
[5 m/s, 6 m/s[	15.6°
[6 m/s, 7 m/s[	15.8°
[7 m/s, 8 m/s[	16.2°
[8 m/s, 10 m/s[	14.8°
Average	15.6°

The analysis showed a speaker angle between 14.8° to 16.2°. Nothing indicate that the angle have to be raise while the wind speed raises in the interval from

[5 m/s, 10 m/s[. As a static interval based on this calculation, the average angle for all wind speed interval is 15.6°.

The last crosswind analysis is based on the absolute added differences between the centre microphone and the upwards and downwards microphone. The following Figure 10.7 shows the box plot of the result and a second order least square fit of the data.

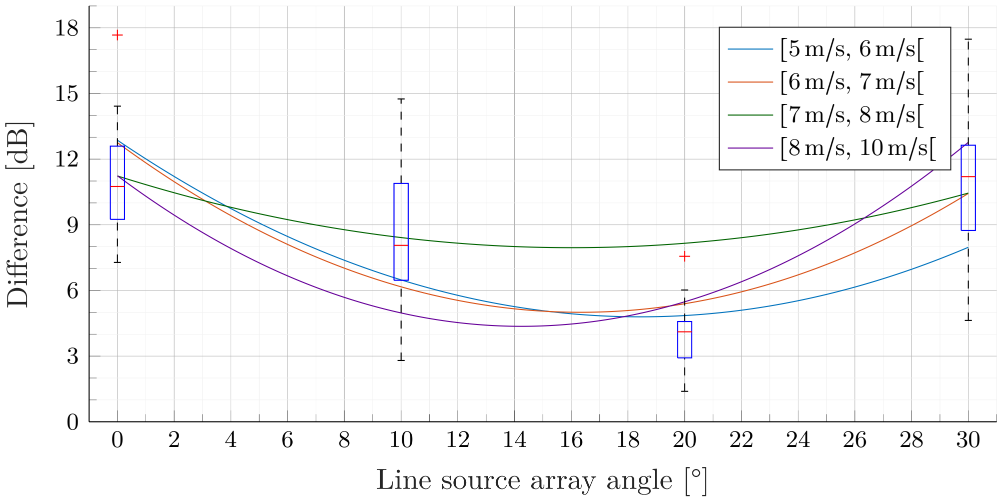

Figure 10.7: The box plot include all absolute average dB differences of all octave band between the center microphone and the upwards and downwards microphone position calculated in section 9.4. The graph shows the second order least square fit of every wind speed interval as a line.

The box plot in Figure 10.7 is calculated with the same settings as in Figure 10.6. The red plus sign indicate outliers, which is points outside 99.3 % of the measurements. The lowest deviation is also in this case in the 20° line source array angle. The second order fit shows an optimal angle between 14.4° to 16.3° line source angle angle. The blue line in the [5 m/s, 6 m/s[interval is not counted here because no data in the 0° angle is present. The mean angle in the interval [6 m/s, 10 m/s[is in this case 15.6°

10.3 Parallel wind data analysis

The parallel data analysis is only based on the approved data shown in Table 9.9. The analysis analyses the SPL measured in line source array downwards tilt angle 3° and 7° for all three microphone position. The analysis is done in the octave band as the shown data from octave band 125 Hz to octave 16 kHz.

The following Figure 10.8 shows the measurement for the front microphone.

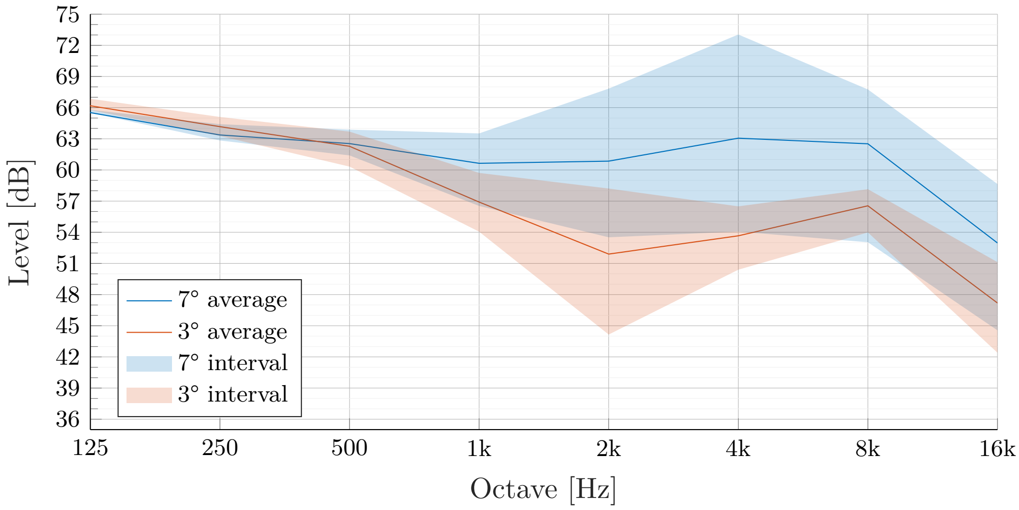

Figure 10.8: The line in the graph shows the average L_{eq} of every octave band and the shaded area shows the L_{eq} differences between all measurement at the given angle. The data is measured at the first microphone position and calculated in section 9.5

The graph in Figure 10.8 shows the average SPL as the line for both microphone and the SPL interval as the transparancy shadded area. It is seen in the graph that the average SPL is higher from 500 Hz to 16 kHz while the speaker is tilted 7°. This SPL differences can be due to two factors. If upwards refraction is present, the upwards refraction refract the sound to the microphone. It can also be due to that the while the line source array is tilted 7° the microphone is within the near-field where at the tilt angle of 3° the microphone is outside the near-field. To be able to see if it is the near-field of the refraction the following Figure 10.9 shows the measurement for the centre microphone where the microphone is within the border of the near-field while the line source array is tilted 3° and outside the near-field, while the line source array is tilted 7°.

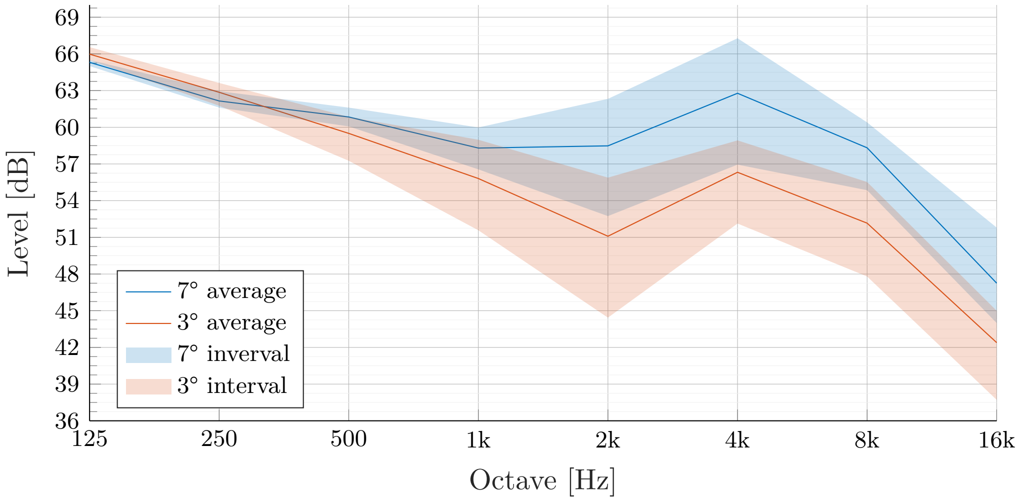

Figure 10.9: The line in the graph shows the average L_{eq} of every octave band and the shaded area shows the L_{eq} differences between all measurement at the given angle. The data is measured at the center microphone position and calculated in section 9.5

The graph in Figure 10.8 shows the average SPL as the line and the SPL interval as the transparency shaded area for the centre microphone. It is clearly seen that the upwards refraction refract the sound to the centre microphone while when the line source array point to the microphone the sound is refracted above the microphone. In this distance, more power is played into the shadow zone, or the shadow zone is moved backwards. The following Figure 10.10 shows the measurement with the back microphone.

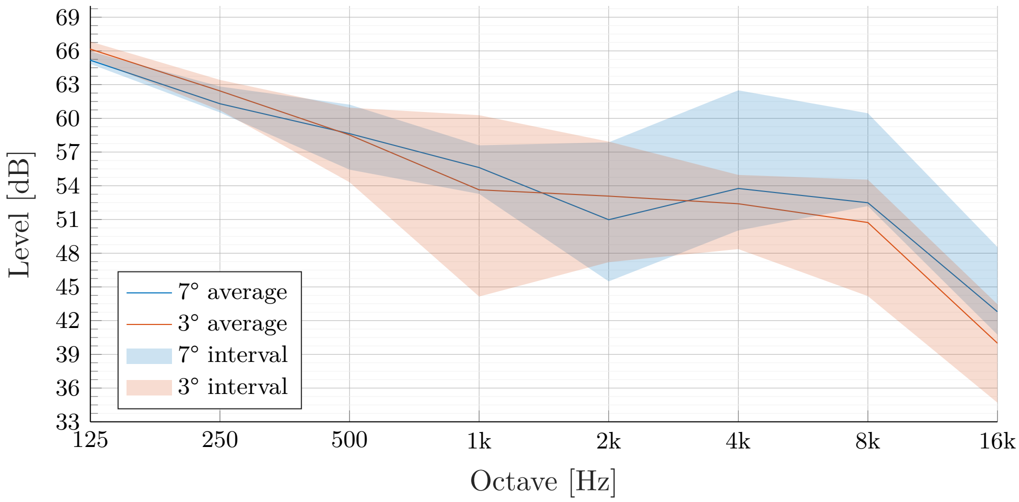

Figure 10.10: The line in the graph shows the average L_{eq} of every octave band and the shaded area shows the L_{eq} differences between all measurement at the given angle. The data is measured at the back microphone position and calculated in section 9.5

The graph in Figure 10.8 shows the average SPL as the line for and the SPL interval as the transparency shaded area for the back microphone. It is seen that the difference is less than the centre microphone but there is still generally more power in the high frequency range from 4.0 kHz and upwards.

By comparing the SPL in every microphone position while the viscosity and distance dependency loss are removed, The SPL decay with distances between the first microphone and the centre microphone from 8.0 kHz octave band and upwards. This indicates that the frequency in the 8.0 kHz and 16 kHz have entered the shadow zone area. The decay is equally in both octave band interval, which indicates that the shadow zone decay is equally for both line source array tilt angle. From the centre microphone to the back microphone the average SPL decay for the 7° tilt angle is higher than the average SPL decay for the 3°. At this measuring position, the shadow zone SPL is more equal than the other but still with more SPL while 7° tilt angle. By tilting the line source array more SPL is obtained in the shadow zone area, but the decay is equally between the front microphone and the back microphone which might indicate that the shadow zone is not moved.

Chapter 11

Discussion

The chapter discusses the observation and further research on the topic. The first observation, which is discussed is the mechanical angle stability of the line source array doing the measurements. The second observation, which is discussed is the wind interval expansion. The third part gives the authors design suggestion for rotating the speaker in windy weather. The last part gives some idea to research the measurement outliers in new measurements.

Line source array angle position stability in windy weather It is observed doing the measurement that the tilt angle of the speaker is very dynamic along with the wind speed and wind direction. While the wind speed changes the line source array swings along with the wind in the wind direction and oscillates in shallow frequency. It is observed that the tilt angle can change more than ± 1° doing a measurement. This oscillation has to be controlled in further research of line source array SPL control in windy weather. Doing the measurement in this theses, the line source array is stabilised by three rope attached underneath of the line source array and guided down to the ground in three directions. This solution stabilised the line source array to oscillate beneath ± 1°. ± 1° is an oscillation of a maximum radius of 8 cm of the laser pointer down on the measuring plate from the centre position. The half circle drawn on the angle plate has a radius on 5 cm. In the measurement, the oscillation is within this circle as the circle was drawn finished. In further research, a mechanical solution for stability is suggested.

Measurements expansion in both lower and higher wind speed It is observed in the measured crosswind data analysis result in section 10.2 that the optimal angle is between 14.8° to 17.3° depending on the optimality criteria. Moreover, it is founded that the highest line source array angle is not at the highest wind speed. The optimal angle seems to be low correlated with the speed change in the speed interval between [5 m/s, 10 m/s[. Therefore it is interesting to analyse the behaviour of the optimal line source angle in the wind speed interval of [0 m/s, 5 m/s[. It is guessed in this wind speed interval that the angle function is logarithmic. Therefore, in the lower part of the interval, the refraction differences change is highly correlated with the speed change, whereas the wind speed raises the correlation decay. The upwards and downwards refraction is due to wind speed differences concerning the hight above ground, this measurement indicates that the speed differences might be stable in the measured wind speed interval. It could furthermore be interesting to measure in higher wind speed interval to research if the measured tendency follows or change.

research the outlier The measured weather data cannot explain the outliers observed in the measurements in section 10.2. It might be due to the oscillation of the line source array or that the two wind measuring point was non-representable of those measurements or some wind turbulence. To research outliers in further research, the oscillation of the line source is suggested to be measured. Furthermore, it is suggested to use ultrasonic anemometer for the measurement, to measure more instantaneous weather condition and maybe a grid of anemometer between the line source array and the microphone. With this information, the turbulence in the wind can be measured, the wind direction is more precise in the data, and the speaker position does not change.

Design suggestion The author suggests that it is the frequency range from 700 Hz and upwards that shall be controlled by the rotation of the line source array for crosswind refraction. This frequency range covers the middle frequency driver and the high frequency driver. At least two possibilities of controlling this frequency range of rotation the line source array is possible. One solution which can be applied to all existing line source array and one solution for a full redesign of the line source element. The solution to the existing line source array is using an adaptive control of the motorized lifting chain for the line source array. By lifting the line source array in two points where the front lifting point is lifted by one chain and the back lifting point is lifted by two change fixes on the truss to the side of the line source array. By this technique, the front chain is the central lifting point, where the two back chain can move the back point from side to side as a power steering solution. For a total redesign of the line source element, the middle frequency driver and high frequency driver shall be build intro one packed as CODA audio does in their line array [audio, 2019]. Furthermore, the drivers shall be fixed such that it can be rotated inside, and the rotation fixpoint is at the mouth of the horn.

Chapter 12

Conclusions

In this chapter, a recapitulation of all results from the master theses is given. This will especially take upon the questions that were stated in chapter 4.

Measurement Design A measurement routine, which allows determining syncronised impulse response and weather information in moving inhomogeneous atmospheric condition of a sound source such as a line source array in different angle has been designed and implemented in MATLAB®section 7.3. The measurement design was tested before the final measurement is performed. The test outsourced a few difficulties, and the final measurement result is analysed.

Proposal solution It has been proposed to rotate the line source array up agents the wind to compensate for the upwards and downwards refraction while the wind is crosswind to the speaker. It has further been proposed to tilt the line source array more downwards to move the shadow zone as far back as possible while parallel wind and upwards refraction is present. It has been founded that the proposal idea is shown to obtain more homogeneous SPL in the crosswind and downwards tilting propagate more sound energy into the shadow zone. The following to paragraph concludes on the crosswind solution and parallel solution, respectively.

Crosswind It can be concluded that the line source array SPL coverage can be optimised by rotating the line source array while upwards and downwards refraction is present. The meaning of optimisation is less differences between the measured SPL between the microphone positions. The optimisation is researched in the octave band from 1.0 kHz to 16 kHz octave. This frequency range is shown to be the refracting part of the frequency range from 20 Hz and up to 20 kHz in the distance of 50 m. It is observed that the SPL at the downwards microphone position is up to 17.67 dB SPL more than at the upwards microphone position in the 2.0 kHz octave band while the line source array is not rotated. While rotating the line source array up against the wind, which means in the upwards direction, the difference is lowered from 17.67 dB to −2.32 dB while the line source array is rotated 20°. This optimisation of the SPL differences by rotating the line source array is measured in the wind speed interval of [5 m/s, 10 m/s[. wind speed above and beneath is not measured or analysed. A linear least square fit is performed on all data in the wind speed interval of [5 m/s, 8 m/s[with wind speed step of [1 m/s and one linear least square fit on the data in the wind speed interval of [8 m/s, 10 m/s[is performed to predict the optimal angle. The least square fit is performed both as single octave band fit and with all octave band for every wind speed interval. No refraction versus wind speed in the measured wind speed area is observed. The optimal angle in the average single octave band spends from 15.0° to 17.3° while 1000 dB SPL octave band linear least square fit is excluded. The execution is based on that the angle is calculated to be negative, which is highly non-realistic based on the refraction theory. The optimal static angle in this interval, while the angle is calculated as an average angle of every linear least square fit, is 16.15°. The optimal angle is also calculated based on a linear least square fit on all data for every wind speed interval. This shows a optimal angle from 14.8° to 16.2° with a average angle of 15.6°. In the end, the optimal angle is also calculated from the absolute difference from the centre microphone to the upwards microphone and the downwards microphone as a second order least square fit. This shows an optimal angle from 14.4° to 16.3° with an average angle of 15.6°.

Three methods of calculating the optimal angle are performed, 15.6° angle is predicted to give the lowest absolute difference between the centre microphone to the upwards and downwards microphone and the lowest difference between the upwards and downwards microphone while all octave band data is used to calculate the least square fit.

It is concluded that the optimal angle for the L-Acoustics KODO line source array is 15.6° up against the wind, while the wind speed is between [5 m/s, 10 m/s[and the wind direction is 90°.

Parallel wind It can be concluded that the shadow zone distance from the line source array can be optimised by tilting the line source array more downwards. It is shown that the SPL in octave band at a distances of both 40 m, 50 m and 60 m is raised while the line source array is tilted from 3° to 7°. While the array is tilted 3° the line source array near-field is pointing directly to the microphone where while the line source array is tilted 7° the near-field is in front of the microphone. Therefore, if no wind were present in the tilt angle of 3°, highest SPL is predicted. Since the highest SPL is measured in the tilt angle of 7° it can be concluded that tilting the line source array produce higher SPL in the shadow zone. The decay in SPL is equally with the tilt angle, and therefore the shadow sone might not be moved back, only the power that enters is higher.

Part IV
Appendix

Appendix A

crosswind effect on line source array

A measurement is made to measure the transfer function differences in two point in the crosswind situation. The used speaker has a horizontal dispersion pattern of 100°.

Materials and setup

To measure the transfer function in a crosswind situation, the following materials are used:

Table A.1: Equipment list

Description	Model	Serial-no	AAU-no
PC	Macbook	W89242W966H	-
Audio interface	RME Fireface UCX	23811948	108230
Microphone	GRAS 26CC	78189	75583
Preamp	GRAS 40 AZ	100268	75551
Microphone	GRAS 26CC	78186	75582
Preamp	GRAS 40 AZ	100267	75550
dB technologies	DVA T4	-	-
Wind measurement tools	Drahtlose Wetterstation	-	2157-45
flying tools	-	-	-

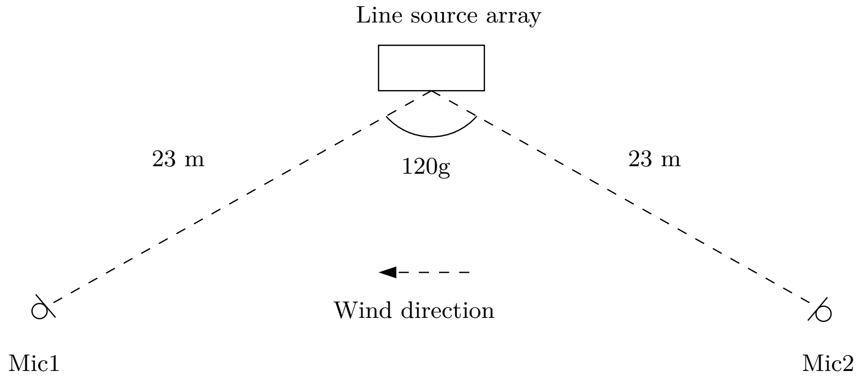

Figure A.1: The figure shows the microphone position versus the position of the line source

(a) The picture shows the speaker setup

(b) The figure shows the wind direction

Figure A.2: The figures shows the measurement set up for Appendix A

Test procedure

1. the microphone is calibrated.
2. The wind direction is measured.
3. The materials are set up as in Figure A.1 where the speaker is placed in crosswind direction, such that the frontal wave direction is orthogonal the wind. The microphone and line source array are connected to the audio interface.
4. The speaker and microphone are placed 1.1 m above the ground
5. the wind direction goes from microphone 2 to microphone 1.
6. 10 sine sweep is performed with a length of 5 s each.
7. The impulse response is calculated and filtered with a 4th order highpass filter at 300 Hz to exclude wind noise.
8. The correlation is calculated for each impulse response to the first impulse response for time alignment [Gunness, 2001] of both microphone channel.

9. The mean impulse response is calculated for the 10 measurements of both microphones.
10. The transfer function is calculated with a 40 sample moving to mean filter.
11. The measurement is repeated three times.
12. The measurement is repeated with an angle of 74° and a distance of 25 m for both microphone.

Measurement area

To be able to measure in a windy area, the football stadium at Fredrick Alfred Nobels Vej 7, 9220 Aalborg is used. The following Figure A.3 shows a picture of the area and the approximate position of the speaker and microphone.

Figure A.3: The picture illustrate the area, where the wind flow is measured

Results

The wind speed was 14 m/s for each measurement and the temperature was 5°. The humidity was not measured.

The following measurement shows the result for 120°

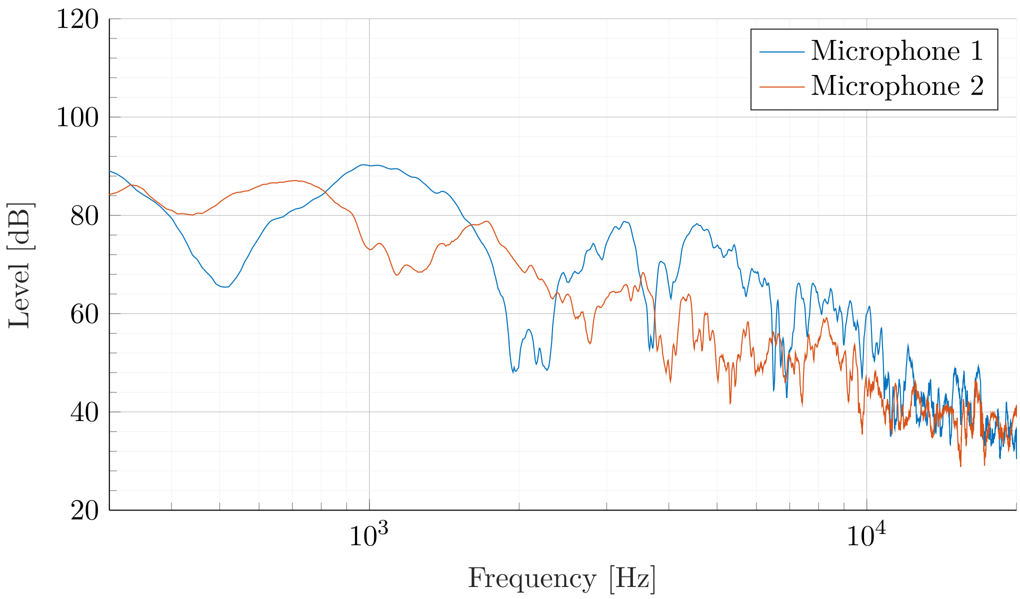

Figure A.4: The graph shows the first transfer function measurement. The $L_{\mathrm{eq},5}$ Sound Pressure Level (SPL) different between the microphones is 5.49 dB SPL (IR_6)

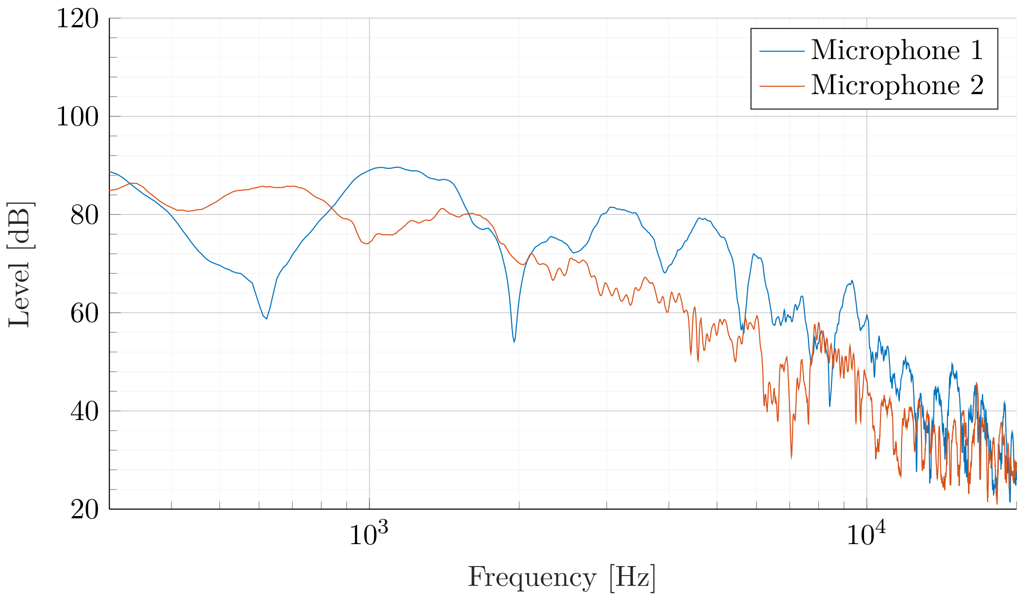

Figure A.5: The graph shows the second transfer function measurement. The $L_{\mathrm{eq},5}$ SPL different between the microphones is 4.40 dB SPL (IR_7)

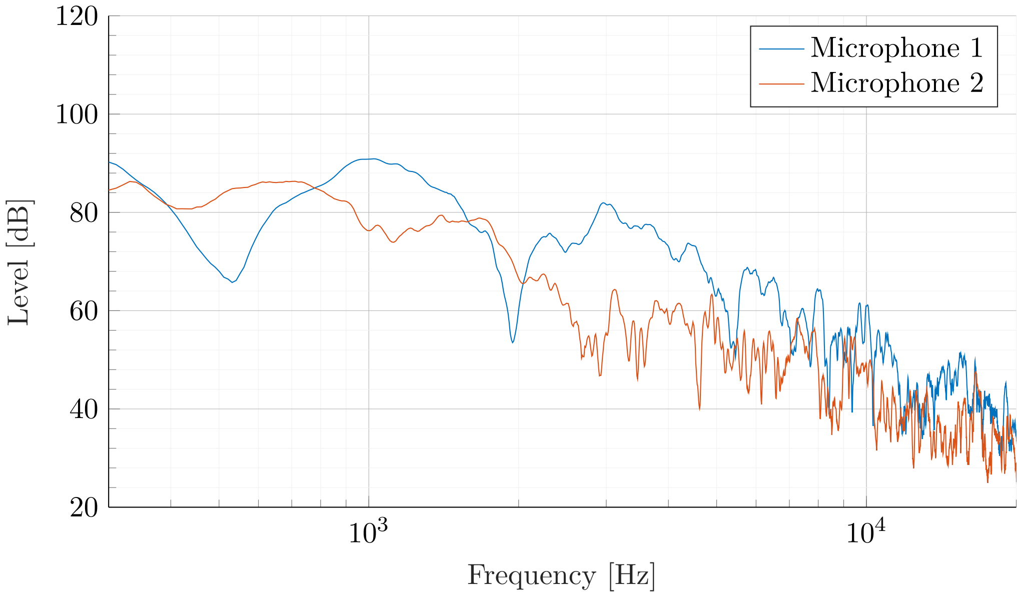

Figure A.6: The graph shows the third transfer function measurement. The $L_{eq,5}$ SPL different between the microphones is 4.23 dB SPL (IR_8)

On Figure A.4, Figure A.5 and Figure A.6 it is seen that the general pressure is higher for microphone 1. It is also seen that ground reflection effect is much higher on microphone 1 than microphone 2. This support the theory about upwards refraction of sound wave on microphone 2 and downwards refraction on microphone 1

The following measurement shows the result for 74°

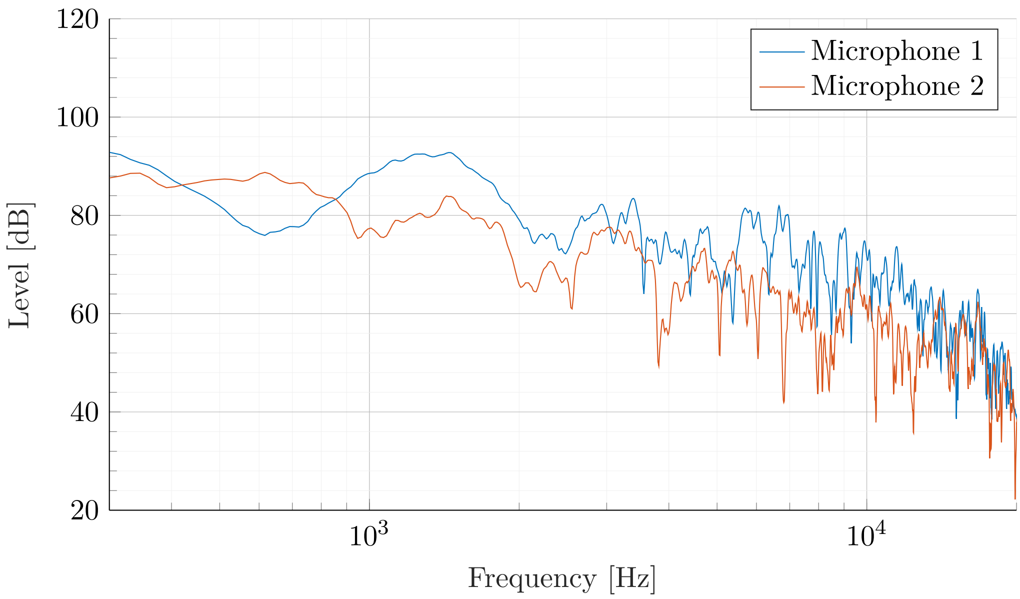

Figure A.7: The graph shows the first transfer function measurement. The $L_{\mathrm{eq},5}$ SPL different between the microphones is 4.41 dB SPL (IR_3)

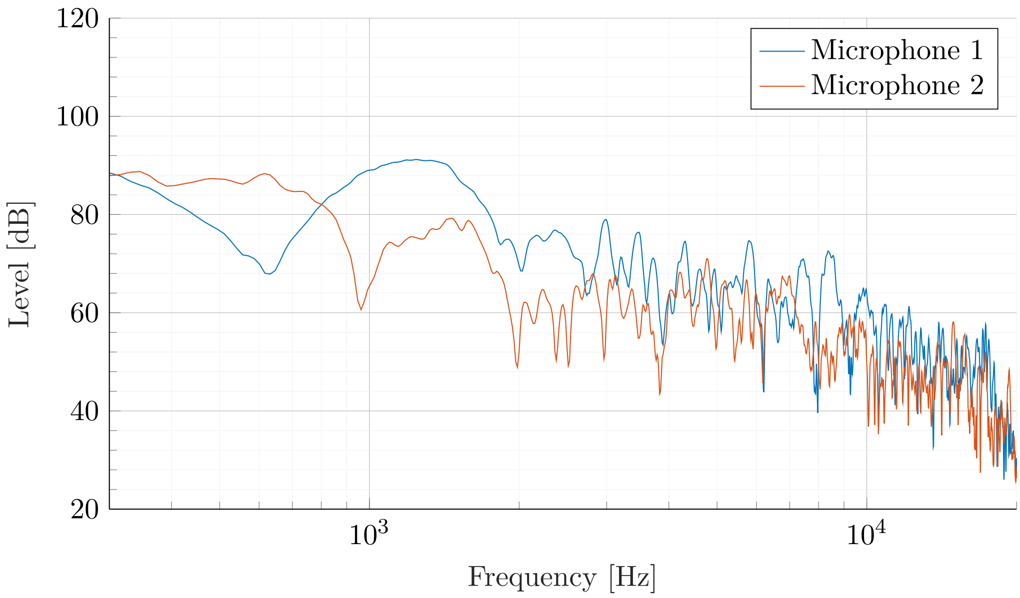

Figure A.8: The graph shows the second transfer function measurement. The $L_{\mathrm{eq},5}$ SPL different between the microphones is 4.81 dB SPL (IR_5)

On Figure A.7 and Figure A.8 it is seen that the general pressure is higher for microphone 1. It is also seen that ground reflection effect is much higher on microphone 1 than microphone 2. This support the theory about upwards refraction of sound wave on microphone 2 and downwards refraction on microphone 1

Appendix B

Design of windscreen

The idea of an additional windscreen is to stop the wind in just at the microphone position with a blocking and non-reflecting surface. The surface shall, therefore, be able to lower the wind speed at the microphone position and have less reflection as possible. The original windscreen is kept on the microphone.

The first two windscreen concept is very identical but just with different size of the material. The idea for the first windscreen is to seal the microphone with foam all around except at the frontal direction. The frontal direction include both 180° angle in the vertical direction and 90° in the horizontal direction. The reason to have a narrow horizontal opening is to be able to get sound inside the opening but still, have a wind-stopping effect. The following Figure B.1 illustrate both windscreen configuration one and windscreen configuration two, just with one size foam wedge.

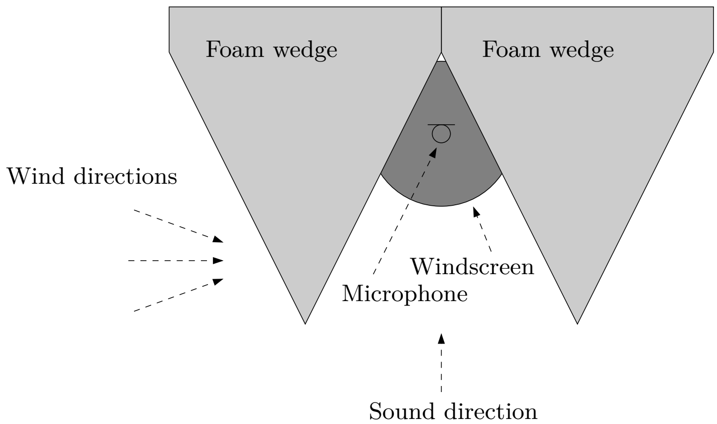

Figure B.1: The figure shows the foam wedge concept. The concept is covering over to different foam wedge, ether two small or too large. The small concept is defined as windscreen configuration one, where the large concept is defined as windscreen configuration two.

The next concept build on the concept in Figure B.1 just with plan surfaces rockwool plates. The opening is also 180° angle in the vertical direction and 90° in the horizontal direction. The concept is defined as windscreen configuration three. The following Figure B.2 illustrate the concept.

The next concept builds on minimizing the reflection from the additional windscreen by only placing the microphone close against one surface, which covers for the wind noise. The concept is defined as windscreen configuration four. The following Figure B.3 illustrate the concept.

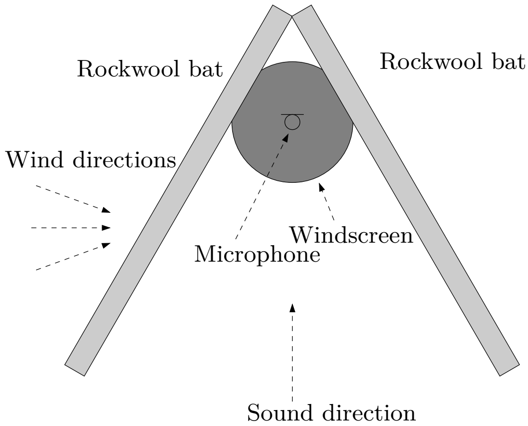

Figure B.2: The figure shows the rockwool concept. This concept is defined as windscreen configuration three.

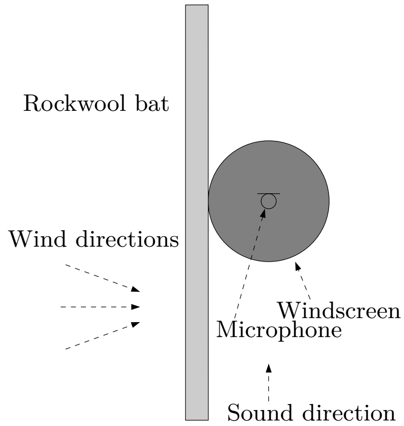

Figure B.3: The figure shows the single rockwool concept. This concept is defined as windscreen configuration four.

Before the optimal windscreen configuration is founded, an optimality criterion is defined, and a test is designed. The optimal criteria for the windscreen are as low wind noise as possible at the microphone position and low sound reflection. To find the windscreen configuration which meets the criteria best, three tests are made on the windscreen configuration. First, the wind speed attenuation of the windscreen configuration is measured to ensure that the windscreen configuration concept does affect the wind speed. Secondly, the frequency response of the windscreen has to be founded to ensure that the windscreen configuration does not have a large influence on the frequency measurement response of the speaker. To test these criteria, the frequency response of a speaker is measured in the anechoic chamber without any windscreen configuration and without the original windscreen. This measurement is compared with the frequency response of the speaker with the windscreen configuration. Finally, the wind noise is measured. To measure the wind noise two low speed and low noise fan is generating 2.5 m/s at the microphone position. The wind noise is measured without any windscreen configuration and the original windscreen and compared with the wind noise in the microphone position in the windscreen configuration. To ensure that the background noise is identically on the wind noise measurement with and without the windscreen configuration two microphones are used and recorded simultaneously. Both the time signal and the frequency content is analysed. The wind speed attenuation is founded in Appendix E. The wind noise attenuation is founded in Appendix C. The frequency response is founded in Appendix D

The result for all configuration is as follows.

Configuration one is the one with the smallest foam wedge and size of the wedge is measured to have the worst wind attenuation. The wind attenuation shows that the wind speed is lowered from 8 m/s to 2 m/s. However, the directional turbulence in the wind is more stable in this configuration compare the configuration three and above. The frequency response of the windscreen configuration is the one that has the lowest effect. At low frequency, up to 100 Hz, the windscreen does not affect the measurement. The frequency above 100 Hz gets off with about 2 dB SPL compare with only the original windscreen. The measured wind noise attenuation is equal to zero. In the measurement, the wind noise is a bit worse compared to only the original windscreen. The attenuation is both approximately 10 dB SPL for both with only the original windscreen and the windscreen configuration in the low frequency below 10 Hz, but at some frequency, the attenuation is lower that 5 dB SPL for the windscreen configuration. For frequency above 10 Hz, the windscreen configuration does not affect.

Configuration two is the one with the largest foam wedge and is measured to have one of the best wind speed and noise attenuations. The wind attenuation shows that the wind speed is lowered from 8 m/s to 1 m/s and have less peek in the wind speed compare to the windscreen with Rockwool. The directional turbulence in the wind is more stable in this configuration compare the configuration three and above, but little less stable compared to configuration one. The frequency response of the windscreen configuration has an amplification in the low frequency range from 80 Hz to 600 Hz of 2 dB SPL. From 1.0 kHz and above the frequency response is very similar compared to only the original windscreen. At low frequency up to 80 Hz, the windscreen does not affect the measurement much. The windscreen attenuates the wind noise 10 dB SPL more than only the original windscreen from 30 Hz and downwards to the measured limit at 2 Hz. The frequency range between 30 Hz and 600 Hz have the same attenuation as the original windscreen, and the frequency above have further 10 dB SPL more attenuation than the original windscreen.

Configuration three is the one with two Rockwool bat formed as an arrow and is measured to have wind attenuation between the small wedge and large wedge. The frequency response of the windscreen configuration is the worst. It alternates between ±6 dB SPL. At the low frequency range from 80 Hz to 600 Hz the amplification goes from 2 dB SPL at 80 Hz to 6.2 dB SPL at 250 Hz and then back to 0 dB SPL at 700 Hz. At 1.0 kHz the attenuation is at 6 dB SPL and above the frequency response alternate around the frequency response of the original windscreen. The windscreen attenuates the wind noise 10 dB SPL more than only the original windscreen from 30 Hz and downwards to the measured limit at 2 Hz. The frequency range between

30 Hz and 600 Hz have the same attenuation as the original windscreen, and the frequency above have further 5 dB SPL to 10 dB SPL more attenuation than the original windscreen. Based on that the frequency response and the wind noise attenuation is worse than configuration two, the configuration is excluded.

Configuration four is the one with only one Rockwool bat where the microphone is situated close to the side of the windscreen and is measured to have one of the best wind speed attenuations. The wind attenuation shows that the mean wind speed is lowered from 8 m/s to 1 m/s, but the directional and wind speed turbulence is less stable compared to the configuration the windscreen with a foam wedge. The wind speed turbulence circulate from 0 m/s to 2 m/s. The frequency response of the windscreen configuration does not change more than approximately ±2 dB SPL in the low and high frequency range. The noise attenuation is not measured in this configuration since the mechanical stability is founded to be poor in wind speed above 5 m/s.

Based on the finding above, the final windscreen concept is designed. The design of the final windscreen concept combines configuration two to and configuration four, where the stability problem is solved.

As the first test of the final windscreen solution, a preliminary setup is done with the available material in the acoustics lab. The preliminary setup is defined as windscreen configuration five. The following Figure B.4 illustrate the concept.

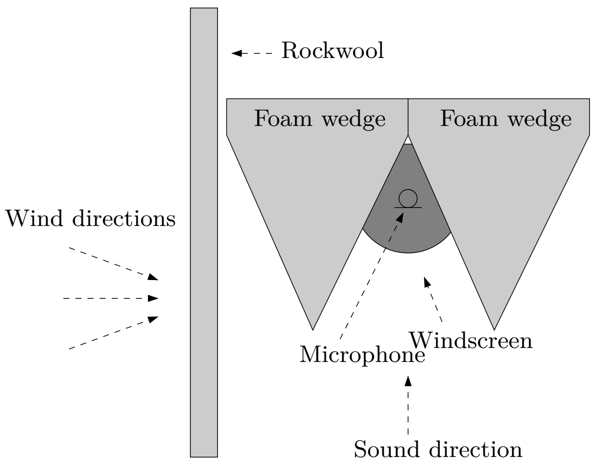

Figure B.4: The figure shows the final windscreen concept. This concept is defined as windscreen configuration five.

This configuration is measured to have more wind speed attenuation that this combination apart. The wind speed attenuation shows that the mean wind speed is lowered from 8 m/s to 0.8 m/s, but the directional turbulence is less stable compared to the configuration the windscreen with only foam wedge. The frequency response of the windscreen configuration is as configuration two but with a little closer fit to without windscreen in the high frequency.

Appendix C

Wind noise attenuation of windscreen

A measurement is made to measure the wind attenuation of difference windscreen configuration. All configuration includes the GRAS AM0069 windscreen with an additional wind stopper surface all around the microphone except the frontal direction. The measurement is done as a preliminary test with low wind speed to test the concept.

Materials and setup

To measure the wind attenuation of the windscreen configuration the following materials are used:

Table C.1: Equipment list

Description	Model	Serial-no	AAU-no
PC	Macbook	W89242W966H	-
Audio interface	RME Fireface UCX	23811948	108230
Microphone	GRAS 26CC	78189	75583
Preamp	GRAS 40 AZ	100268	75551
Microphone	GRAS 26CC	78186	75582
Preamp	GRAS 40 AZ	100267	75550

Table C.2: Equipment list

Description	Model	Serial-no	AAU-no
Fan	IMPEGA	-	-
Fan	IMPEGA	-	-
Windscreen	GRAS AM0069	-	-
Windscreen	GRAS AM0069	-	-
large foam wedge	-	-	-
Small foam wedge	-	-	-
Rockwool bat	-	-	-

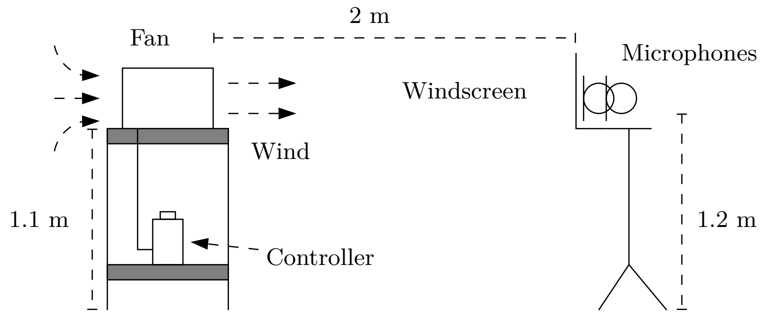

Figure C.1: The figure shows the measurement setup for the wind noise measurement in the microphone position and outside the windscreen. The two microphone seems to lay onto each other but it shall show that one is inside the windscreen and one is outside the windscreen

Figure C.2: The picture shows the measurement set up

Test procedure

1. The materials are set up as in Figure C.1 where the two microphone connected to the audio interface.

2. Both microphones are calibrated.
3. Both fans is activated
4. A 7 s time signal is measured three times synchronise on both microphones.
5. The frequency content is calculated by `fft` on all six measured time signal.
6. The average of the frequency response for each microphone is calculated
7. The difference between the microphone is calculated to find the attenuation of the windscreen configuration
8. The procedure is done for all windscreen configuration and one where no additionally wind stopper is added around the microphone. This last configuration is defined as the reference configuration.
9. A no wind measurement is measured the same way just without the fan activated and only with GRAS AM0069 windscreen in the end.
10. The wind speed is measured.

Measurement area

To be able to generate a controlled wind flow, the hallway in Fredrick Bajers vej 7B5, 9200 Aalborg is used. The following Figure C.3 shows a drawing of the area and the position of the fan and windscreen.

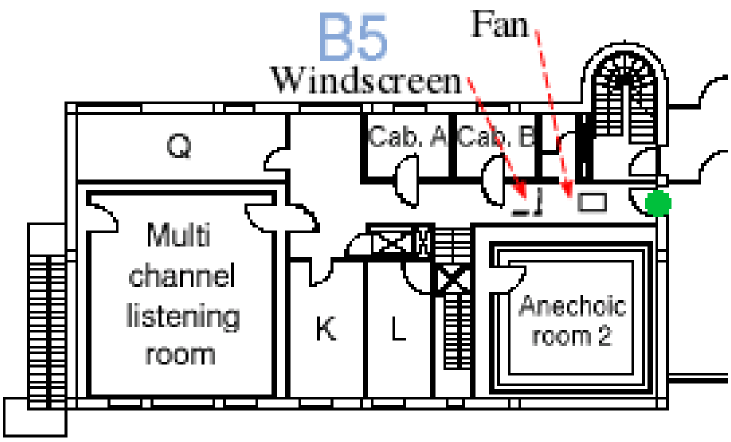

Figure C.3: The picture illustrate the area, where the wind flow is measured

Results

The following graphs show the result of the measurements. The wind speed is measured to be 2.5 m/s.

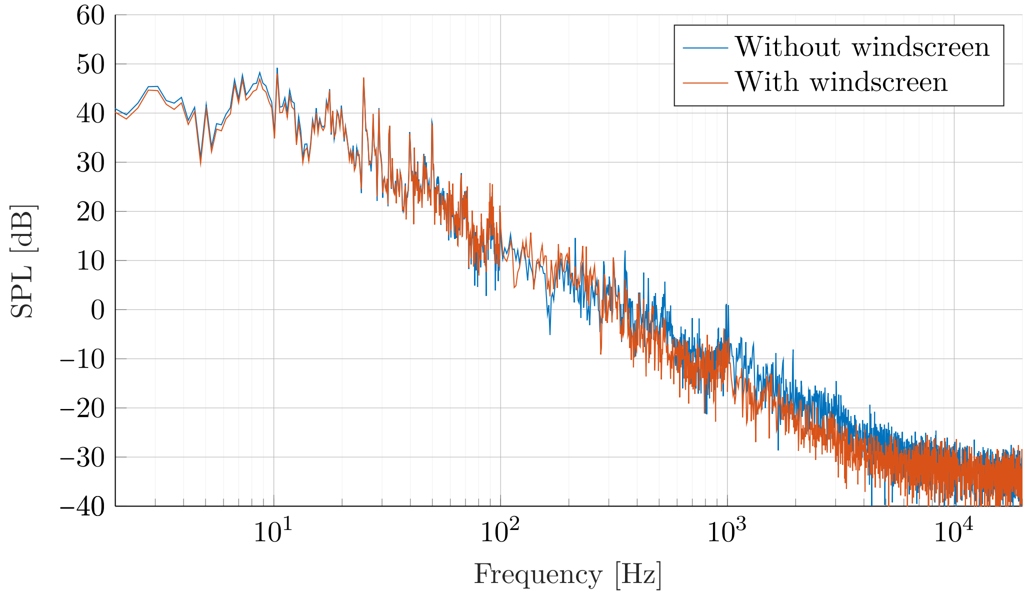

Figure C.4: The graph shows the frequency content without the fan activated

The Figure C.4 shows the frequency content in the measuring area without the fan activated for both microphone and the reference windscreen configuration.

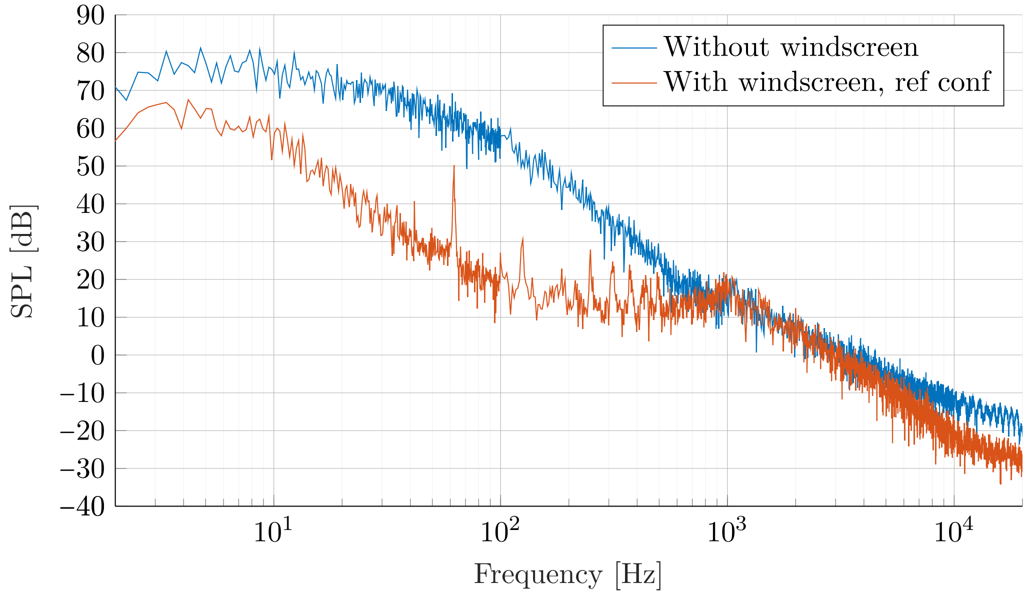

Figure C.5: The graph shows the frequency content with the fan activated

The Figure C.5 shows the frequency content in the measuring area with the fan activated for both microphone and the reference windscreen configuration. It is seen that the highest attenuation is at 900 Hz but the general attenuation is

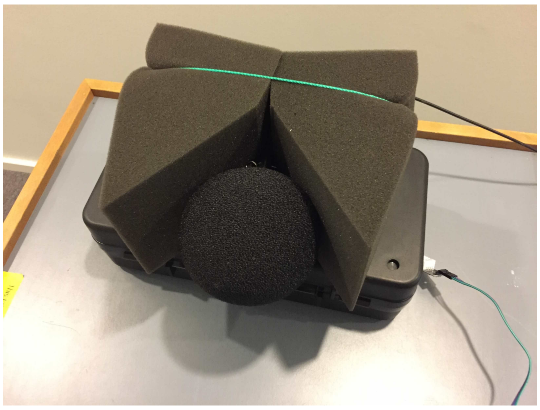

Figure C.6: The picture shows the microphone covered with windscreen and the Small foam wedge windscreen configuration. This configuration is defined as configuration one

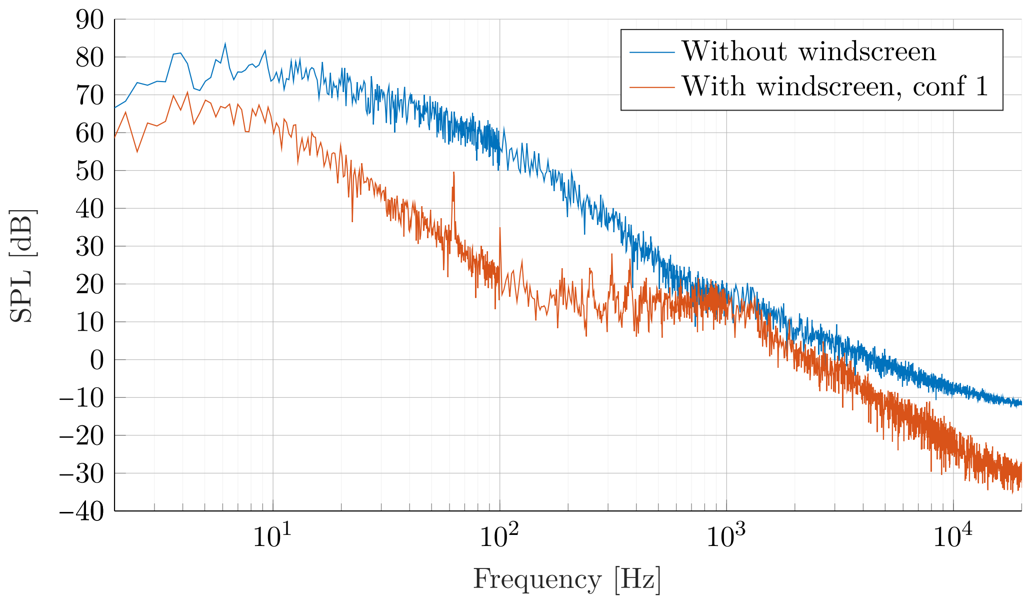

Figure C.7: The graph shows the frequency content of the measurement with configuration one

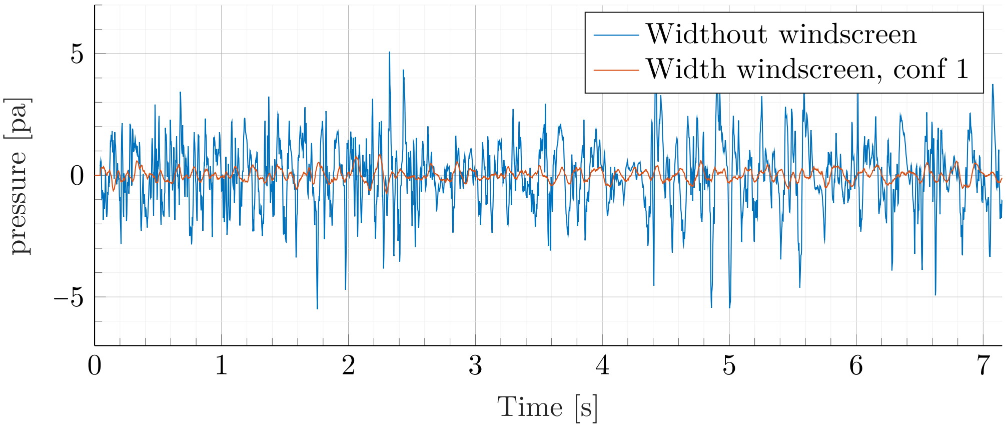

Figure C.8: The graph shows one of the time measurement with configuration one

The Figure C.7 and Figure C.8 shows the measurement with configuration one in frequency and time domain respectively. It can be seen that the general windscreen attenuation is not lowered compared to the reference windscreen measurement.

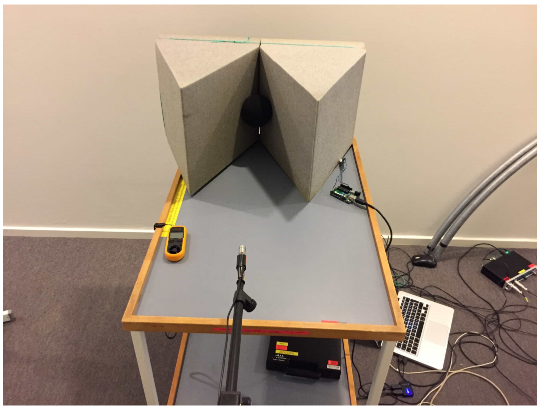

Figure C.9: The picture shows the microphone covered with windscreen and the large foam wedge windscreen. This configuration is defined as configuration two.

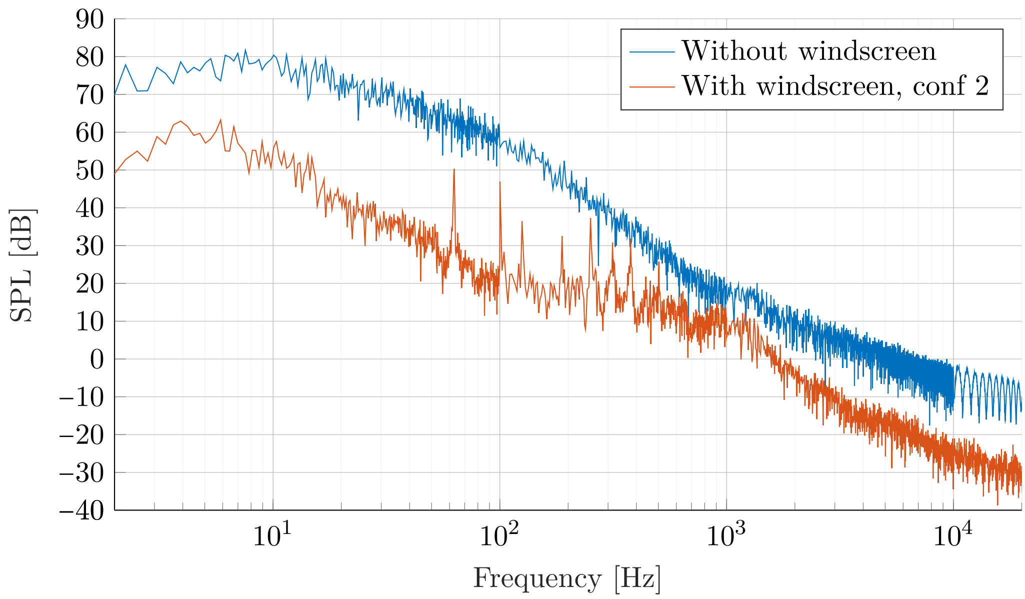

Figure C.10: The graph shows the frequency content of the measurement with configuration two

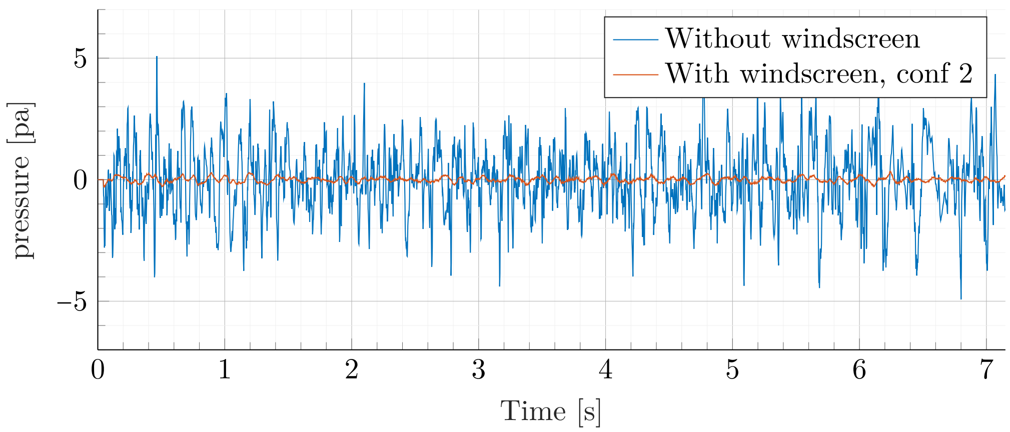

Figure C.11: The graph shows one of the time measurement with configuration two

The Figure C.10 and Figure C.11 shows the measurement with configuration two in frequency and time domain respectively. The measurement shows that the windscreen attenuation does have an effect compare to the reference windscreen measurement. The attenuation is nearly greater for all frequency especially in the low and high frequency range.

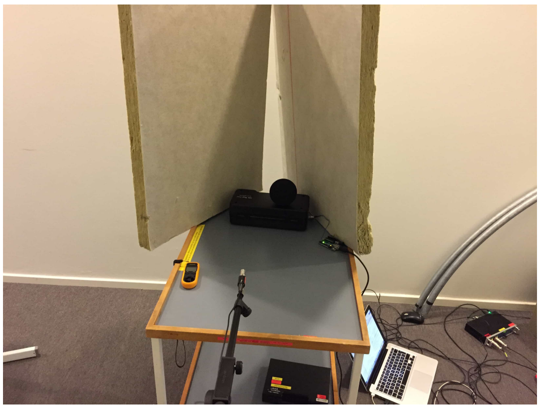

Figure C.12: The picture shows the microphone covered with windscreen and the Rockwool wind stopper. This configuration is defined as configuration three.

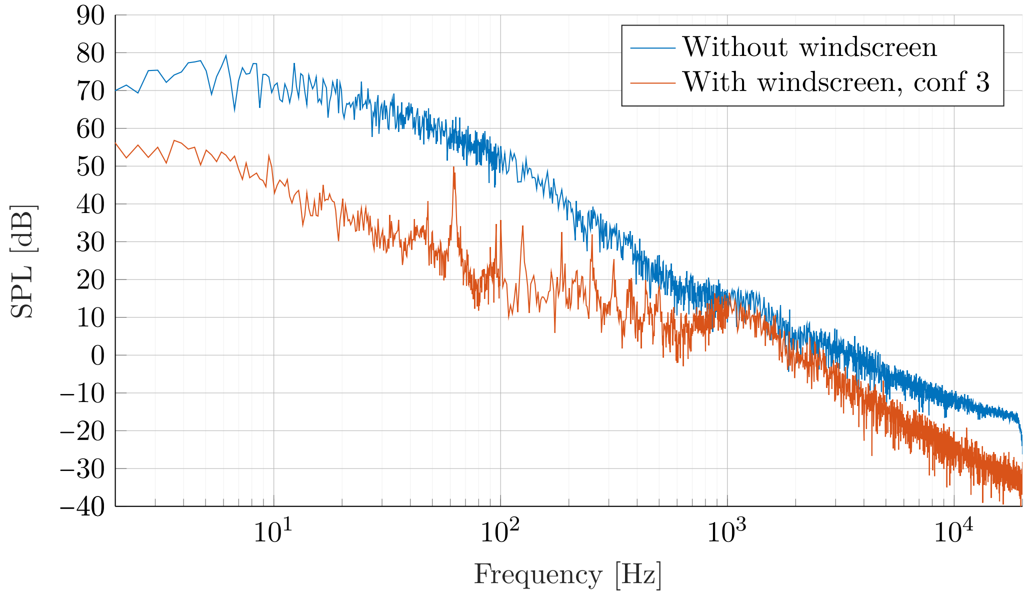

Figure C.13: The graph shows the frequency content of the measurement with configuration three

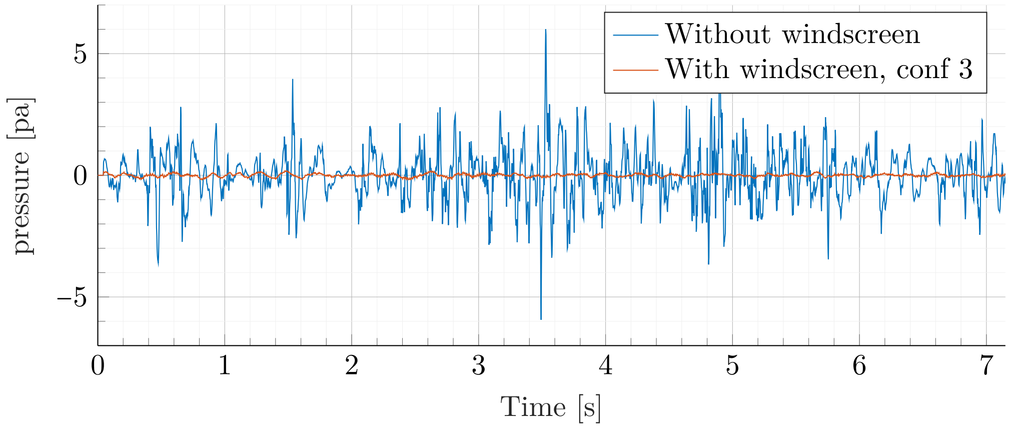

Figure C.14: The graph shows one of the time measurement with configuration three

The Figure C.13 and Figure C.14 shows the measurement with configuration three in frequency and time domain respectively. The measurement shows that the windscreen attenuation does affect compare to the reference windscreen measurement, but the attenuation is not as good as in configuration two. There is better attenuation is the low frequency compared to the reference windscreen measurement, but in the high frequency, the attenuation is worse than the reference windscreen measurement, that might be due to reflection on the surface of the Rockwool.

Appendix D

Windscreen response measurement

A measurement is made to measure the frequency response of difference windscreen configuration. All configuration includes the GRAS AM0069 windscreen with an additional wind stopper surface all around the microphone except the frontal direction. The measurement is done in the anechoic chamber. The measurement is done to analyse the effect of the windscreen in the frequency domain to ensure that the chosen windscreen does not add reflect on the measurement. The optimal criteria, therefore as profound difference as possible.

Materials and setup

To measure the frequency response of the windscreen configuration the following materials are used:

Table D.1: Equipment list

Description	Model	Serial-no	AAU-no
PC	Macbook	W89242W966H	-
Audio interface	RME Fireface UCX	23811948	108230
Microphone	GRAS 26CC	78189	75583
Preamp	GRAS 40 AZ	100268	75551
Windscreen	GRAS AM0069	-	-
large foam wedge	-	-	-
Small foam wedge	-	-	-
Rockwool bat	-	-	-

Table D.2: Equipment list

Description	Model	Serial-no	AAU-no
Speaker stand	-	-	-
Speaker stand	-	-	-
Speaker	Dynaudio	03508438	1441-0

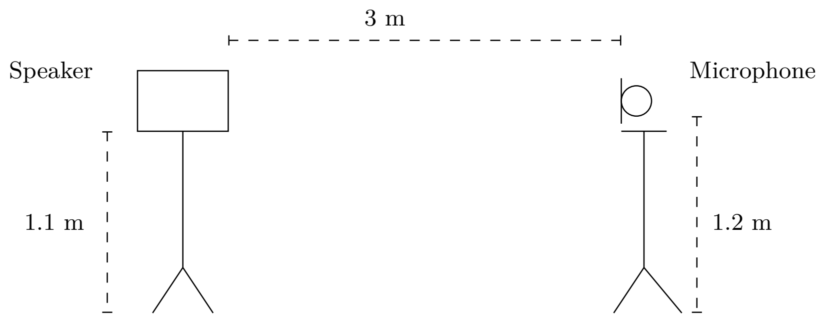

Figure D.1: The figure shows the measurement setup in the anechoic chamber

Test procedure

1. The materials are set up as in Figure D.1 where the microphone is connected to the audio interface.
2. The microphone is calibrated
3. The speaker is placed 3 m from the microphone and pointing in the direction of the microphone.
4. The windscreen configuration is placed such that the microphone has approximately the same position as without the windscreen.
5. The transfer function is measured
6. The procedure is started over until all windscreen is measured.
7. The transfer function is calculated and plotted versus the transfer function without windscreen MATLAB®.
8. The difference between the transfer function with and without windscreen is calculated and plotted in MATLAB®.

Measurement area

To be able to measure the windscreen frequency response, the anechoic chamber in Fredrick Bajers vej 7B4, 9220 Aalborg is used. The following Figure D.2 shows a drawing of the area and the position of the fan and windscreen.

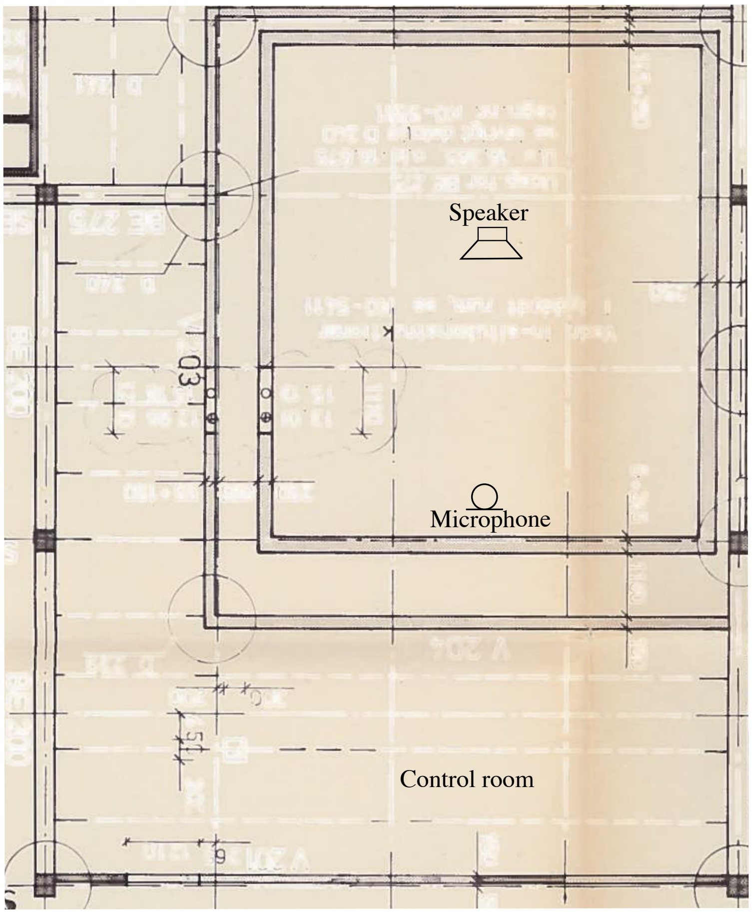

Figure D.2: The picture illustrate the area, where the wind flow is measured

Results

The following Figure D.3 shows the speaker.

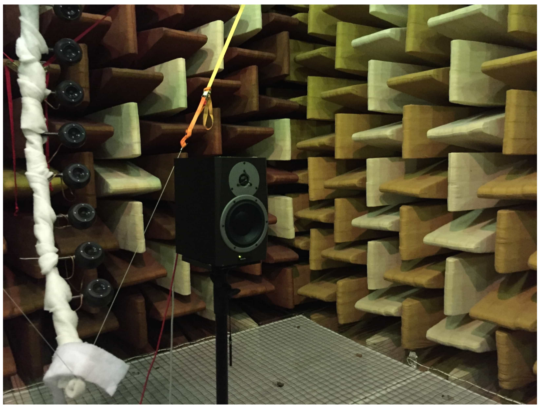

Figure D.3: The picture shows the used speaker

The following graphs shows the result of the measurement.

Figure D.4: The picture shows the measurement microphone with the original windscreen

The measurement shown in Figure D.5 shows frequency response of the speaker with and without the windscreen. The Figure D.4 shows the microphone position with the windscreen. The position is not changed for the measurement without windscreen.

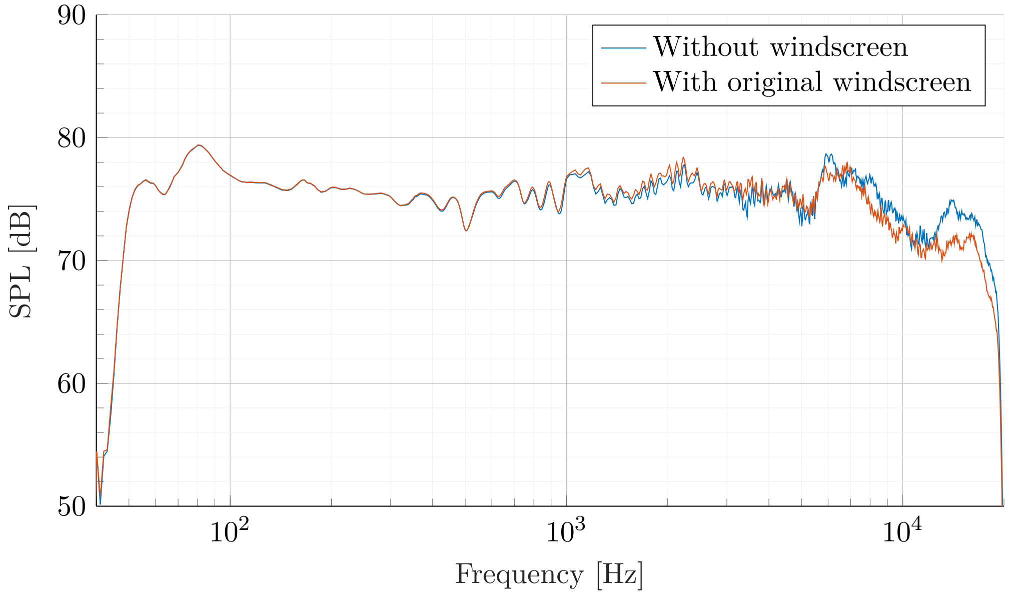

Figure D.5: The graph shows frequency response of the speaker measured without windscreen and with the original windscreen

The measurement shown in Figure D.6 shows the difference SPL between the measurement with and without original windscreen.

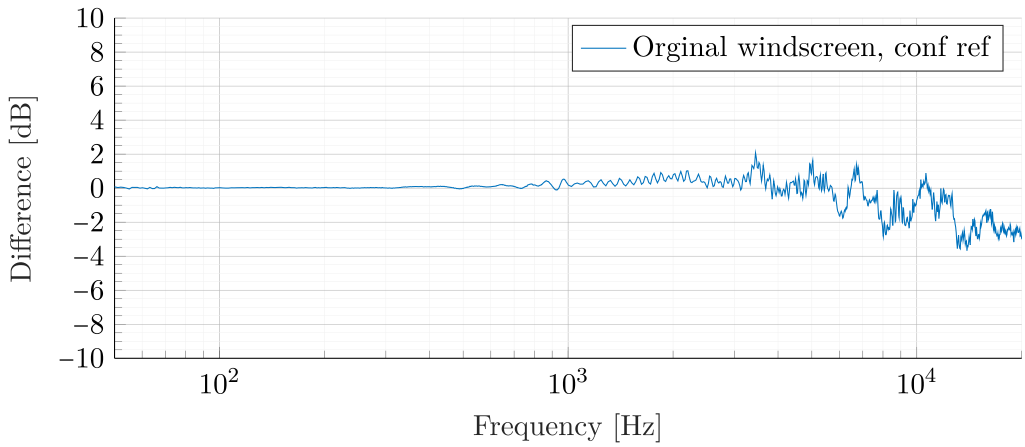

Figure D.6: The graph shows frequency response of the windscreen, where the frequency characteristic for the speaker is out calculated.

Figure D.7: The picture shows the measurement microphone with the large foam wedge configuration two

The measurement shown in Figure D.8 shows the difference in frequency response of the speaker without the windscreen and with the windscreen configuration one. The Figure D.7 shows the measured set up.

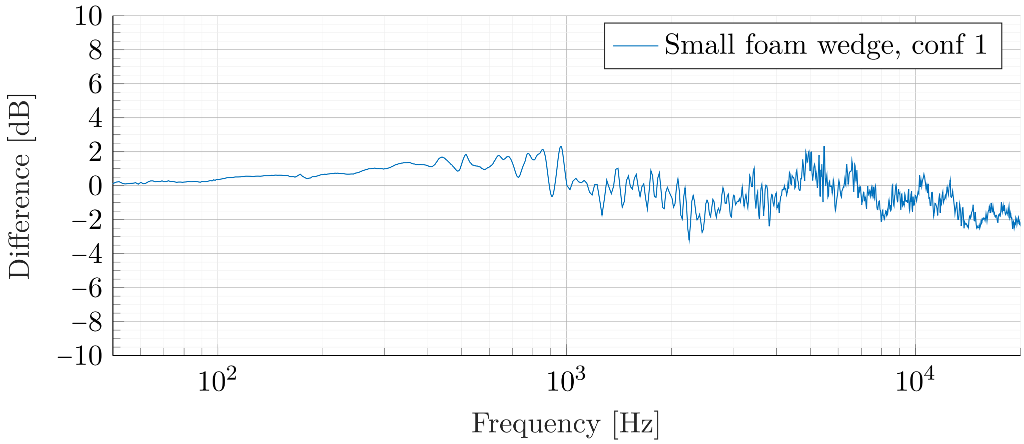

Figure D.8: The graph shows frequency response of the windscreen, where the frequency characteristic for the speaker is out calculated.

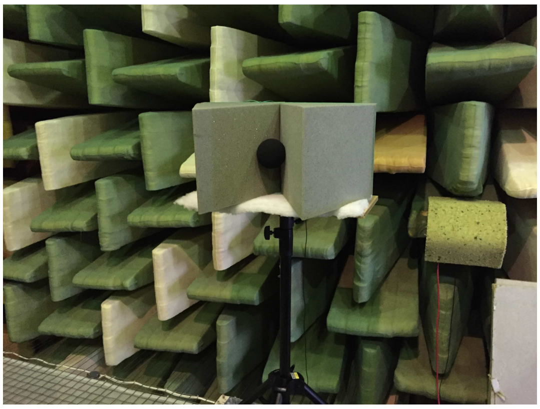

Figure D.9: The picture shows the measurement microphone with the large foam wedge configuration two

The measurement shown in Figure D.10 shows the difference in frequency response of the speaker without the windscreen and with the windscreen configuration two. The Figure D.9 shows the measured set up.

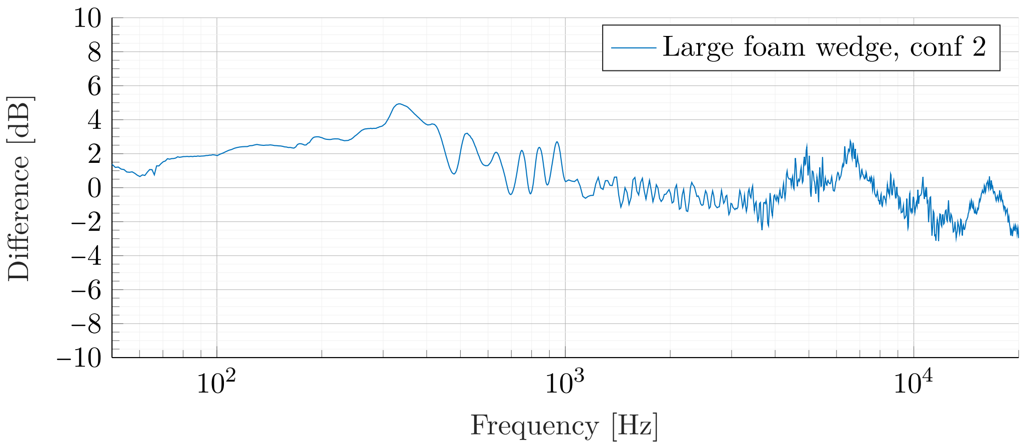

Figure D.10: The graph shows frequency response of the windscreen, where the frequency characteristic for the speaker is out calculated.

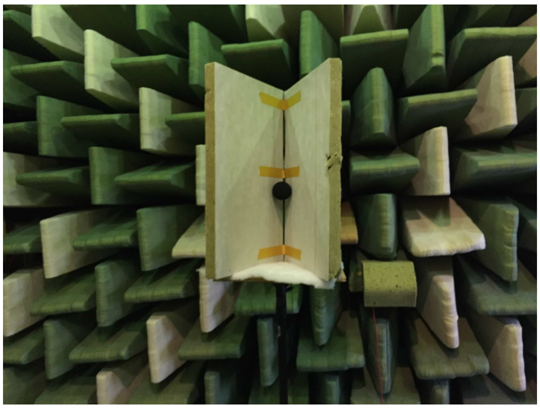

Figure D.11: The picture shows the measurement microphone with the Rockwool bat configuration three

The measurement shown in Figure D.12 shows the difference in frequency response of the speaker without the windscreen and with the windscreen configuration three. The Figure D.11 shows the measured set up. In this measurement both the speaker and the microphone is lifted 20 cm

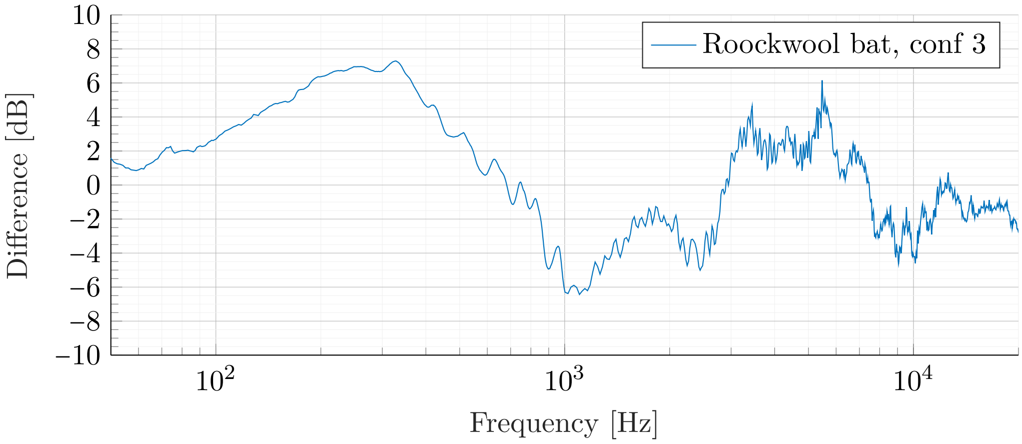

Figure D.12: The graph shows frequency response of the windscreen, where the frequency characteristic for the speaker is out calculated.

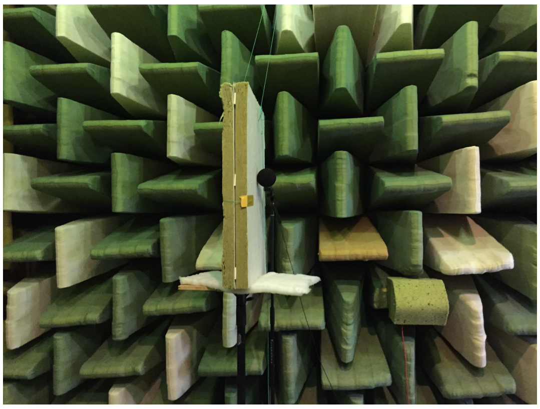

Figure D.13: The picture shows the measurement microphone with the Rockwool bat configuration four

The measurement shown in Figure D.14 shows the difference in frequency response of the speaker without the windscreen and with the windscreen configuration four. The Figure D.13 shows the measured set up. In this measurement both the speaker and the microphone is lifted 30 cm

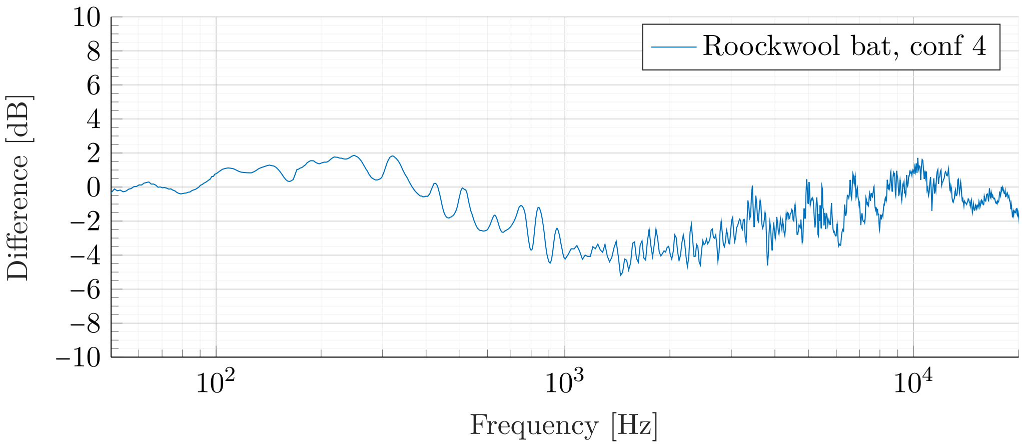

Figure D.14: The graph shows frequency response of the windscreen, where the frequency characteristic for the speaker is out calculated.

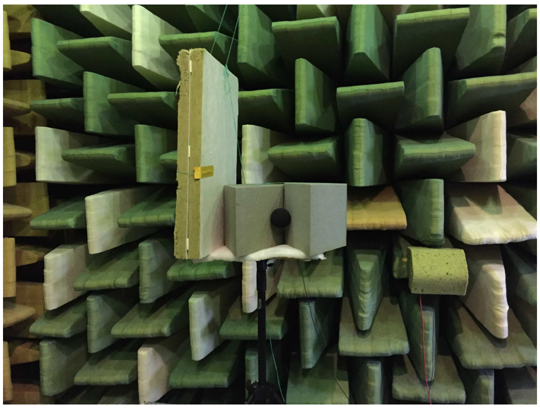

Figure D.15: The picture shows the measurement microphone with the Rockwool bat configuration four

The measurement shown in Figure D.16 shows the difference in frequency response of the speaker without the windscreen and with the windscreen configuration four. The Figure D.15 shows the measured set up.

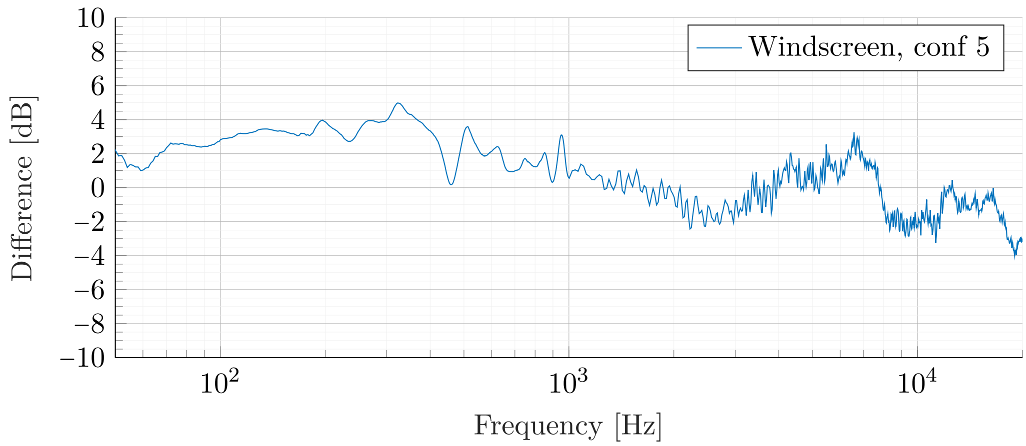

Figure D.16: The graph shows frequency response of the windscreen, where the frequency characteristic for the speaker is out calculated.

Appendix E

Windscreen wind speed measurement

A measurement is made to measure the wind attenuation in the microphone position with the difference windscreen configuration.

Materials and setup

To measure the wind attenuation of the windscreen configuration the following materials are used:

Table E.1: Equipment list

Description	Model	Serial-no	AAU-no
PC	Macbook	W89242W966H	-
large foam wedge	-	-	-
Small foam wedge	-	-	-
Rockwool bat	-	-	-
Fast fan	-	-	-
Fan control	tranformator	-	60398
Windspeed tools	FT technologies FT742-D-SM	9002-922	105634

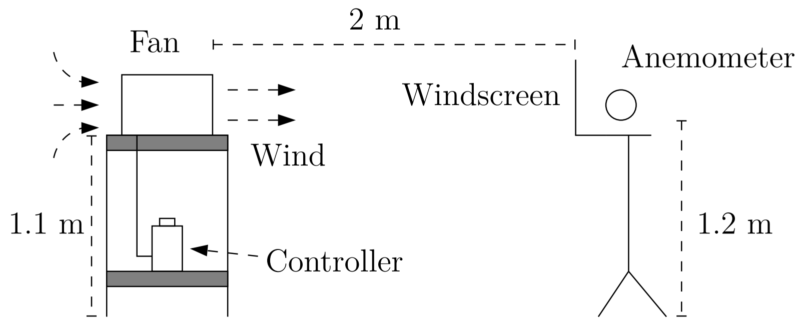

Figure E.1: The figure shows the measurement setup for the wind speed measurement in the microphone position

Test procedure

1. The materials are set up as in Figure E.1.
2. The fan is placed such that is produce directly crosswind.
3. The fan is activated
4. The anemometer is activated to record.
5. The anemometer is placed in the wind for approximately 10 s.
6. Then the anemometer is moved into the microphone position for approximately 10 s.
7. Then the anemometer is moved back in the wind for approximately 10 s.
8. Then the anemometer is moved into the microphone position for approximately 10 s again.
9. The wind speed measurement is plotted in MATLAB®with a moving mean filter with two samples and as m/s versus s.
10. Next the wind direction measurement is plotted in MATLAB®with a moving mean filter with two samples and as ° versus s.
11. The measurement is done for all windscreen configuration the same way.

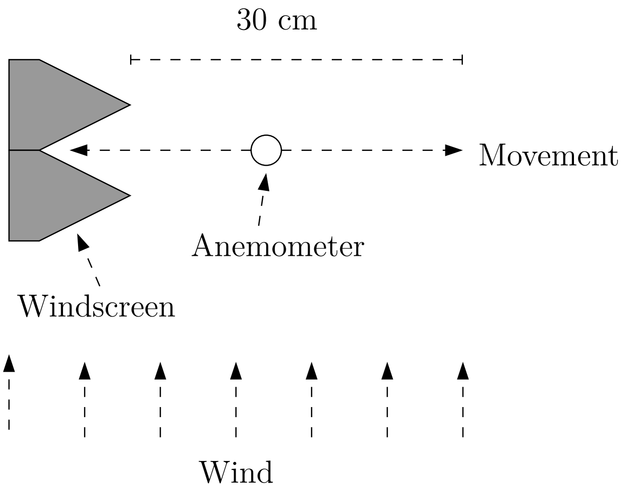

Figure E.2: The figure shows the movement of the anemometer doing the measurement

The following Figure E.3 shows the anemometer used for the measurement.

Figure E.3: The picture shows anemometer used for the measurement

Measurement area

To be able to generate a controlled wind flow, the hallway in Fredrick Bajers vej 7B5, 9220 Aalborg is used. The following Figure C.3 shows a drawing of the area and the position of the fan and windscreen.

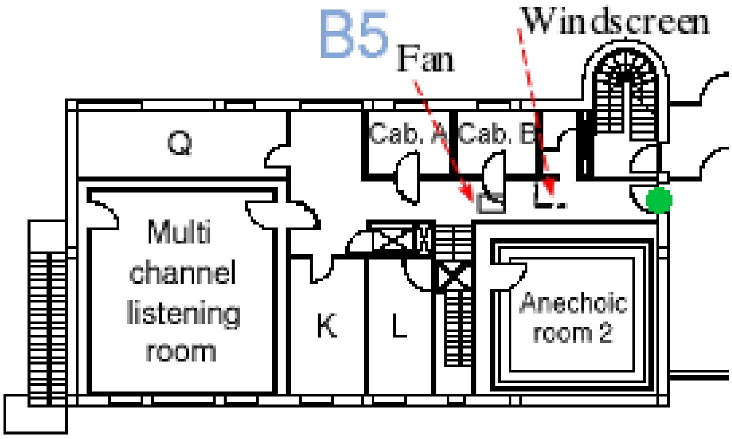

Figure E.4: The picture illustrates the area, where the wind flow is measured

Results

The following graphs show the result of the measurement.

Figure E.5 shows the measurement setup of the foam wedge, where the Figure E.6 shows the result.

Figure E.5: The picture shows the measurement setup with the small wedge, configuration one

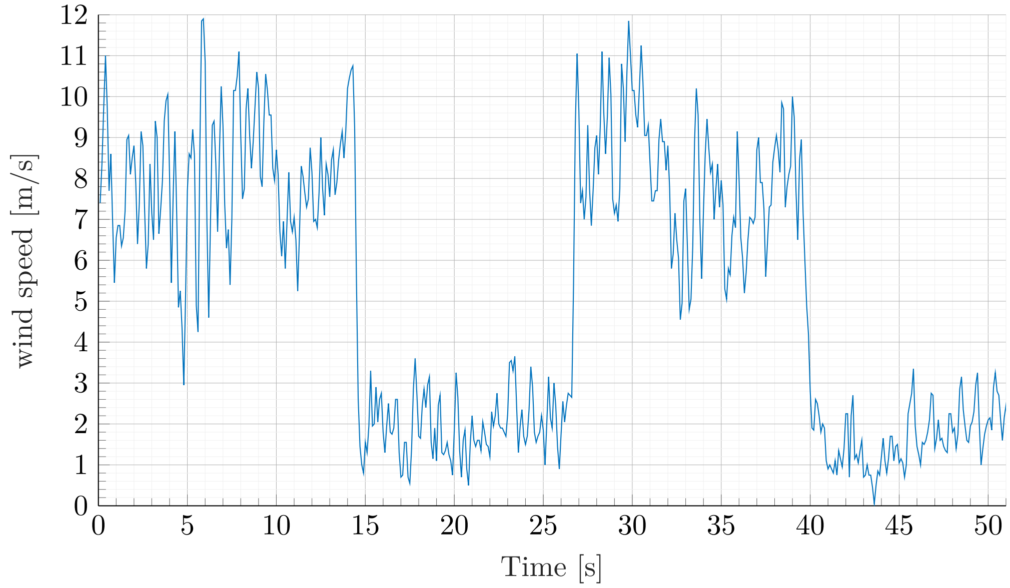

Figure E.6: The graph shows the wind speed versus time for configuration one. The grape has a high-speed period, and a low-speed period, in the high-speed period, the anemometer is in the wind approximately 30 cm from the windscreen wherein the low-speed period, the anemometer is inside the windscreen.

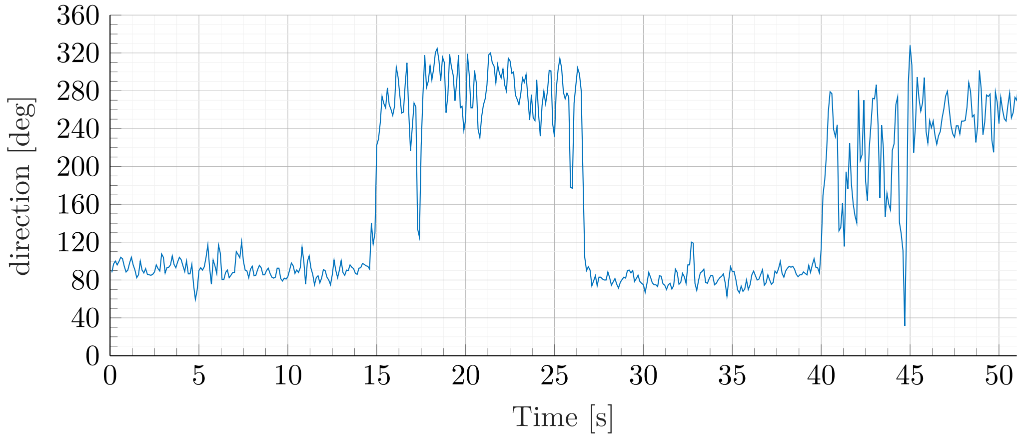

Figure E.7: The graph shows the synchronous direction of the wind with respect the the wind speed in Figure E.6

It is seen in Figure E.6 that the wind speed is lowered from approximately 8 m/s to 2 m/s. It is seen in Figure E.7 that the windscreen produces turbulence in the windscreen and the direction of the wind change approximately 180°.

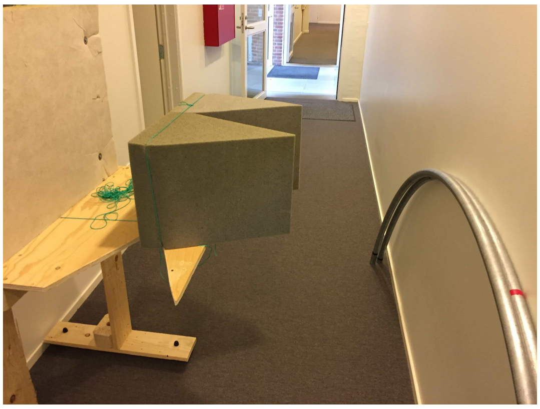

Figure E.8: The picture shows the measurement setup for the large wedge, configuration two

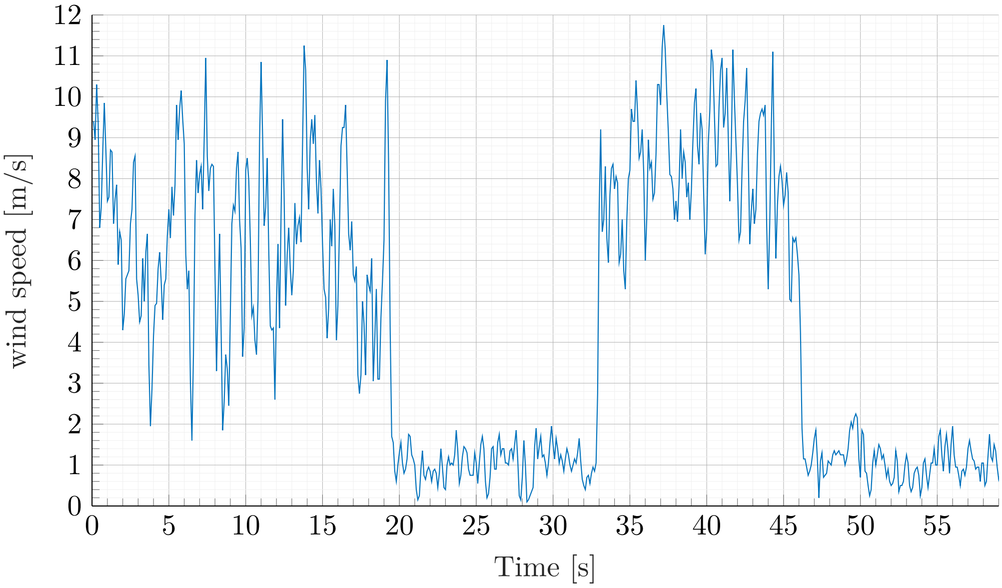

Figure E.9: The graph shows the wind speed versus time for configuration two. The grape has a high-speed period, and a low-speed period, in the high-speed period, the anemometer is in the wind approximately 30 cm from the windscreen wherein the low-speed period, the anemometer is inside the windscreen.

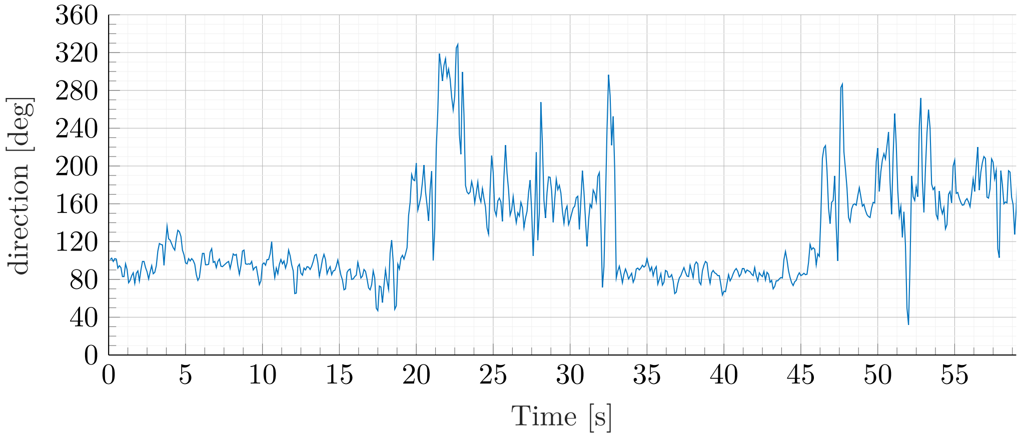

Figure E.10: The graph shows the synchronous direction of the wind with respect the the wind speed in Figure E.9

It is seen in Figure E.9 that the wind speed is lowered from approximately 7.5 m/s to 1 m/s. It is seen in Figure E.10 that the windscreen produces turbulence as high as with the small foam wedge in the windscreen and the direction of the wind change approximately 70°.

Figure E.11: The picture shows the measurement setup for the single rockwool bat, configuration four

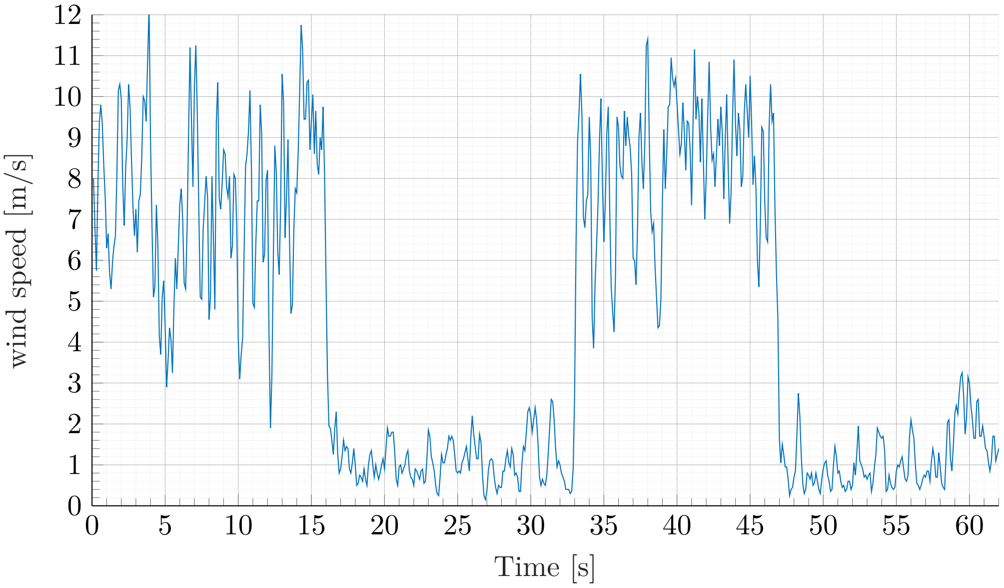

Figure E.12: The graph shows the wind speed versus time for configuration four. The grape have a high speed period and a low speed period, in the high speed period, the anemometer is in the wind approximatly 30 cm from the windscreen where in the low speed period, the anemometer is inside the windscreen.

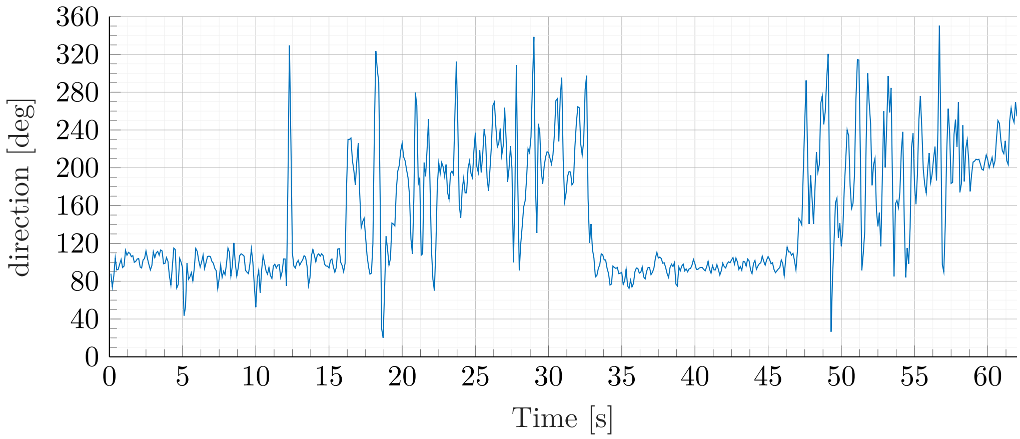

Figure E.13: The graph shows the synchronous direction of the wind with respect the the wind speed in Figure E.12

It is seen in Figure E.12 that the wind speed is lowered from approximately 8 m/s to 1 m/s. It is seen in Figure E.13 that the windscreen produces higher turbulence compare to the foam wedge windscreen. The direction of the wind change is approximately 100°.

Figure E.14: The picture shows the measurement with the large wedge and single rockwool bat, configuration five.

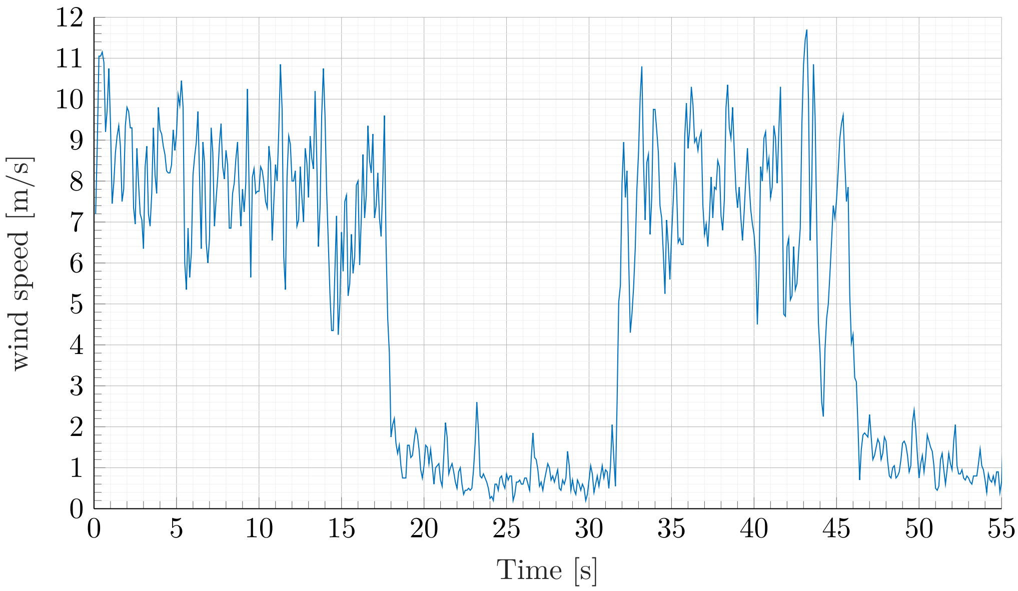

Figure E.15: The graph shows the wind speed versus time for configuration five. The grape have a high speed period and a low speed period, in the high speed period, the anemometer is in the wind approximatly 30 cm from the windscreen where in the low speed period, the anemometer is inside the windscreen.

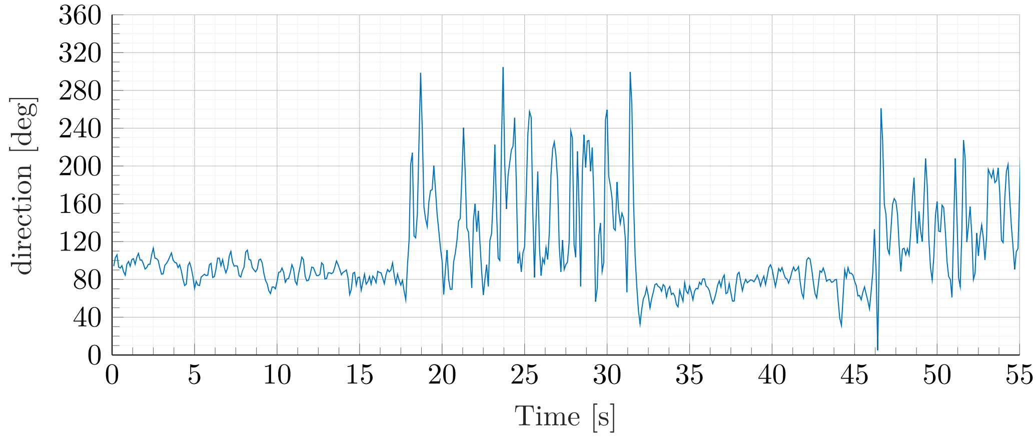

Figure E.16: The graph shows the synchronous direction of the wind with respect the the wind speed in Figure E.15

It is seen in Figure E.15 that the wind speed is lowered from approximately 8 m/s to 0.8 m/s. It is seen in Figure E.16 that this windscreen produces the highest turbulence of all windscreen. The direction of the wind change approximately 60°.

Appendix F

Windscreen attenuation measurement

A measurement was made to measure the wind attenuation in the microphone position with the difference windscreen configuration.

Materials and setup

To measure the wind attenuation of the windscreen configuration the following materials are used:

Table F.1: Equipment list

Description	Model	Serial-no	AAU-no
PC	Macbook	W89242W966H	-
Optimised windscreen	-	-	-
Fast fan	-	-	-
Fan control	tranformator	-	60398
Windspeed tools	FT technologies FT742-D-SM	9002-922	105634

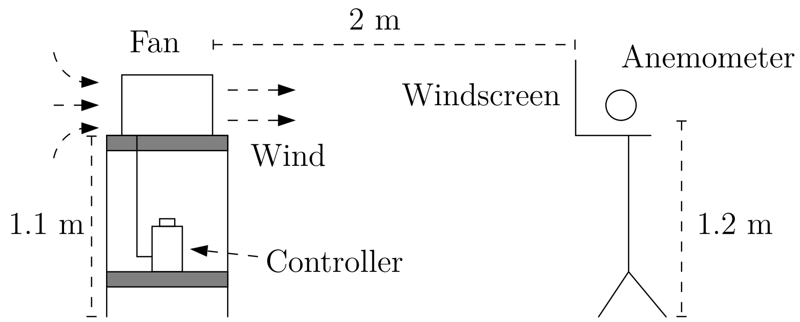

Figure F.1: The figure shows the measurement setup for the wind speed measurement in the microphone position

Test procedure

1. The materials are set up as in Figure F.1.
2. The fan is placed such that is produce directly crosswind.
3. The fan is activated
4. The anemometer is activated to record.
5. The anemometer is placed in the wind for approximately 10 s.
6. Then the anemometer is moved into the microphone position for approximately 10 s.
7. Then the anemometer is moved back in the wind for approximately 10 s.
8. Then the anemometer is moved into the microphone position for approximately 10 s again.
9. The wind speed measurement is plotted in MATLAB®with a moving mean filter with two samples and as m/s versus s.
10. Next the wind direction measurement is plotted in MATLAB®with a moving mean filter with two samples and as ° versus s.

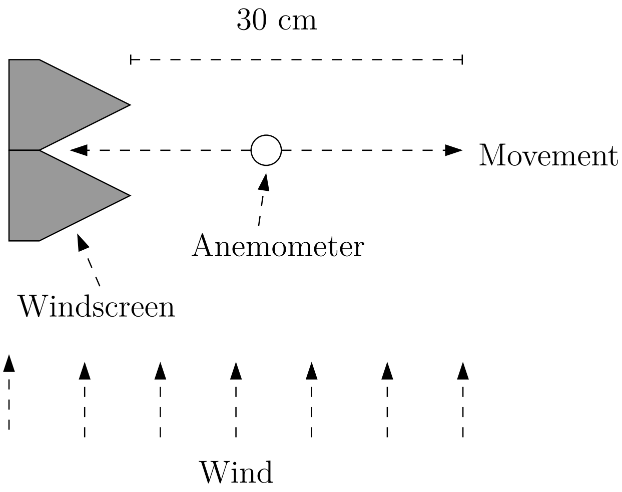

Figure F.2: The figure shows the movement of the anemometer doing the measurement

Measurement area

To be able to generate a controlled wind flow, the hallway in Fredrick Bajers vej 7B5, 9220 Aalborg is used. The following Figure F.3 shows a drawing of the area and the position of the fan and windscreen.

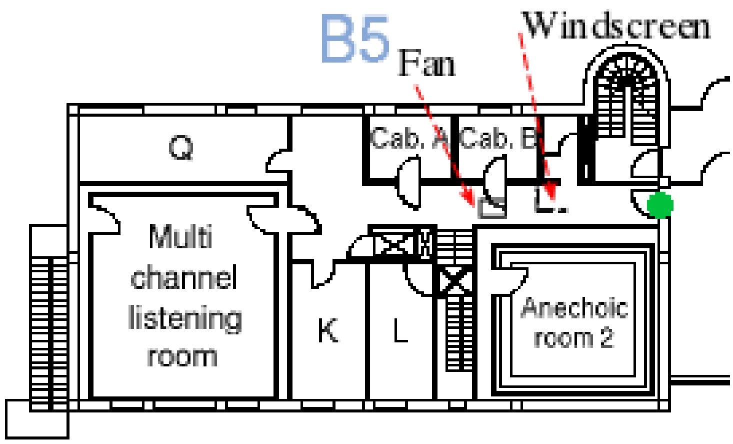

Figure F.3: The picture illustrate the area, where the wind flow is measured

Results

The following graphs show the result of the measurement.

Figure E.5 shows the measurement setup of the foam wedge, where the Figure F.5 shows the result.

(a) The picture shows the measurement setup for the optimised windscreen configuration five from back

(b) The picture shows the measurement setup for the optimised windscreen configuration five in front

Figure F.4: ap:wind:large_opt_pic

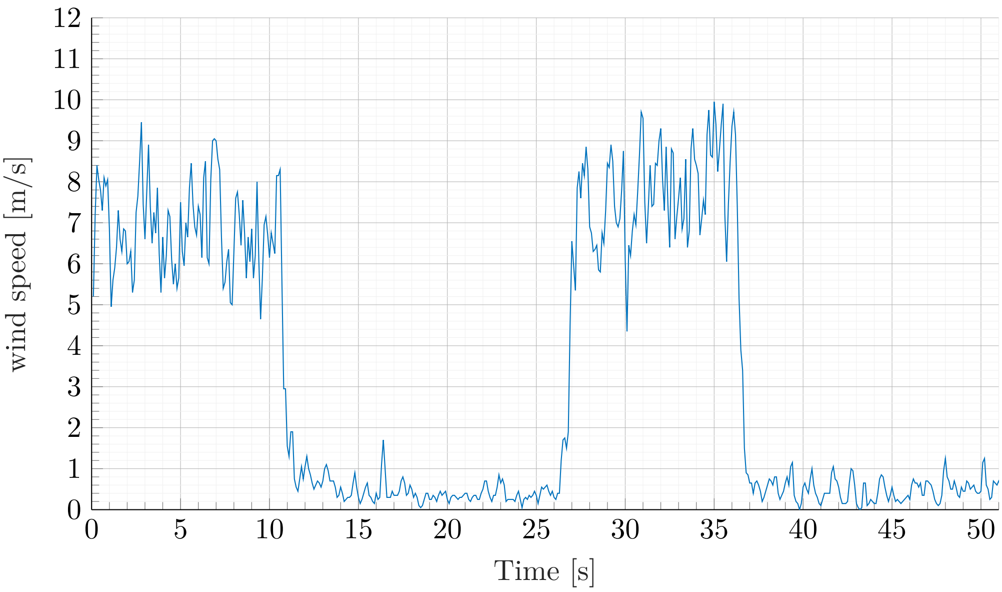

Figure F.5: The graph shows the wind speed versus time for the optimised configuration five. The grape have a high speed period and a low speed period. In the high speed period, the anemometer is in the wind approximately 30 cm from the windscreen where in the low speed period, the anemometer is inside the windscreen.

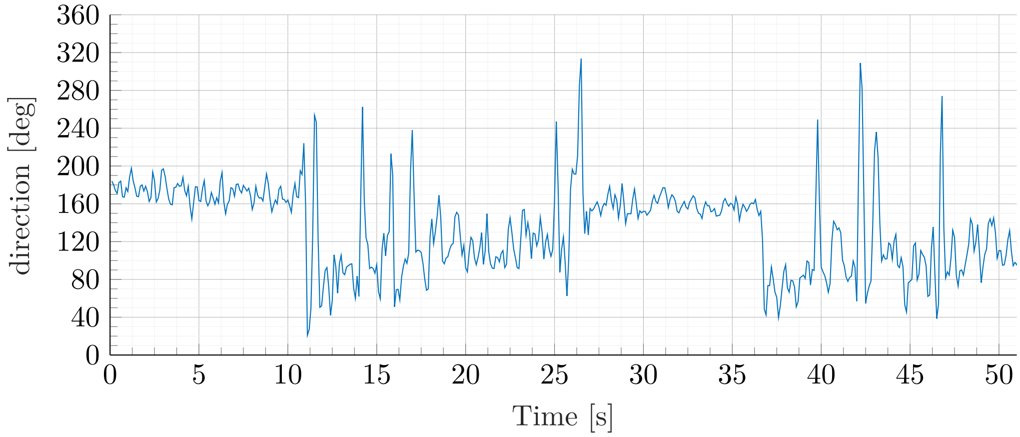

Figure F.6: The graph shows the synchronous direction of the wind with respect the the wind speed in Figure F.5

It is seen in Figure F.5 that the wind speed is lowered from approximately 8 m/s to 0.5 m/s. It is seen in Figure F.6 that the windscreen produces turbulence in the windscreen and the direction of the wind change approximately −100°. The reason that the angle is negative in this measurement is that the anemometer is turned 180° in the vertical plan for practical reason.

Appendix G

Outline ET 250-3D turntable control

In this appendix, the control of an Outline ET 250-3D turntable is described. The turntable can be controlled by User Datagram Protocol (UDP) commands through Ethernet. For controlling the turntable by MATLAB, the Ethernet-based control method is designed. The usage of UDP leads to short and simple scripts, where the script opens a UDP channel as a file, and, e.g. the script shall only edit the file in the right position to move the turntable. The MATLAB®software is not designed by the author but is delivered from OUTLINE.

Materials and setup

The following materials are used:

Table G.1: Equipment list

Description	Model	Serial-no	AAU-no
PC	Macbook	W89242W966H	-
Turntable	Outline ET 250-3D	REIBO012	-
PC - software	MATLAB 2018b	-	-

The UDP setup of the computer

To establish connection between the turntable and computer, both have to run at the same SUBNET MASK. The turntable comes with a factory setting for Ethernet connection which is as follows:

Table G.2: Turntable network address

Internet Protocol (IP)	192.168.1.34
SUBNET MASK	255.255.255.0
DEFAULT GATEWAY	192.168.1.250
BROADCAST IP	192.168.1.255

Turntable control command

The software is implemented as a function, where the user can retrieve the turntable position, specify a position and stop the turntable. The function name is:

Code snippet G.1: The turntable control function | ET250_3D.m

```
function [angle] = ET250_3D(cmd, angle)
```

The function is made as a switch case with input variable "cmd", and an angle input. The following command can be sent to the "cmd" of the function:

Table G.3: Function commands

cmd = 'udp_start'	Which start a connection on port 7000
cmd = 'set'	Which move the turntable to the specified angle
cmd = 'get'	Which get the position of the turntable
cmd = 'stop'	Which stop the turntable from moving
cmd = 'udp_stop'	Which stop the connection on port 7000

The MATLAB function

Code snippet G.2: The turntable control function | ET250_3D.m

```
function [angle] = ET250_3D(cmd, angle)


switch cmd

    case 'udp_start'
        echoudp('on',7000)
        u = udp('192.168.1.34',7000);
        fopen(u)


    case 'set'
        %request current position
        fwrite(u,hex2dec(['04';'00';'00';'04']))
        x = fread(u,7);
        angle_current = (x(4)*256+x(5))/10;

        %calc shortest way
```

```
        angle_delta = angle-angle_current;
        if angle_delta > 180
            angle_delta = angle_delta - 360;
        end
        if angle_delta < -180
            angle_delta = angle_delta + 360;
        end

        cmd(1) = uint8( 1.5-sign(angle_delta)/2 );    %1st byte = direction
        cmd(2) = uint8( floor(abs(angle_delta*10)/256) );    %angle in degree*10
        cmd(3) = uint8( mod(floor(abs(angle_delta*10)),256) );    %angle in degree*10
        cmd(4) = 0;

        fwrite(u,cmd)
        x = dec2hex(fread(u,2));                                    %receive ACK


    case 'get'
        %request current position
        fwrite(u,hex2dec(['04';'00';'00';'04']))
        x = fread(u,7);
        angle = (x(4)*256+x(5))/10;

    case 'stop'
        fwrite(u,hex2dec(['03';'00';'00';'03']))                    %send stop stop
        x = dec2hex(fread(u,2));

    case 'udp_stop'
        echoudp('off')
        fclose(u)
end


end
```

Appendix H

Weather measurement

This appendix shows the ardoino code for the weather samples. This code is based on the code designed by [cactus.io, 2019]

The firmware

Code snippet H.1: The weather firmware | weather_program.ino

```
#include <math.h>
#include <dht.h>
dht DHT;
#include "TimerOne.h"


//Constants
#define DHT22_PIN 4     // DHT 22  (AM2302) - what pin we're connected to

#define WindSensorPin1 (2) // The pin location of the anemometer sensor
#define WindSensorPin2 (3) // The pin location of the anemometer sensor

//Variables


volatile bool IsSampleRequired; // this is set true every 2.5s. Get wind speed
volatile unsigned int TimerCount; // used to determine 2.5sec timer count
volatile unsigned long Rotations1; // cup rotation counter used in interrupt routine
volatile unsigned long Rotation_old1; // cup rotation counter used in interrupt routine
volatile unsigned long ring1; // cup rotation counter used in interrupt routine
```

```
volatile unsigned long ContactBounceTime1; // Timer to avoid contact bounce in isr
volatile unsigned long Rotations2; // cup rotation counter used in interrupt routine
volatile unsigned long Rotation_old2; // cup rotation counter used in interrupt routine
volatile unsigned long ring2; // cup rotation counter used in interrupt routine
volatile unsigned long ContactBounceTime2; // Timer to avoid contact bounce in isr
volatile unsigned long timet1 = 0;
volatile unsigned long timet2 = 0;
float WindSpeed1; // speed miles per hour
float WindSpeed2; // speed miles per hour

int analogPin1 = A2;
int analogPin2 = A3;
int vaneValue1;
int vaneValue2;
int count1;
int count2;
int buffersize = 16;
int ringbuffer1[16];
int ringbuffer2[16];
float hum;  //Stores humidity value
float temp; //Stores temperature value

void setup() {



IsSampleRequired = false;
TimerCount = 0;
count1 = 0;
count2 = 0;
Rotations1 = 0; // Set Rotations to 0 ready for calculations
Rotation_old1 = 0;
Rotations2 = 0; // Set Rotations to 0 ready for calculations
Rotation_old2 = 0;
ring1 = 0;
ring2 = 0;
Serial.begin(115200);
pinMode(WindSensorPin2, INPUT);
// Setup the timer interupt
attachInterrupt(digitalPinToInterrupt(WindSensorPin1), isr_rotation1, FALLING);
attachInterrupt(digitalPinToInterrupt(WindSensorPin2), isr_rotation2, FALLING);
Timer1.initialize(26500);// Timer interrupt every 2.5 seconds 500000 (25000))
Timer1.attachInterrupt(isr_timer);
}

```

```
void loop() {
  if(IsSampleRequired) {


    ringbuffer1[count1] = Rotations1 - Rotation_old1;
    Rotation_old1 = Rotations1;
    ring1 = 0;

    for(int i = 0; i <= buffersize; i++){
      ring1 = ring1+ringbuffer1[i];
    }

    if(count1 == buffersize){
      Rotations1 = 0; // Reset count for next sample
      Rotation_old1 = 0;
      count1 = 0;
    }

    else{
      count1++;
    }


    ringbuffer2[count2] = Rotations2 - Rotation_old2;
    Rotation_old2 = Rotations2;
    ring2 = 0;

    for(int i = 0; i <= buffersize; i++){
      ring2 = ring2+ringbuffer2[i];
    }

    if(count2 == buffersize){
      Rotations2 = 0; // Reset count for next sample
      Rotation_old2 = 0;
      count2 = 0;
    }

    else{
      count2++;
    }

  IsSampleRequired = false;
  }

  int chk = DHT.read22(DHT22_PIN); //Read data and store it to
      variables hum and temp
  vaneValue1 = analogRead(analogPin1);
  vaneValue2 = analogRead(analogPin2);
  temp = DHT.temperature;
  hum = DHT.humidity;
  WindSpeed1 = ring1*(2.25/2.960)*0.44704;
  WindSpeed2 = ring2*(2.25/2.960)*0.44704;
  Serial.print(WindSpeed1);
```

```
  Serial.print("\t");
  Serial.print(vaneValue1);
  Serial.print("\t");
  Serial.print(WindSpeed2);
  Serial.print("\t");
  Serial.print(vaneValue2);
  Serial.print("\t");
  Serial.print(temp);
  Serial.print("\t");
  Serial.println(hum);
  delay(88);

}


// isr handler for timer interrupt
void isr_timer() {
TimerCount++;
  if(TimerCount == 7) {
    timet2 =  millis();
    IsSampleRequired = true;
    TimerCount = 0;
  }
}

// This is the function that the interrupt calls to increment the
    rotation count
void isr_rotation1() {
  if((millis() - ContactBounceTime1) > 15 ) { // debounce the
      switch contact.
    Rotations1++;
    ContactBounceTime1 = millis();
  }
}

 void isr_rotation2() {
  if((millis() - ContactBounceTime2) > 15 ) { // debounce the
      switch contact.
    Rotations2++;
    ContactBounceTime2 = millis();
  }
}
```

Appendix I

Impulse response measuring software

The software measures the impulse response of a line source array while it read weather information on the serial bus.

The firmware

Code snippet I.1: The impulse and weather measuring software | IRmeas_fft.m

```
if ~isempty(instrfind)
    fclose(instrfind);
    delete(instrfind);
end

port = seriallist;
s = serial(port(5));
s=serial(port(5),'InputBufferSize',512,'Baudrate',115200);
fopen(s)
tic
    while(toc<10)
        buff=strsplit(fscanf(s),'\t');
    end


            % Perform capture
            %audiowrite("sweep.wav",dataOut,fs)
            L = 4096;
            fileReader =
                dsp.AudioFileReader('sweep.wav','SamplesPerFrame',L);
            fs = fileReader.SampleRate;

            aPR = audioPlayerRecorder('SampleRate',fs,...
                                  % Sampling Freq.
                              'RecorderChannelMapping',inputChannel,...
                                  % Input channel(s)
```

```
                          'PlayerChannelMapping',[1 2],... % Output channel(s)
                          'SupportVariableSize',true,...    % Enable variable buffer size
                          'BufferSize',L);                  % Set buffer size


                      out = [];
                      data = [];
                      while ~isDone(fileReader)
                          audioToPlay = fileReader();
                          [audioRecorded,nUnderruns,nOverruns] = aPR(audioToPlay);
                          out = [out; audioRecorded];
                          dat=strsplit(fscanf(s),'\t');
                          data = [data; dat];
                          if nUnderruns > 0
                              fprintf('Audio player queue was underrun by %d samples.\n',nUnderruns);
                                res = 1;
                          end
                          if nOverruns > 0
                              fprintf('Audio recorder queue was overrun by %d samples.\n',nOverruns);
                                res = 1;
                          end
                      end
                      release(fileReader);
                      release(aPR);
                      fclose(s)
                      delete(s)
                      clear s



weather = str2double(data);
weather = weather(23:end,:);
weathertime = [0 ([1:length(weather)-1]./(fs/L))]';

            load('calibration.mat')



            for k=1:length(inputChannel)-1
            % convelution of signal
            input    = out(:,k+1);
            ref   =
                out(:,1)/(rms(out(:,1))/calibration.mic_sensitivity(k));
            eps = 0.1;
            L = numel(ref);
            W = hann(L);
```

```
            uz1f = fft(W.*input,L);
            uz2f = fft(W.*ref,L);
            ir(:,k) =
                real(ifft((uz1f.*conj(uz2f))./(uz2f.*conj(uz2f)+eps*mean(uz2f.*conj(uz2f))))
            irtime = ([1:length(ir)]./fs)';
            end


      end
```

Appendix J

The directionality of L-acoustics KUDO

A measurement was made to measure the directionality of an L-acoustics KUDO. The goal of this appendix is to measure the polar response and calculate transfer functions of the line source array element in a free field environment with calibrated measuring equipment. During the measurement of the polar response, impulse responses are measured with a specified degree step size all around the speaker. E.g. if the step is one degree, the loudspeaker is turned 1 degree for every impulse response measurement, until 360° is achieved.

Materials and setup

To measure the directionality of the line source element, the following materials are used:

Table J.1: Equipment list

Description	Model	Serial-no	AAU-no
PC	Macbook	W89242W966H	-
Audio interface	RME Fireface UCX	23811948	108230
Microphone	GRAS 26CC	78189	75583
Preamp	GRAS 40 AZ	100268	75551
Speaker	L-acoustics KUDO	7733	-
Turntable	Outline ET 250-3D	REIBO012	-
PC - software	MATLAB 2018b	-	-

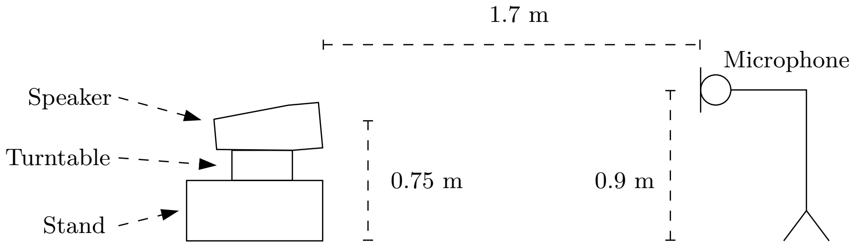

Figure J.1: The figure shows the measurement setup in the anechoic chamber

Test procedure

1. The materials are set up as in Figure J.1 where the microphone is connected to the audio interface.
2. The microphone is calibrated
3. The speaker is placed 1.7 m from the microphone and pointing in the direction of the microphone.
4. The impulse response is measured for every 5°
5. The −3 dB SPL step contour is calculated until −21 dB SPL and plotted.

Measurement area

To be able to measure the windscreen frequency response, the anechoic chamber in Fredrick Bajers vej 7B4, 9220 Aalborg is used. The following Figure J.2 shows a drawing of the area and the position of the fan and windscreen.

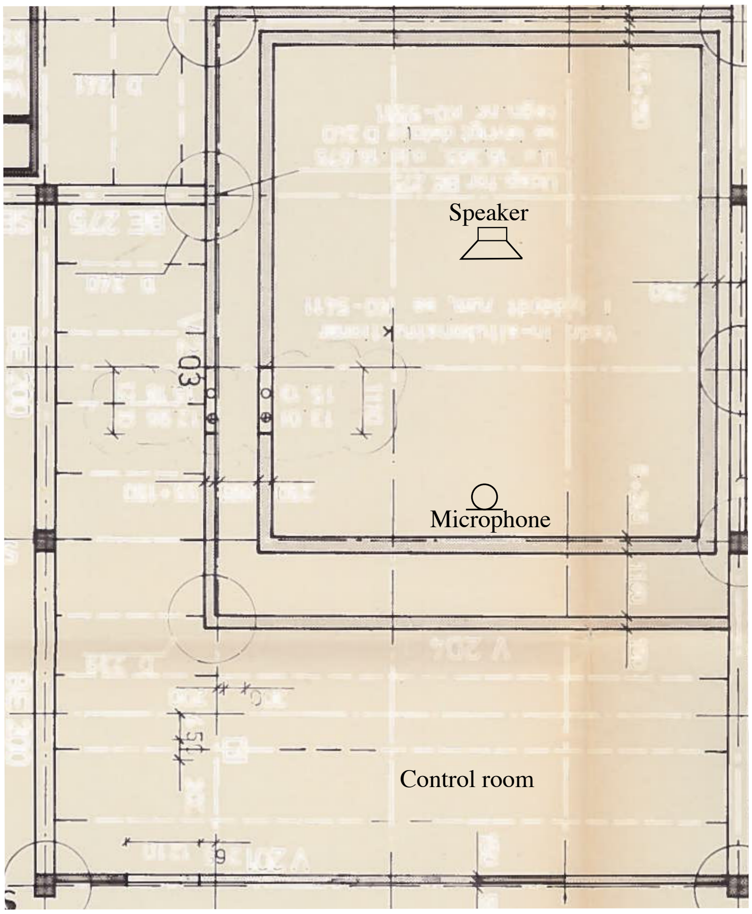

Figure J.2: The picture illustrate the position of the microphone and the speaker

Results

The following Figure J.3 shows the measurement setup.

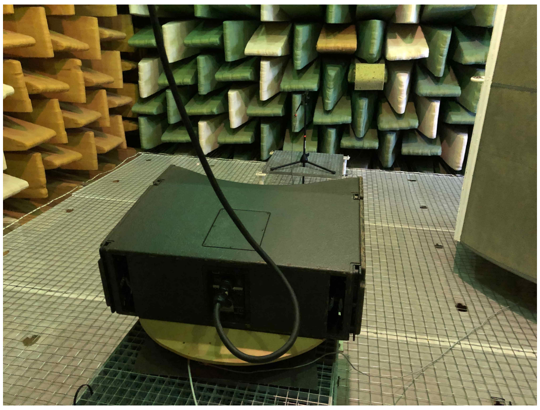

Figure J.3: The picture shows the measurement setup

The following graphs show the result of the measurement.

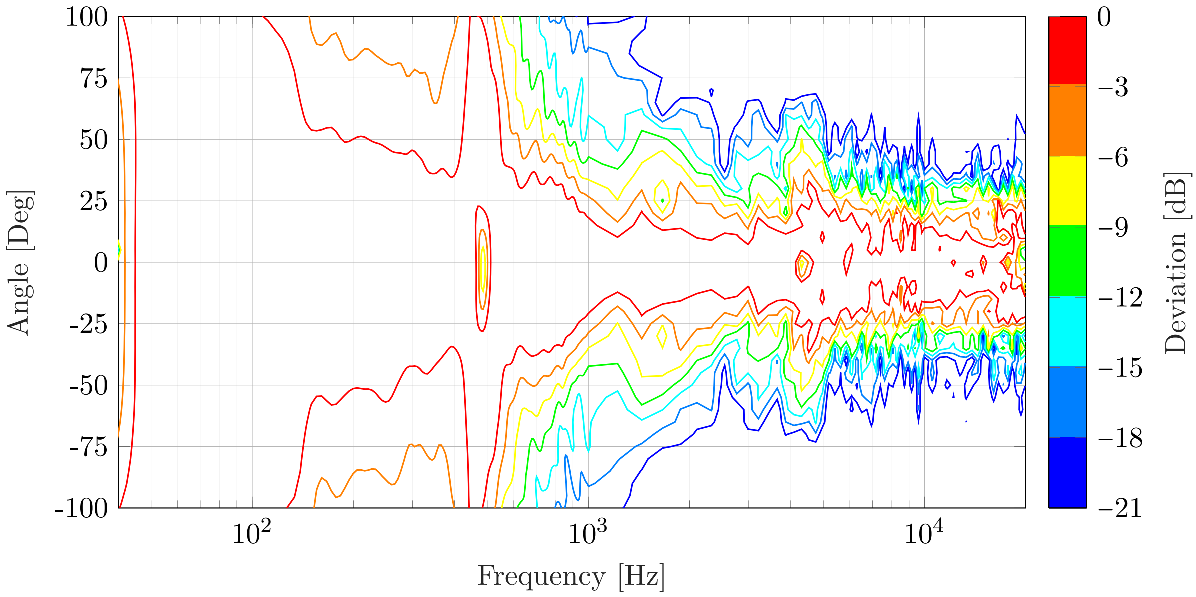

Figure J.4: The graph shows a contour plot with 3 dB SPL step of the directionally of the L-acoustics KUDO with 25° / 25° settings. The lower black contour line indicate the dBdirectionality for the maximum rotation of the speaker

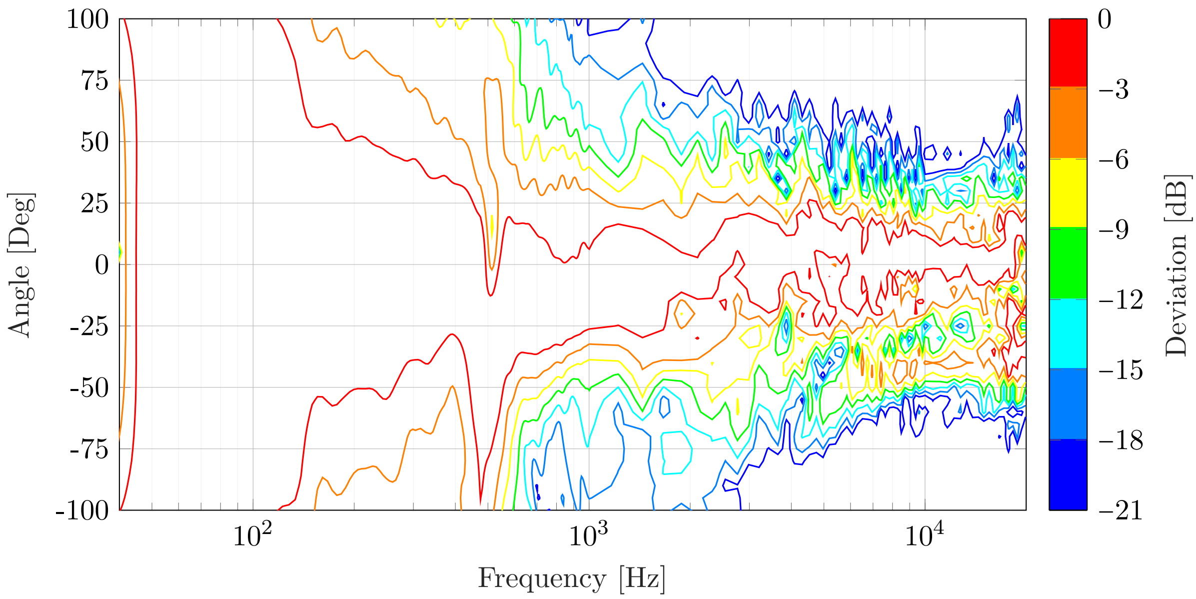

Figure J.5: The graph shows a contour plot with 3 dB SPL step of the directionally of the L-acoustics KUDO with 25° / 55° settings. The lower black contour line indicate the dBdirectionality for the maximum rotation of the speaker

Appendix K

crosswind effect on line source array

A measurement is made to measure the transfer function differences in three measurement point in the crosswind. One microphone situated in downwards direction, one microphone situated in upwards direction and one microphone situated in the centre, which is between the other two microphones. The used speaker has a horizontal dispersion pattern of 80°.

Materials and setup

To measure the transfer function in a crosswind situation, the following materials are used:

Table K.1: Equipment list

Description	Model	Serial-no	AAU-no
PC	Macbook	W89242W966H	-
Audio interface	RME Fireface UCX	23811948	108230
Microphone	GRAS 26CC	78189	75583
Preamp	GRAS 40 AZ	100268	75551
Microphone	GRAS 26CC	78186	75582
Preamp	GRAS 40 AZ	100267	75550
Microphone	GRAS 26CC	??	
Preamp	GRAS 40 AZ		
3 Windscreen	Author design	-	-
Line source element	L-acoustics KUDO		
Line source element	L-acoustics KUDO		
Line source element	L-acoustics KUDO		
Line source element	L-acoustics KUDO		
Line source element	L-acoustics KUDO		
Amplifier	Lab PLM10000Q		
Amplifier	Lab PLM10000Q		
Mixer	Yamaha LS9		
Wind measurement tools	Davis	-	
Angling tools	Author design	-	
flying tools	-	-	-

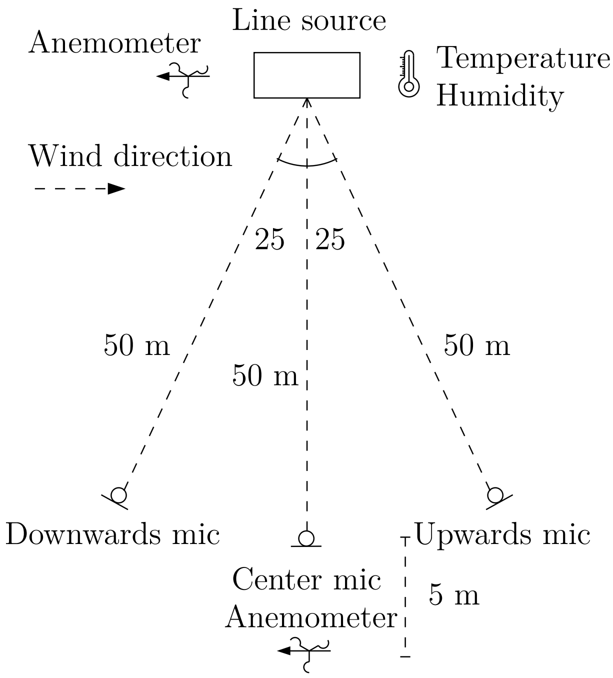

Figure K.1: The figure shows the microphone position versus the position of the line source, while the array is 0° horizontal turned

(a) The picture shows the speaker setup

(b) The figure shows the wind direction

Figure K.2: The figures shows the measurement set up for Appendix A

Test procedure

1. The microphone is calibrated.
2. The wind direction is measured.
3. The materials are set up as in Figure P.1 where the speaker is placed in cross-wind direction, such that the frontal wave direction is orthogonal the wind. The microphone and speaker are connected to the audio interface.
4. The speaker is placed 2.92 m above the ground.
5. The speaker is tilted 5° pointing down agents the ground.
6. The microphone is placed 1.68 m above the ground, 50 m from the speaker. One 25° to the left of the speaker, one 25° to the right of the speaker and one in the centre between the other microphone.
7. The anemometer at the speakers is situated on the speaker tower in the same side as shown on the setup and a hight of 4.64 m
8. The anemometer at the microphone position is lifted 1.68 m above the ground.
9. The wind direction goes from the upwards microphone to the downwards microphone.
10. The humidity and temperature are measured at the speaker position.
11. 10 sine sweep is performed with a length of 5 s each while the wind direction and speed is measured.
12. The impulse response is calculated and filtered with a 4th order highpass filter at 20 Hz.
13. The correlation is calculated for each impulse response to the first impulse response for time alignment [Gunness, 2001] of all microphone channels.
14. The mean impulse response is calculated for the 10 measurements of all three microphone.
15. The transfer function is calculated with a 10 sample moving mean filter.

16. The the transfer function is downsampled to fit the plotting program.
17. The transfer function is calculated with a 5 sample moving mean filter.
18. The wind measurement is synchronised to the transfer function in time.
19. The measurement is repeated 6 times with different horizontal speaker angle from 0° to 30° in step of 5°

Measurement area

To be able to measure in a windy area, parking lot at Tryvej 13, 9320 Hjallerup is used. The following Figure P.3 shows a picture of the area and the approximate position of the speaker and microphone.

Figure K.3: The picture illustrate the area, where the wind flow is measured

Results

All measuring result is not shown here. The rest can be founded in the attached file. One synchronised measurement is shown for the upwards microphone where the speaker is turned 0°. The shown measurement result is for one measurement and is not a mean from 10. This shows the time synchronised result.

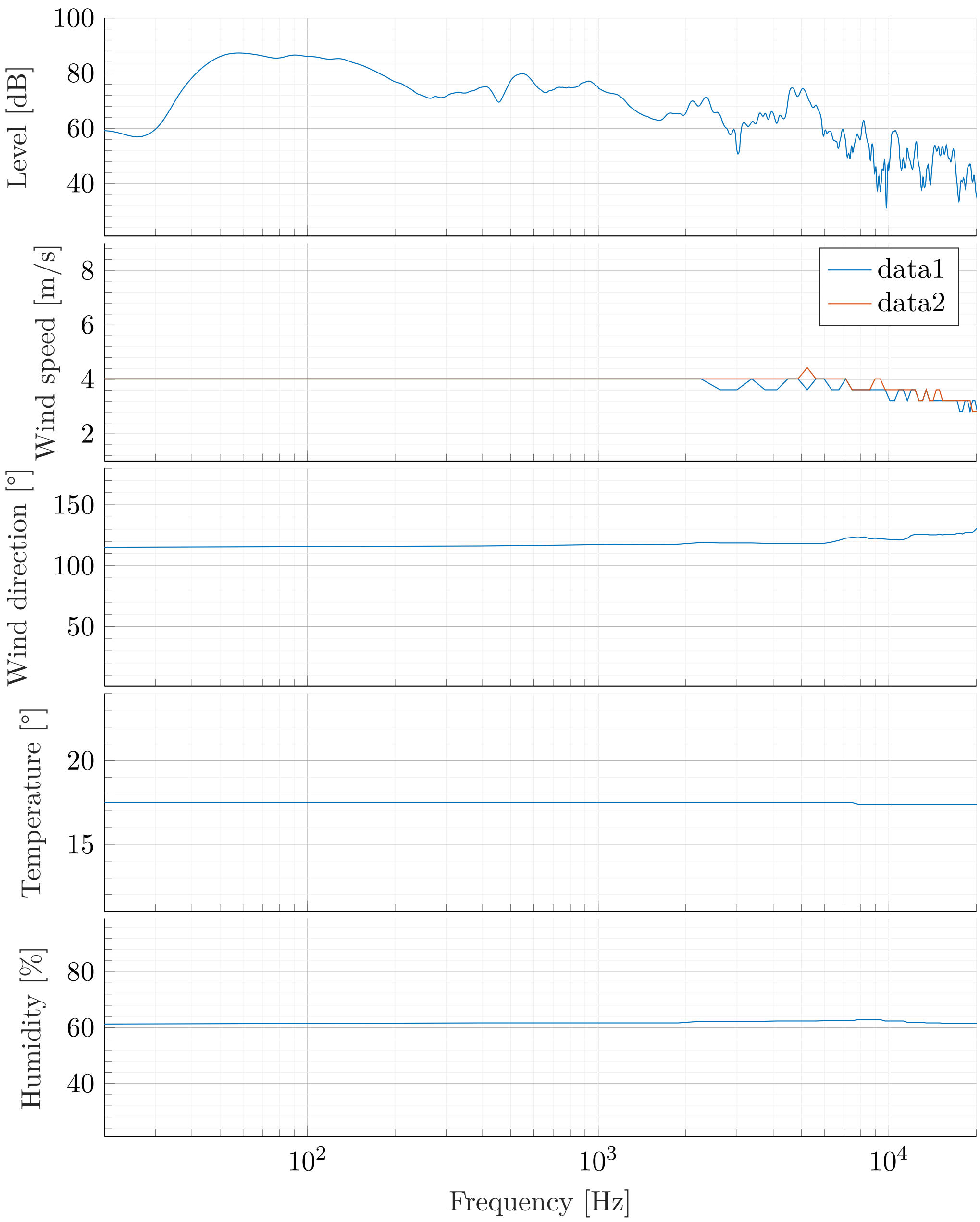

Figure K.4: the graph shows

Appendix L

Line source array angle measuring design

To measure the angle of the speaker, a angle plate with coloured laser indicator is designed.

Materials and setup

The following martial is used

Table L.1: Equipment list

Description	Model	Serial-no	AAU-no
Laser pen	Red	-	-
Laser pen	Green	-	-
Angle plate	-	-	-
Laser pen holder	-	-	-

(a) The picture shows the angle finder plate

(b) The figure shows the lasers and the laser holder

Figure L.1: The figures shows the angle finder martial for the used line source array

Adjusting the line source horizontal angle

1. The materials are set up as in Figure L.1.
2. The line source array is turned until the laser pointers light is on the drawn line of the angle or with the same distance to the line.

Appendix M

Windscreen influence of frequency response

A measurement is made to measure the frequency influence of the designed windscreen. The configuration includes the modified GRAS AM0069 windscreen. The measurement is done to analyse the effect of the windscreen in the frequency domain to analyse the observed frequency differences.

Materials and setup

To measure the frequency response of the windscreen configuration the following materials are used:

Table M.1: Equipment list

Description	Model	Serial-no	AAU-no
PC	Macbook	W89242W966H	-
Audio interface	RME Fireface UCX	23811948	108230
Microphone	GRAS 26CC	78189	75583
Preamp	GRAS 40 AZ	100268	75551
Windscreen	GRAS AM0069	-	-
large foam wedge	-	-	-
Speaker stand	-	-	-
Speaker	Dynaudio	03508438	1441-0

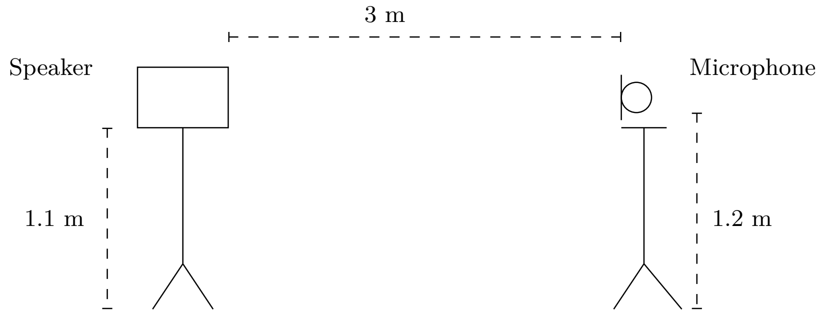

Figure M.1: The figure shows the measurement setup in the anechoic chamber

The following Figure M.2 shows the speaker.

Figure M.2: The picture shows the used speaker

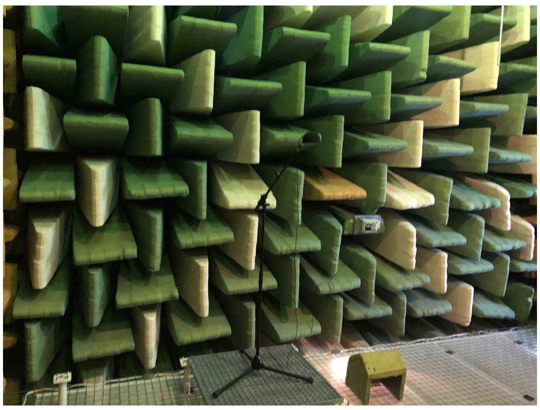

Figure M.3: The picture shows the measurement microphone with the original modified windscreen

Test procedure

1. The materials are set up as in Figure M.1 where the microphone is connected to the audio interface.
2. The microphone is calibrated
3. The speaker is placed 3 m from the microphone and pointing in the direction of the microphone.
4. The transfer function is measured of the speaker without the designed windscreen and with the modified windscreen.
5. The windscreen configuration is placed such that the microphone has approximately the same position as without the designed windscreen, (while the windscreen is tilted the microphone is closer to the speaker).
6. The transfer function is measured
7. The transfer function is calculated and plotted versus the transfer function without designed windscreen but with modified original windscreen MATLAB®.
8. The position of the windscreen is changed both with tilting and rotation while the measuring is repeated.
9. , In the end, the designed windscreen is measured without the foam wedge.

Measurement area

To be able to measure the windscreen frequency response, the anechoic chamber in Fredrick Bajers vej 7B4, 9220 Aalborg is used. The following Figure M.4 shows a drawing of the area and the position of the fan and windscreen.

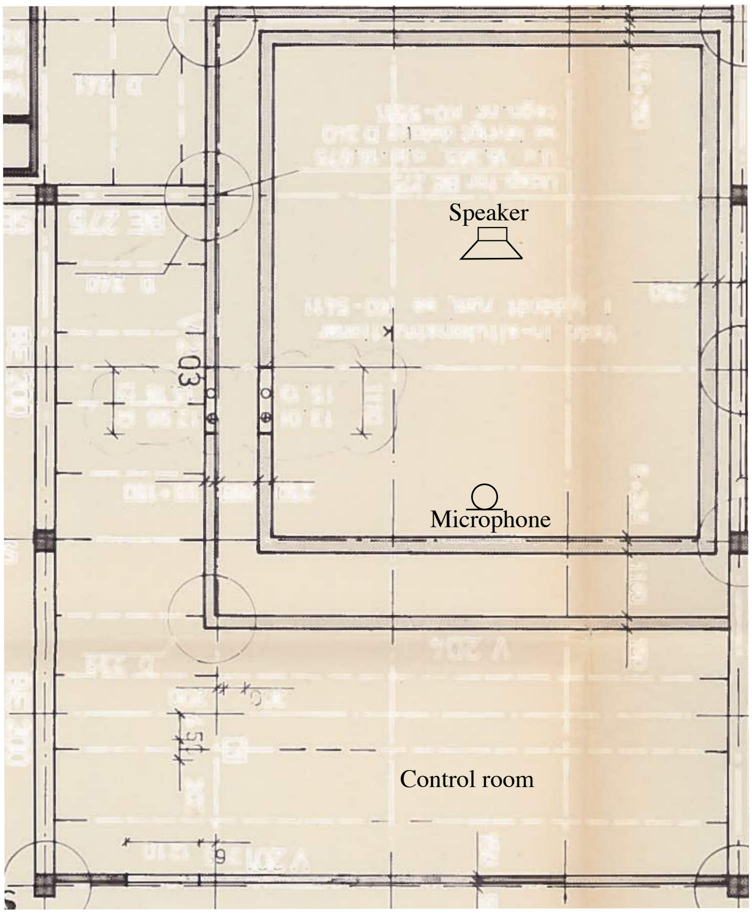

Figure M.4: The picture illustrate the area, where the wind flow is measured

Results

The following graphs show the result of the measurement.

The first measurement in Figure M.5 shows the transfer function while the foam wedge is at its designed position and without tilting and rotation. Therefore the windscreen point with 0° to the speaker and the windscreen plate have vertical and horizontal of 0°

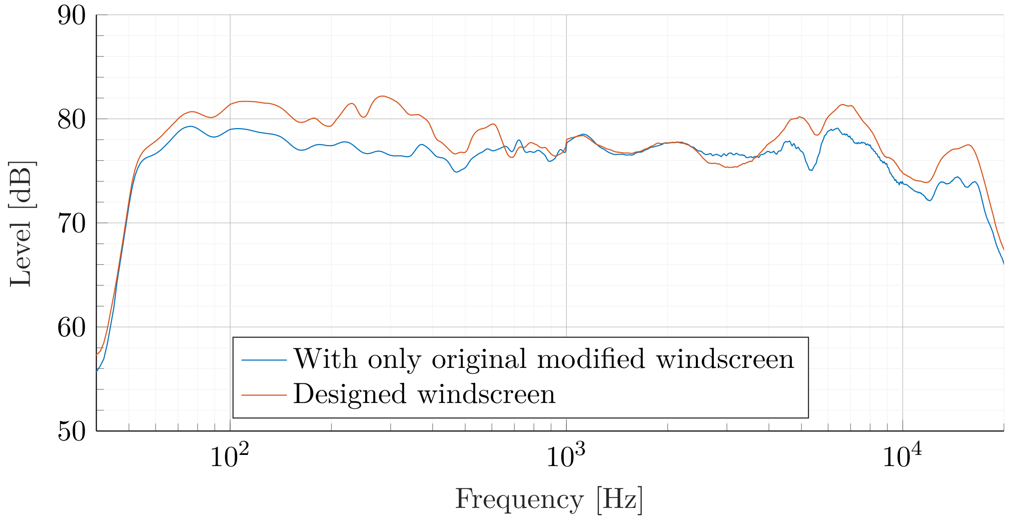

Figure M.5: The graph shows frequency response of the speaker measured without windscreen and with the designed windscreen with no rotation and no tilting

The next measurement in Figure M.6 shows the transfer function while the foam wedge is moved 20 cm back compare to its designed position and without tilting and rotation.

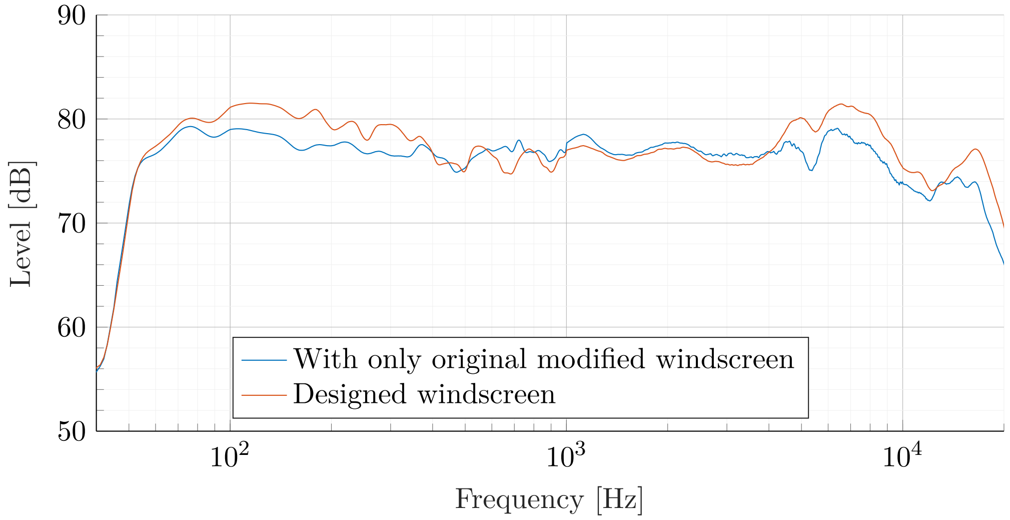

Figure M.6: The graph shows frequency response of the speaker measured without windscreen and with the designed windscreen with no rotation and no tilting while the foam wedge is moved 20 cm back

As see in Figure M.6 the frequency response does not change markelibly compare to Figure M.5. It is seen that the general level is 0.5 dB SPL lower as expected since the microphone is moved back.

The next measurement in Figure M.7 shows the transfer function while the foam wedge is at its designed position and without tilting and with 30° right rotation. Therefore the white PVC plate covers more the opening to the microphone and the windscreen plate have vertical and horizontal of 0°

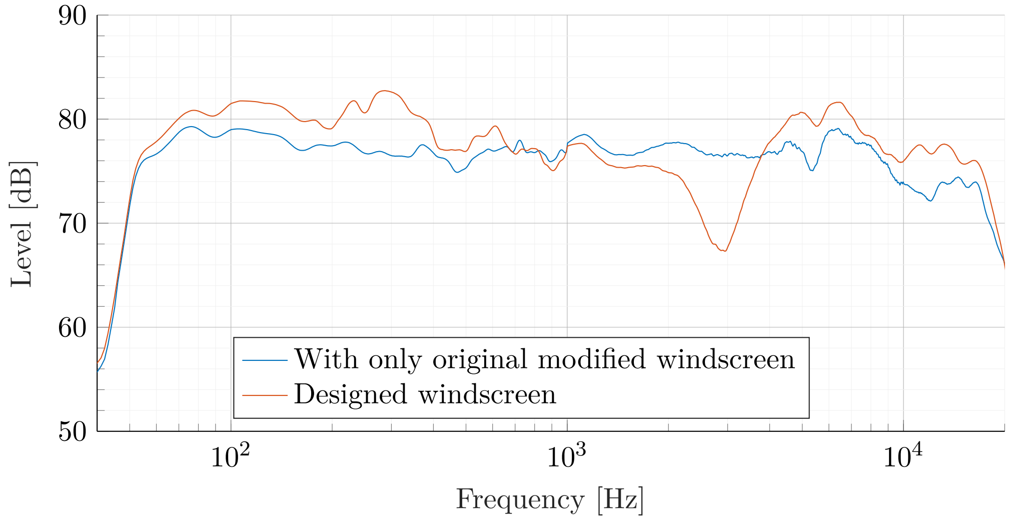

Figure M.7: The graph shows frequency response of the speaker measured without windscreen and with the designed windscreen with no no tilting and a right rotation of 30°

It is seen in Figure M.7 that 30° right rotation gives a SPL depth between 1.0 kHz and 4.0 kHz otherwise the frequency response is similar to Figure M.5

The next measurement in Figure M.8 shows the transfer function while the foam wedge is at its designed position and without tilting and with 30° left rotation. Therefore the foam wedge covers more the opening to the microphone and the windscreen plate have vertical and horizontal of 0°

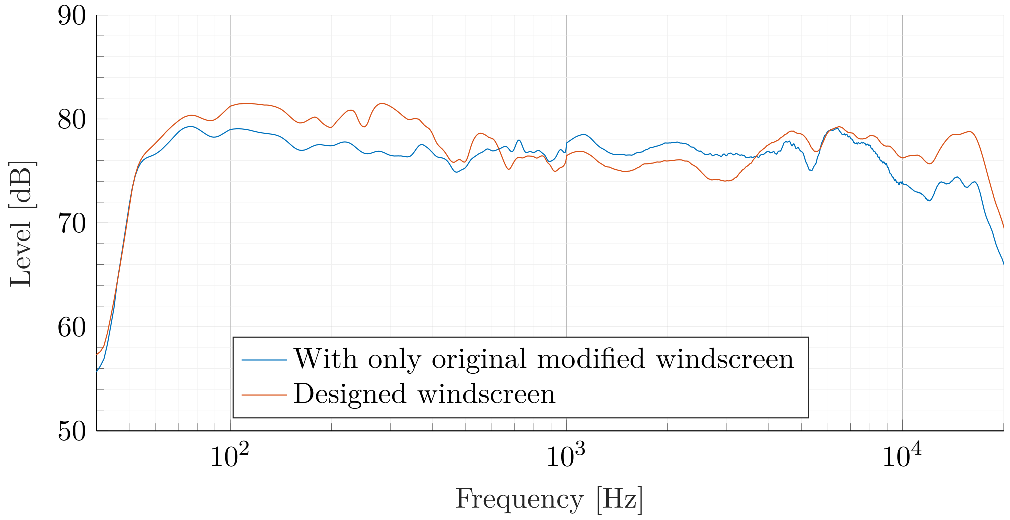

Figure M.8: The graph shows frequency response of the speaker measured without windscreen and with the designed windscreen with no no tilting and a left rotation of 30°

It is seen in Figure M.8 that 30° left rotation also gives a SPL depth between 1.0 kHz and 4.0 kHz but much less than Figure M.7. Otherwise the frequency response is similar to Figure M.5

The next measurement in Figure M.9 shows the transfer function while the foam wedge is at its designed position and with a tilting of 9° and without rotation. Therefore the windscreen point with 0° to the speaker and the windscreen plate have horizontal of 0°

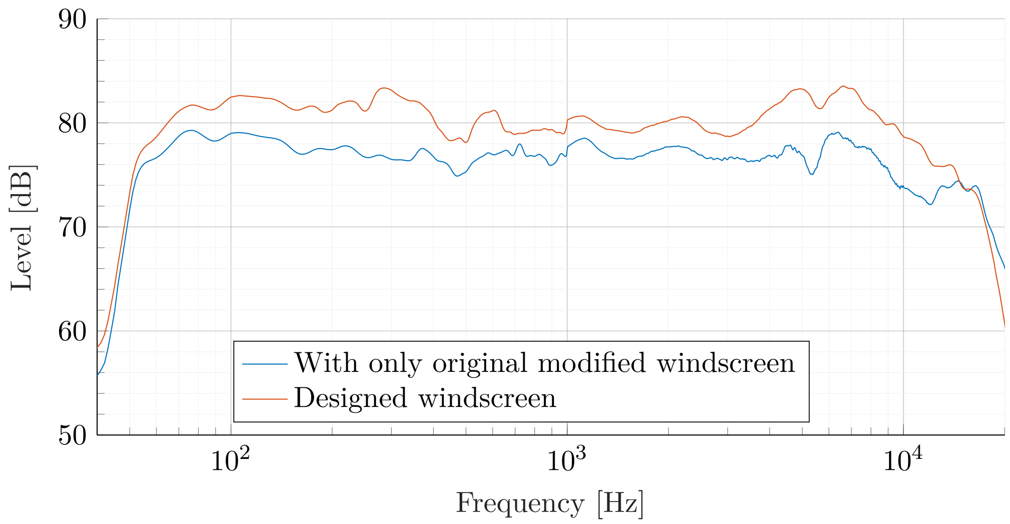

Figure M.9: The graph shows frequency response of the speaker measured without windscreen and with the designed windscreen with no rotation and a frontal tilting of 9°

As see in Figure M.9 the frequency response does not change markelibly compare to Figure M.5. It is seen that the general level is 2 dB SPL higher as expected since the microphone is moved closer to the speaker as shown in Figure M.10.

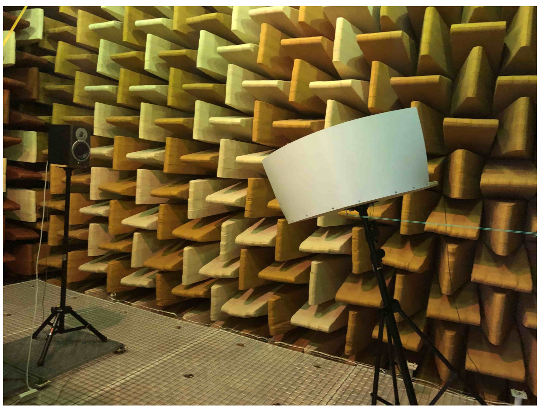

Figure M.10: The picture shows the measurement microphone with the tilted designed windscreen

Moreover there is a roll off in the frequency higher that 10 kHz which might result from a plate reflection of the sound since the microphone is lifted by the modified original windscreen. To research the roll off the tilting of the plate is raised to 20°. The result of tilting 20° is shown in Figure M.11

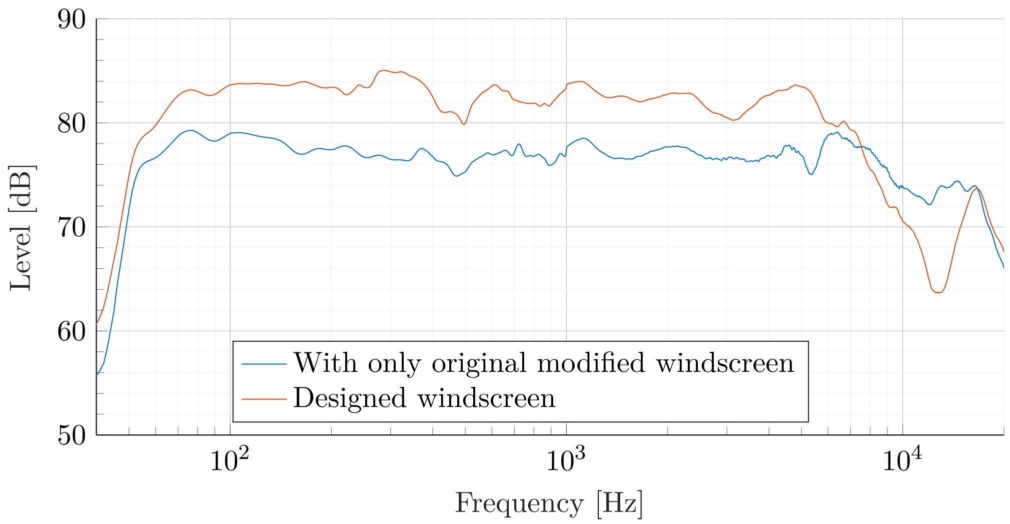

Figure M.11: The graph shows frequency response of the speaker measured without windscreen and with the designed windscreen with no rotation and a frontal tilting of 9°

As seen in Figure M.11, the roll off is due to a plate reflection. While tilting 20° the reflection frequency is lowered which means that the sound path differences of the reflected sound path grows.

A tilting of the windscreen while the foam wedge is moved 20 cm is measured as the last measurement while the foam wedge is on the plate. The following Figure M.12 shows the result with a tilt of 8° and no rotation.

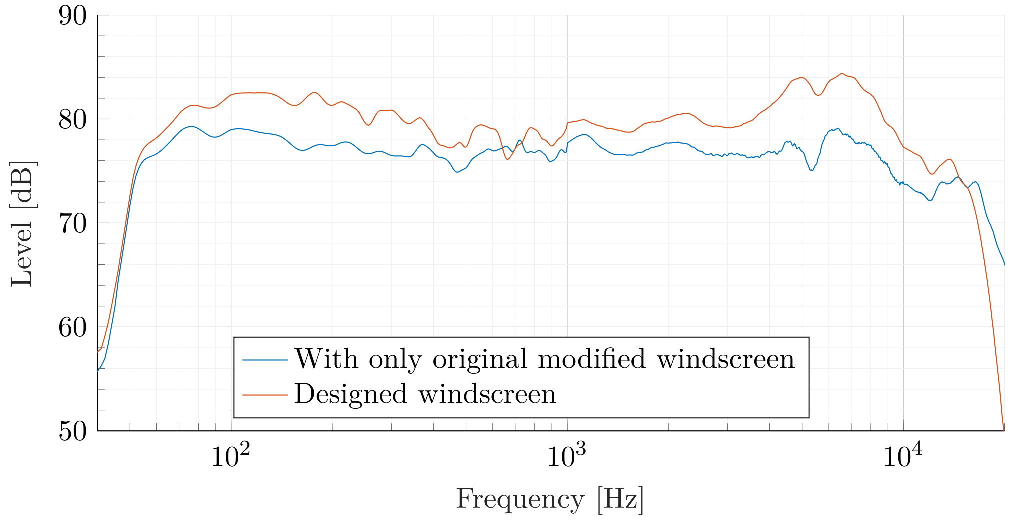

Figure M.12: The graph shows frequency response of the speaker measured without windscreen and with the designed windscreen moved 20 cm back with no rotation and a frontal tilting of 8°

The last two measurement shows the frequency response while the foam wedge is removed. The first measurement in Figure M.13 shows the frequency response without tilting and rotation. The second measurement in Figure M.14 shows the frequency response without tilting and a rotation of 30° to the right.

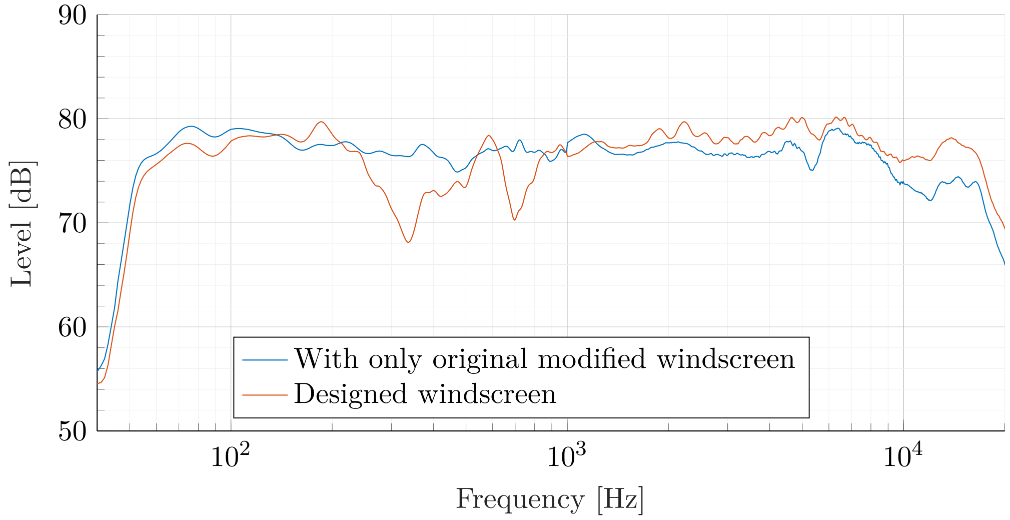

Figure M.13: The graph shows the frequency response of the speaker measured without windscreen and the designed windscreen without the foam wedge and with no rotation and no tilting

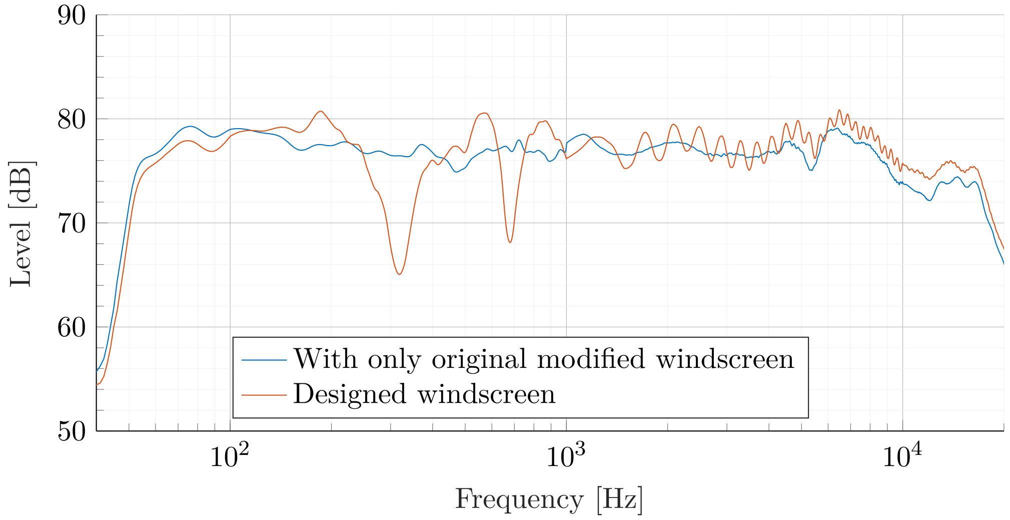

Figure M.14: The graph shows frequency response of the speaker measured without windscreen and with the designed windscreen without the foam wedge and with no tilting and a right turn of 30°

It is seen in measurement Figure M.13 and Figure M.14 that removing the foam wedge gives depth in 310 Hz and 690 Hz and the frequency response shows generally more reflections that with foam wedge.

Appendix N

Wind noise attenuation of the designed windscreen

A measurement is made to measure the wind noise attenuation of the designed windscreen. All measurement include the modified GRAS AM0069 windscreen. The measurement is done in a real scenario outside on a flat area with high wind speed than 5 m/s. The measurement is done to ensure that the measured wind noise does not overload the preamp of the microphone at the measured wind speed.

Materials and setup

To measure the wind attenuation of the windscreen configuration the following materials are used:

Table N.1: Equipment list

Description	Model	Serial-no	AAU-no
PC	Macbook	W89242W966H	-
Audio interface	RME Fireface UCX	23811948	108230
Microphone	GRAS 26CC	78189	75583
Preamp	GRAS 40 AZ	100268	75551
Windscreen	GRAS AM0069	-	-
Designed windscreen	-	-	-

Table N.2: Equipment list

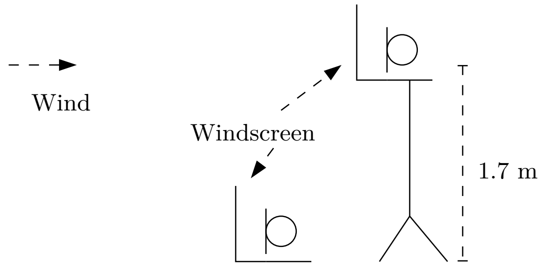

Figure N.1: The figure shows the measurement setup for the wind noise measurement.

Figure N.2: The picture shows the measurement set up

Test procedure

1. The materials are set up as in Figure N.1 where the microphone is connected to the audio interface.
2. The microphone is calibrated.
3. A 7 s time signal is measured.
4. The frequency content is calculated by `fft` after a Hanning window windows the time signal.
5. The procedure is done with, and without the windscreen
6. The procedure is done where the windscreen is rotated 50° and −50°
7. The result is plotted in MATLAB®
8. The measurement is done over for every position until similar wind speed is measured with about 8.5 m/s

Measurement area

To be able to measure in a windy area, the football stadium at Fredrick Alfred Nobels Vej 7, 9220 Aalborg is used. The following Figure N.3 shows a picture of the area and the approximate position of the speaker and microphone.

Figure N.3: The picture illustrate the area, where the measured is done

Results

The following graphs show the result of the measurement.

The graph in Figure N.4 shows a measurement where the modified original windscreen is on the ground and in the hight of 1.7 m.

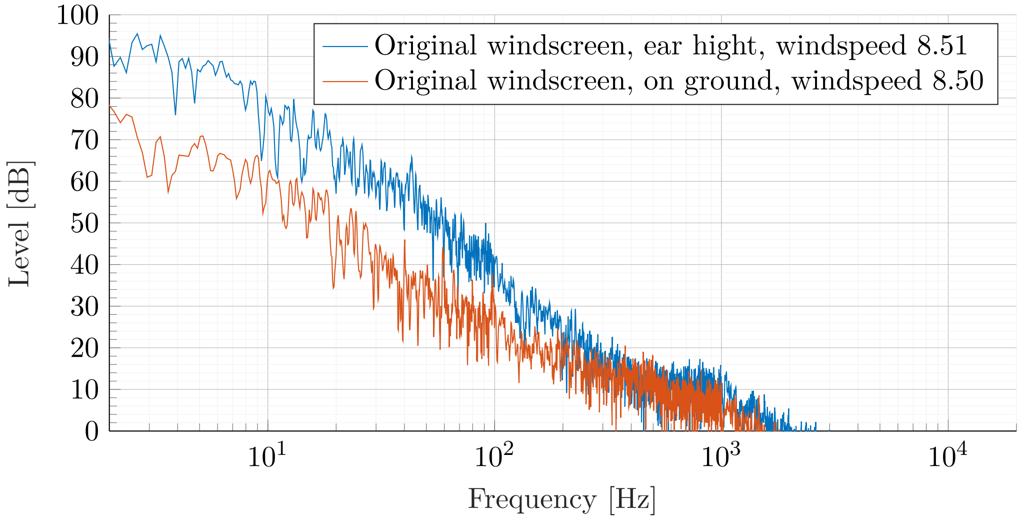

Figure N.4: The graph shows the frequency content of the measurement without the windscreen

As seen in Figure N.4, the wind noise is more than 10 dB SPL lower while the modified original windscreen is moved from the hight of 1.7 m to the ground.

The graph in Figure N.5 shows a measurement where the designed windscreen is on the ground and in the hight of 1.7 m. The windscreen is 90° to the wind in both measurements, which mean that the wind is orthogonal to the middle of the white PVC plate.

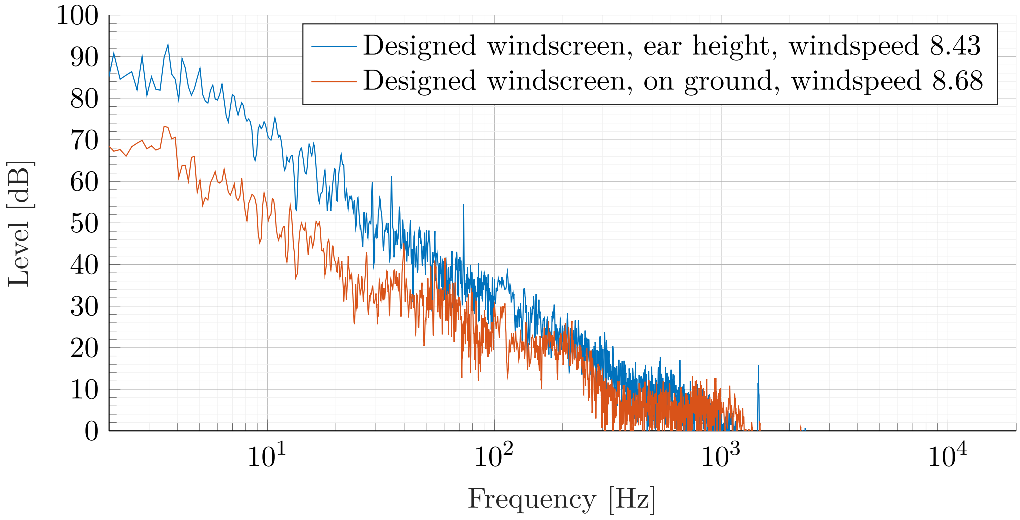

Figure N.5: The graph shows the frequency content of the measurement without the windscreen

As in Figure N.4 The wind noise is lowered more that 10 dB SPL in Figure N.5. Furthermore, the wind noise is lowered approximately 5 dB SPL to 10 dB SPL from 100 Hz and below while the designed windscreen is used. The highest attenuation is while the windscreen is lifted above the ground.

Based on the observed ground reflection shown in section 8.1.1 and the large noise differences founded in the above measurement, only the measurement on the ground is shown in the rest of the measurement. The measurement in ear height is chosen to be irrelevant since the measurement for the final test is done with a microphone on the ground. The measurement in the hight of the ear can be founded in the file. The following measurement Figure N.6 shows the measurement with and without the designed windscreen.

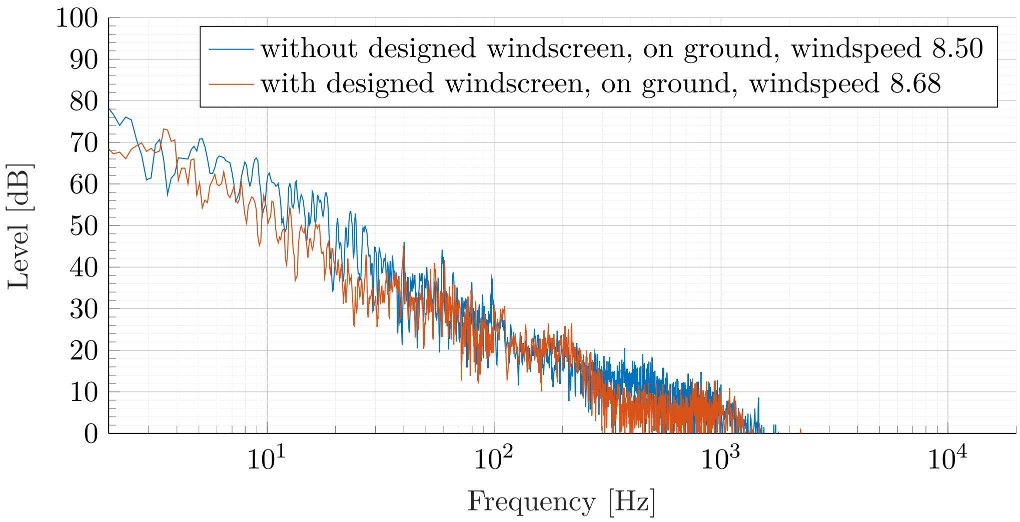

Figure N.6: The graph shows the frequency content of the measurement without the windscreen

As it is seen in Figure N.6 and explained above, it is clearly seen that the designed windscreen attenuate the wind noise. The next measurement Figure N.7 shows the differences in wind noise while the windscreen is ether rotated 50° to the left and to the right.

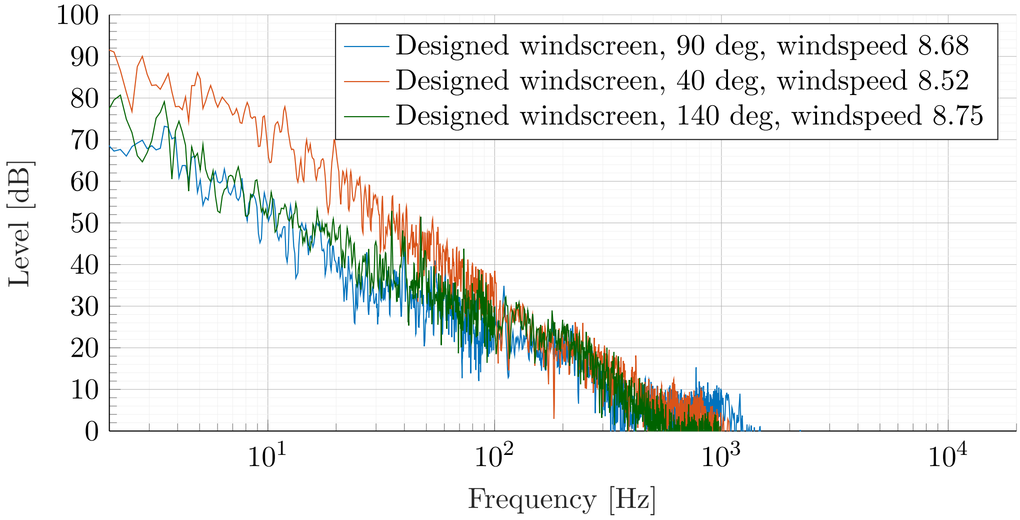

Figure N.7: The graph shows the frequency content of the measurement without the windscreen

As seen in Figure N.7, the wind noise depends on the angle of the wind to the designed windscreen. While the designed windscreen is rotated 50° to the left, the windscreen does not have any wind noise attenuation compared to the measurement with only the modified windscreen. While the designed windscreen is rotated 50° to the right, the wind noise follows the wind noise while the designed windscreen is not rotated unless around 2 Hz where the noise is 10 dB SPL higher.

Appendix O

Hardware

(a) The picture shows the anemometer.

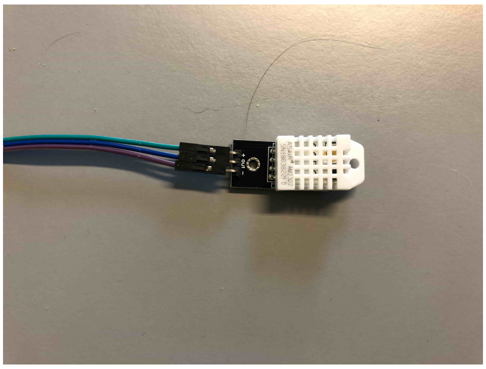

(b) The picture shows the temperature and humidity censor

Figure O.1: The figures shows the measurement sensors

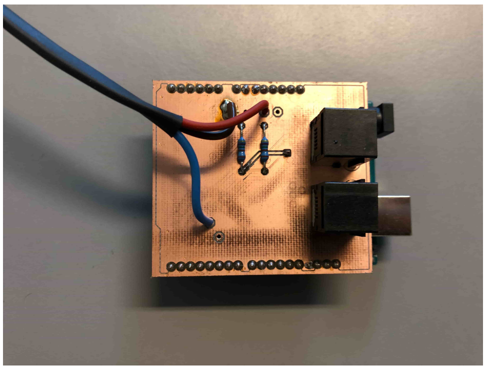

(a) The picture shows the Arduino shield

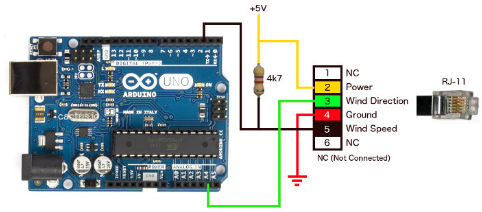

(b) The picture shows the wire connection. The connection schematic is founded at [cactus.io, 2019]

Figure O.2: The figure shows the Arduino shield and the connection of the anemometer

Appendix P

Final measurement

A measurement was made to measure the transfer function differences in three point in crosswind. One microphone situated in downwards direction, one microphone situated in upwards direction and one microphone situated in center, which is between the other two microphone. The used speaker have a horizontal dispersion pattern of 80°, but it is the 50° angle which is used as explained in ??

Materials and setup

To measure the transfer function in a crosswind situation, the following materials are used:

Table P.1: Equipment list

Description	Model	Serial-no	AAU-no
PC	Macbook	W89242W966H	-
Audio interface	RME Fireface UCX	23811948	108230
Microphone	GRAS 26CC	78189	75583
Preamp	GRAS 40 AZ	100268	75551
Microphone	GRAS 26CC	78186	75582
Preamp	GRAS 40 AZ	100267	75550
Microphone	GRAS 26CC	??	
Preamp	GRAS 40 AZ		
3 Windscreen	Author design	-	-
Line source element	L-acoustics KUDO		
Line source element	L-acoustics KUDO		
Line source element	L-acoustics KUDO		
Line source element	L-acoustics KUDO		
Line source element	L-acoustics KUDO		
Amplifier	Lab PLM10000Q		
Amplifier	Lab PLM10000Q		
Mixer	Yamaha LS9		
Wind measurement tools	Davis	-	
Angling tools	Author design	-	
flying tools	-	-	-

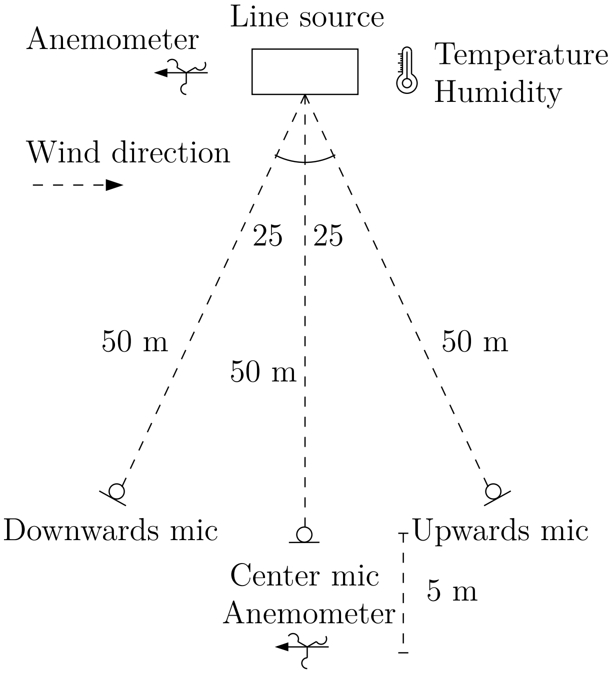

Figure P.1: The figure shows the microphone position versus the position of the line source, while the array is 0° horizontal turned

(a) The picture shows the speaker setup　　**(b)** The figure shows the wind direction

Figure P.2: The figures shows the measurement set up for Appendix A and **??**

Test procedure

1. The microphone i calibrated.
2. The wind direction is measured.
3. The materials are set up as in Figure P.1 where the speaker is placed in cross wind direction, such that the frontal wave direction is orthogonal the the wind. The microphone and speaker is connected to the audio interface.
4. The speaker is placed 2.92 m above the ground.
5. The speaker is tilted 5° pointing down agents the ground.
6. The microphone is placed 1.68 m above the ground, 50 m from the speaker. One 25° to the left of the speaker, one 25° to the right of the speaker and one in center between the to other microphone.
7. The anemometer at the speakers is situated on the speaker tower in the same side as shown on the setup and a hight of 4.64 m
8. The anemometer at the microphone position is lifted 1.68 m above the ground.
9. The wind direction goes from the upwards microphone to the downwards microphone.
10. The humidity and temperature is measured at the speaker position.
11. 10 sine sweep is performed with a length of 5 s each while the wind direction and speed is measured.
12. The impulse response is calculated and filtered with a 4th order highpass filter at 20 Hz.
13. The correlation is calculated for each impulse response to the first impulse response for time alignment [Gunness, 2001] of all microphone channels.
14. The mean impulse response is calculated for the 10 measurement of all three microphone.
15. The transfer function is calculated with a 10 sample moving mean filter.

16. The the transfer function is down sampled to fit the plotting program.
17. The transfer function is calculated with a 5 sample moving mean filter.
18. The wind measurement is synchronised to the transfer function in time.
19. The measurement is repeated 6 times with different horizontal speaker angle from 0° to 30° in step of 5°

Measurement area

To be able to measure in a windy area, parking lot at Tryvej 13, 9320 Hjallerup is used. The following Figure P.3 shows a picture of the area and the approximate position of the speaker and microphone.

Figure P.3: The picture illustrate the area, where the wind flow is measured

Results

All measuring result is not shown here, the rest can be founded in the attached file. One synchronised measurement is shown for the upwards microphone where the speaker is turned 0°, 10°, 20° and 30°. The shown measurement result is for one measurement and is not a mean from 10. This shows the time synchronised result. The average result can be founded in **??**.

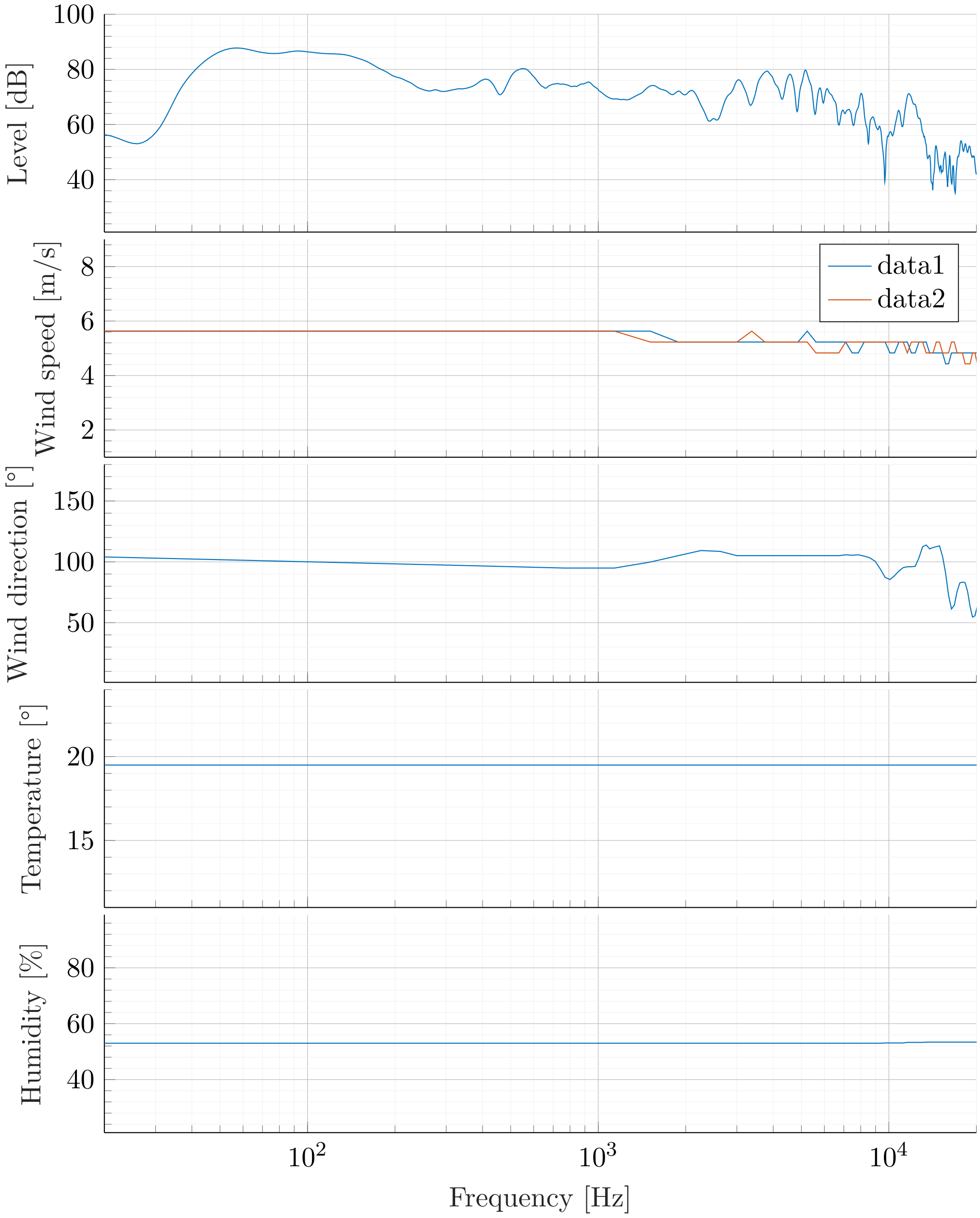

Figure P.4: the graph shows

Appendix Q

Questionnaire

A questionnaire was made to find the maximum coverage distance for a line array.

Question	Answer	Unit
Company	Profox	
What is the distances between the main stage to the first delay tower at large concert	50	[m]
How many audiences attempt to a large concert you produces	15000+	Number
What is the distances between the main stage to the first delay tower at medium concert	30	[m]
How many audiences attempt to a medium concert you produces	5000+	Number
Flying hight of top speaker	12 - 16	[m]
Does the wind direction and speed influence on the distance decision	No	
Do you want to know the result	Yes	

Question	Answer	Unit
Company	Nordic sales	
What is the distances between the main stage to the first delay tower at large concert	75	[m]
How many audiences attempt to a large concert you produces	100000+	Number
What is the distances between the main stage to the first delay tower at medium concert	50	[m]
How many audiences attempt to a medium concert you produce	30000	Number
Flying hight of top speaker	?	[m]
Does the wind direction and speed influence on the distance decision	Yes	
Do you want to know the result	No	

Question	Answer	Unit
Company	Moto rental	
What is the distances between the main stage to the first delay tower at large concert	50-60	[m]
How many audiences attempt to a large concert you produces	20000+	Number
What is the distances between the main stage to the first delay tower at medium concert	50	[m]
How many audiences attempt to a medium concert you produces	5000+	Number
Flying hight of top speaker	12 - 16	[m]
Does the wind direction and speed influence on the distance decision	Yes	
Do you want to know the result	Yes	

Question	Answer	Unit
Company	Roskilde festival	
What is the distances between the main stage to the first delay tower at large concert	73	[m]
How many audiences attempt to a large concert you produces	100000+	Number
What is the distances between the main stage to the first delay tower at medium concert	?	[m]
How many audiences attempt to a medium concert you produces	?	Number
Flying hight of top speaker	?	[m]
Does the wind direction and speed influence on the distance decision	No	
Do you want to know the result	No	

Question	Answer	Unit
Company	AV-center Aalborg	
What is the distances between the main stage to the first delay tower at large concert	60	[m]
How many audiences attempt to a large concert you produces	20000+	Number
What is the distances between the main stage to the first delay tower at medium concert	30	[m]
How many audiences attempt to a medium concert you produces	5000+	Number
Flying hight of top speaker	14 - 16	[m]
Does the wind direction and speed influence on the distance decision	Yes	
Do you want to know the result	Yes	
comment: The biggest problem lays in the frequency range from 1.0 kHz to 7.0 kHz where the understanding of the music despisers and the music sound muddy	-	

Question	Answer	Unit
Company	Kinovox	
What is the distances between the main stage to the first delay tower at large concert	60	[m]
How many audiences attempt to a large concert you produces	20000+	Number
What is the distances between the main stage to the first delay tower at medium concert	30	[m]
How many audiences attempt to a medium concert you produce	10000	Number
Flying hight of top speaker	14 - 16	[m]
Does the wind direction and speed influence on the distance decision	Yes	
Do you want to know the result	No	
comment: He uses to rotate the line array agents the wind if he knows that the wind is crosswind and the wind will continue along the concert time. Moreover, he would stop the concert if the wind speed is above 10 m/s	-	

Bibliography

AOSONG. *Temperature and humidity module*, AOSONG. Available at: <https://akizukidenshi.com/download/ds/aosong/AM2302.pdf>.

Association, D. W. I., 2003. *The Geostrophic Wind*, Danish Wind Industry Association. [Website]. Available at: <http://dr\T1\omst\T1\orre.dk/wp-content/wind/miller/windpower%20web/en/tour/wres/geostro.htm>. [Accessed 18 feb 2019].

audio, C., 2019. *DDP and DDC-Driver*, CODA audio. [Website]. Available at: <https://codaaudio.com/ddp-driver/>. [Accessed 28 maj 2019].

Ballou, G. Focal Press, Oxford, fourth edition edition, 2008. ISBN 978-0-240-80969-4. doi: https://doi.org/10.1016/B978-0-240-80969-4.50002-X. Available at: <http://www.sciencedirect.com/science/article/pii/B978024080969450002X>.

Bauman, P., Urban, M., and Heil, C. Wavefront Sculpture Technology. In *Audio Engineering Society Convention 111*, Nov 2001. Available at: <http://www.aes.org/e-lib/browse.cfm?elib=9813>.

Beranek, L. L., 2006. Analysis of Sabine and Eyring equations and their application to concert hall audience and chair absorption. *The Journal of the Acoustical Society of America*, 120(3), pp. 1399–1410. doi: 10.1121/1.2221392. Available at: <https://doi.org/10.1121/1.2221392>.

Bohn, D. A. Environmental Effects on the Speed of Sound. In *Audio Engineering Society Convention 83*, Oct 1987. Available at: <http://www.aes.org/e-lib/browse.cfm?elib=4916>.

cactus.io, 2019. *How to Hookup Davis Anemometer to Arduino (Part 1 of 3)*, cactus.io. [Website]. Available at: <http://cactus.io/hookups/weather/anemometer/davis/hookup-arduino-to-davis-anemometer>. [Accessed 21 maj 2019].

Corteel, E., Sugden, S., and Montignies, F. Large Scale Open Air Sound Reinforcement in Extreme Atmospheric Conditions (Engineering Brief). In *Audio Engineering Society Conference: 2017 AES International Conference on Sound Reinforcement – Open Air Venues*, Aug 2017. Available at: <http://www.aes.org/e-lib/browse.cfm?elib=19184>.

Crocker, M. J. *Handbook of Acoustics*. John Wiley & Sons, New York, 1998. ISBN 978-0-471-25293-1.

Czerwinski, E., Voishvillo, A., Alexandrov, S., and Terekhov, A., 1999. Air-Related Harmonic and Intermodulation Distortion in Large Sound Systems. *J. Audio Eng. Soc*, 47(6), pp. 427–446. Available at: <http://www.aes.org/e-lib/browse.cfm?elib=12102>.

Davis. *Anemometer Vantage Pro2TM Accessories*, Davis. Available at: <https://www.davisinstruments.com/product_documents/weather/spec_sheets/6410_SS.pdf>.

d&b audiotechnik, 2019. *d&b Soundscape*, d&b audiotechnik. [Website]. Available at: <https://www.dbsoundscape.com/global/en/>. [Accessed 21 feb 2019].

de Oliveira, A. F. G. P., 2012. The effect of wind and turbulence on sound propagation in the atmosphere. Speciale, Instituto Superior Technico Universidad Tecnica de Lisboa. Available at: <https://fenix.tecnico.ulisboa.pt/downloadFile/395144345754/dissertacao.pdf>.

Embleton, T. F. W., 1996. Tutorial on sound propagation outdoors. *The Journal of the Acoustical Society of America*, 100(1), pp. 31–48. doi: 10.1121/1.415879. Available at: <https://doi.org/10.1121/1.415879>.

Gunness, D. W. Loudspeaker Transfer Function Averaging and Interpolation. In *Audio Engineering Society Convention 111*, Nov 2001. Available at: <http://www.aes.org/e-lib/browse.cfm?elib=9850>.

ISO 9613-1:1993. *Acoustics – Attenuation of sound during propagation outdoors – Part 1: Calculation of the absorption of sound by the atmosphere.*

L-Acoustics, a. *KUDO Multi-Mode WST Enclosure*, L-Acoustics. Available at: <http://www.dreamsound.com/downloadable/211>.

L-Acoustics, b. *KUDO*, L-Acoustics. Available at: <http://impact-even.com/wp/wp-content/uploads/2012/03/procedure_d_accrochage_kudo.pdf>.

L-Acoustics, 2019. *Live Sound*, L-Acoustics. [Website]. Available at: <https://www.l-isa-immersive.com/live-sound/>. [Accessed 21 feb 2019].

Letowski, T. R. and Scharine, A. A., 2017. Correlational Analysis of Speech Intelligibility Tests and Metrics for Speech Transmission, US Army Research Laboratory. [Online], DEFENSE TECHNICAL INFORMATION CENTER. Available at: <http://www.dtic.mil/dtic/tr/fulltext/u2/1043203.pdf>. [Accessed 27.09.2018].

Levine, D. R., Calza, P., Di Cola, M., Martignon, P., and Chisari, L. Influence of Horn's Surface Temperature on its Directivity Control. In *Audio Engineering Society Convention 145*, Oct 2018. Available at: <http://www.aes.org/e-lib/browse.cfm?elib=19746>.

Müller, S. and Massarani, P., 2001. Transfer-Function Measurement with Sweeps. *J. Audio Eng. Soc*, 49(6), pp. 443–471. Available at: <http://www.aes.org/e-lib/browse.cfm?elib=10189>.

Ostashev, V. E., Wilson, D. K., Liu, L., Aldridge, D. F., Symons, N. P., and Marlin, D., 2005. Equations for finite-difference, time-domain simulation of sound propagation in moving inhomogeneous media and numerical implementation. *The Journal of the Acoustical Society of America*, 117(2), pp. 503–517. doi: 10.1121/1.1841531. Available at: <https://doi.org/10.1121/1.1841531>.

Piercy, J. E., Embleton, T. F. W., and Sutherland, L. C., 1977. Review of noise propagation in the atmosphere. *The Journal of the Acoustical Society of America*, 61 (6), pp. 1403–1418. doi: 10.1121/1.381455. Available at: <https://doi.org/10.1121/1.381455>.

Prospathopoulos, J. M. and Voutsinas, S. G., 2007. Determination of equivalent sound speed profiles for ray tracing in near-ground sound propagation. *The Journal of the Acoustical Society of America*, 122(3), pp. 1391–1403. doi: 10.1121/1.2764476. Available at: <https://doi.org/10.1121/1.2764476>.

Roozen, N. B., Vael, J. E. M., and Nieuwendijk, J. A. Reduction of Bass-Reflex Port Nonlinearities by Optimizing the Port Geometry. In *Audio Engineering Society Convention 104*, May 1998. Available at: <http://www.aes.org/e-lib/browse.cfm?elib=8519>.

Rossing, T. *Springer Handbook of Acoustics*. 01 2014. ISBN 978-1-4939-0754-0. doi: 10.1007/978-1-4939-0755-7.

Vanderkooy, J. Nonlinearities in Loudspeaker Ports. In *Audio Engineering Society Convention 104*, May 1998. Available at: <http://www.aes.org/e-lib/browse.cfm?elib=8432>.

Voishvillo, A. Comparative Analysis of Nonlinear Distortion in Compression Drivers and Horns. In *Audio Engineering Society Convention 117*, Oct 2004. Available at: <http://www.aes.org/e-lib/browse.cfm?elib=12849>.

Wilson, D. K., 2003. Wind noise and the spectrum of atmospheric turbulence pressure fluctuations. *The Journal of the Acoustical Society of America*, 113(4), pp. 2248–2248. doi: 10.1121/1.4780400. Available at: <https://doi.org/10.1121/1.4780400>.

Wong, G. S. K. and Embleton, T. F. W., 1985. Variation of the speed of sound in air with humidity and temperature. *The Journal of the Acoustical Society of America*, 77 (5), pp. 1710–1712. doi: 10.1121/1.391918. Available at: <https://doi.org/10.1121/1.391918>.

Yang, X. *Atmospheric Acoustics*. Walter de Gruyter GmbH Co KG, Berlin, 2016. ISBN 978-3-110-31153-2.